Electroanalytical Sensors using Lipophilic Cyclodextrins

by

Simon Richard Faunch Palmer

Department of Chemistry
University of Durham

A thesis submitted for the degree of Doctor of Philosophy

November, 1997

Abstract

Electroanalytical Sensors using Lipophilic Cyclodextrins

Lipophilic dialkylated-α-, β- and γ-cyclodextrin derivatives were used as selective ionophores for a series of clinically relevant ammonium ions, and as enantioselective ionophores for both α- and β-aryl ammonium ions.

Sensitive and selective potentiometric detection of the local anaesthetics lidocaine and bupivacaine was achieved by using 2,3,6 trioctyl-β-cyclodextrin as the ionophore, leading to micromolar detection limits. Interference studies showed that the simulated clinical electrolyte background caused minimal interference whereas organic interferents of similar size and charge caused some perturbation of the electrode response at a concentration of 10 mmol dm^{-3}. An electrode comprising a plasticised biocompatible membrane matrix, TECOFLEX, with 2,6 didodecyl-β-cyclodextrin was incorporated in a flow injection analysis system and the response to lidocaine studied in the presence of human serum. Human serum caused no adverse effects to the electrochemical response of the electrode. These electrodes are, therefore, very suitable for on-line detection of local anaesthetics.

Potentiometric detection of tricyclic antidepressants using didodecyl-α-, β- and γ-cyclodextrins as the ionophore, gave micromolar detection limits. Interference from simulated clinical electrolyte background and selected organic interferents gave similar results to those discussed above. In order to lower the detection limit to sub-nanomolar levels modified amperometric electrodes were assembled by depositing a membrane comprising plasticised TECOFLEX, 2,3,6 triethyl-β-cyclodextrin and TKB on the working electrode of a screen printed electrode.

Lipophilic 2,6 didodecyl-α- and β-cyclodextrins exhibited enantiomeric discrimination in the binding of propranolol, ephedrine, amphetamine and methamphetamine. These results were confirmed using potentiometric and NMR techniques.

Declaration

The work described herein was carried out in the Department of Chemistry at the University of Durham between October 1994 and September 1997. All the work is my own, unless stated to the contrary, and it has not been submitted for a degree at this or any other university.

Statement of Copyright

Acknowledgements

I would like to thank my supervisors, Professor David Parker and Doctor Ritu Kataky, for their help, advice and guidance during the course of my work. The members, past and present, of the research group are thanked for their help and friendship during the last three years.

I would also like to thank Ian Mckeag for running numerous NMR spectra. I would also like to thank the rest of the technical staff for all their help during the last three years. Thanks must also go to Professor Yoram Cohen of the school of chemistry, Tel-Aviv University for providing the PGSE data.

I would also like to thank Professors Zsofia Feher, Klara Toth and their research groups for the support they gave me during my work at the Technical University of Budapest. Thanks especially goes to Robbie who showed me around Budapest.

David, Steve, Rosy and Ritu are thanked for their rapid and helpful proof reading of the thesis.

Financial assistance from the University of Durham is gratefully acknowledged.

Most of all I would like to thank my parents for their love and support. This thesis is for them.

Once you have exhausted all possibilities and failed
There will be one solution, simple and obvious,
Highly visible to everyone else.

Snafu

To Mum and Dad

Contents

Abbreviations

A_g, A_o	Echo intensities in presence and absence of pulsed gradient
γ	gyromagnetic ratio
τ_c	rotational correlation time
AAG	α_1-acid glycoprotein
BBPA	bis(1-butylpentyl)adipate
BSA	bovine serum albumin
CDA	chiral derivatising agents
CSA	chiral solvating agent
CVD	constant volume dilution
CZE	capillary zone electrophoresis
D	self-diffusion coefficient
DOS	bis(2-ethylhexyl)sebacate
E^0	standard electrode potential
E^0_{init}	initial potential
E^0_{internal}	internal electrode potential
ECE	electrochemical – chemical – electrochemical mechanism
ES	electrospray
ESMS	electrospray mass spectrometry
FAB	fast atom bombardment
FET	field effect transistor
FIA	flow injection analysis
FIM	fixed interferent method
FTIR	fourier transform infra-red spectroscopy
$\Delta G^0_{complex}$	free Energy of complexation
g	magnetic gradient strength (in PGSE)
GLC	gas liquid chromatography
GSE	gas-sensing electrode
HPLC	high performance liquid chromatography
HS	human serum
IR	infra-red

ISE	ion-selective electrode
ISFET	ion-selective field effect transistor
$K_{+/-}$	enantioselectivity
K_{ij}^{pot}	selectivity coefficient
K_a	association constant
KTClPB	potassium tetrakis(4-chlorophenyl)borate
LD	limit of detection
LSR	lanthanide shift reagents
NMR	nuclear magnetic resonance
N_p	1-napthyl group
*o*NPOE	ortho-2-nitrophenyloctyl ether
PGSE	pulsed gradient spin-echo
Ph	phenyl group
pK_a	acidity constant
Poly-HEMA	poly-2-hydroxy ethylmethacralate
PS	plasmaspray
PVC	poly vinyl chloride
R_1	relaxation rate
RIA	radioimmunoassay
SPE	screen printed electrode
SQW	square wave voltammetry
T_1	relaxation time
THF	tetrahydrofuran
TKB	sodium tetrakis[3,5-bis(trifluoromethyl)phenyl]borate
TSP	thermospray
UV/VIS	ultraviolet/visible spectroscopy

Chapter One

Introduction

1.1 Clinical Analysis and Enantiomer Discrimination

This thesis is based upon the application of alkylated cyclodextrins; in clinical analysis and enantiomer discrimination. This chapter discusses the processes involved in molecular recognition (section 1.2), the electrochemical sensors designed for analysis of clinically relevant substances (section 1.3). Sections 1.4 – 1.8 discuss the properties and uses of cyclodextrins.

1.2 Molecular Recognition

1.2.1 Host Structure

Molecular recognition is the basis of many biochemical processes, but it has only been relatively recently that synthetic molecules have been produced that can recognise other ions and molecules. The host molecules most often used in these areas of research are either modified naturally occurring receptors or synthetic molecules which are often macrocycles. To be suitable for ion recognition the molecule should typically possess the following features[1,2],

1. A stable conformation that defines a 'cavity' into which polar groups may be directed (binding sites), while non-polar groups form a lipophilic shell around the 'cavity'.
2. There should be preferably 4 to 8, but no more than 9 co-ordination sites.
3. High selectivity may be achieved with convergent co-ordination.
4. The ligand should be sufficiently flexible to allow fast ion-exchange.

These criteria have been statisfied by a variety of hosts such as spherands, cryptaspherands, cryptands, crown ethers and certain naturally occurring antibiotics such as valinomycin, all of which have been studied as hosts.

The degree of pre-organisation in the host has a profound influence upon both the binding strength and the selectivity of the host. Cram[3] studied a series of macrocyclic hosts and showed that spherands are highly preorganised, possessing a single

conformation ideally suited to the binding of lithium. The free energy cost for binding site organisation had already been paid during synthesis and therefore did not contribute to a less favourable $\Delta G^0_{complex}$ for complex formation. Thus the spherand (figure 1.2.1.1) was preorganised for binding. As less preorganised compounds are considered (crown ethers), the less favourable $\Delta G^0_{complex}$ can be attributed to a greater need for binding site reorganisation prior to complexation.

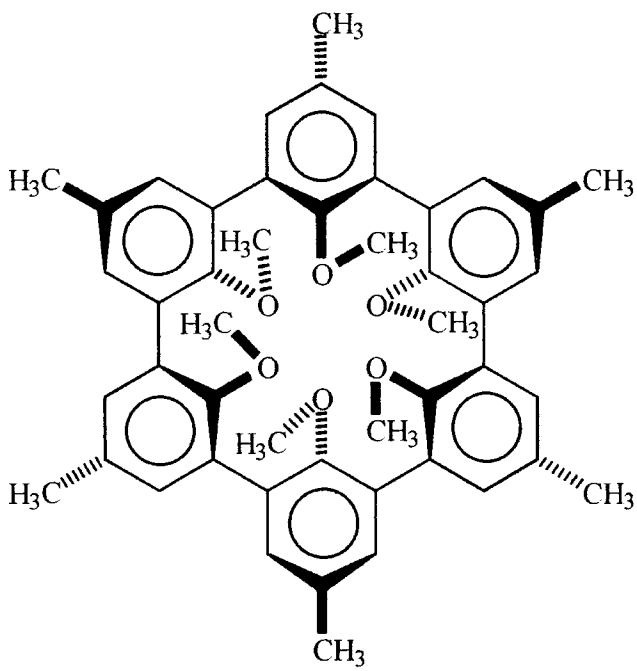

Figure 1.2.1.1 The preorganised Spherand-6.

Although binding site preorganisation to some extent determines the binding power of the host, complementarity of the host and guest binding sites is central in determining the extent of structural recognition. The binding energy at a single contact site is at most a few kilojoules per mole (hydrogen bonding of alcohols, bond strength = 20 kJ/mol), much lower than that of a covalent bond (C-H bond (av.) = 420 kJ/mol). Contacts at several sites between the host and guest are required for formation of complexes. Such contacts depend on the relative placements of binding sites in the complexing partners. This aspect is fundamental in chiral recognition. The host is chiral, and binding site complementarity has a chiral as well as structural aspect. For chiral discrimination to occur, the binding interaction of the host must favour one guest

enantiomer. The other enantiomer must give rise to an unfavourable interaction, such as a repulsive steric interaction.

The ability to selectively recognise a specific guest species has led to host molecules being used in a variety of chemical sensors. However, host-guest complexation is not sufficient on its own, the complexation must lead to a change in a detectable physical property. The properties most frequently used are electrochemical[4] and optical[5,6].

1.2.2 Recognition of ammonium ions and related structures

Ammonium ions frequently play an important role in clinical chemistry so it is not surprising that receptor molecules capable of recognising such substrates have been developed.

Crown ether macrocycles are the host molecules which have been studied most often in this area. Primary ammonium ions are bound via the anchoring of the protonated ammonium group through three C_3-related $^+$NH—O hydrogen bonds, as shown in figure 1.2.2.1.

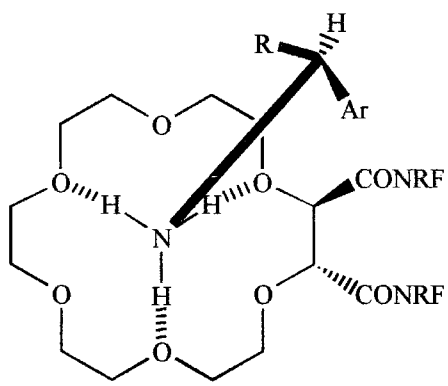

Figure 1.2.2.1 Binding of a primary ammonium ion by an 18-crown-6 derivative.

Chiral polyethers have been used to bind chiral ammonium ions with fairly high enantiomer selectivity. The most successful of these have been devised by Cram[7] and Lehn[8]. Figure 1.2.2.2 shows the structure of these host molecules. The host devised by Cram was tested using partition experiments (between D_2O and a solution containing

CD_3CN and $CDCl_3$) and showed enantioselective binding towards a series of chiral α-amino acids. The tetracarboxamide 18-crown-6 derivative, developed by Lehn[8], bound the (+)-α-phenylethylammonium ion in preference to its enantiomer ($K_{+/-} = 2.6$). Selectivity against selected other ammonium ions was also investigated, for example, the selectivity over the ephedrinium ion (a protonated secondary amine) when present as the interferent was $-\log K^{pot}_{PEA,EPH} = 2.0$. However, the selectivities against inorganic cations such as sodium ($-\log K^{pot}_{PEA,Na^+} = 1.4$) or potassium ($-\log K^{pot}_{PEA,K^+} = 0.5$) were poor.

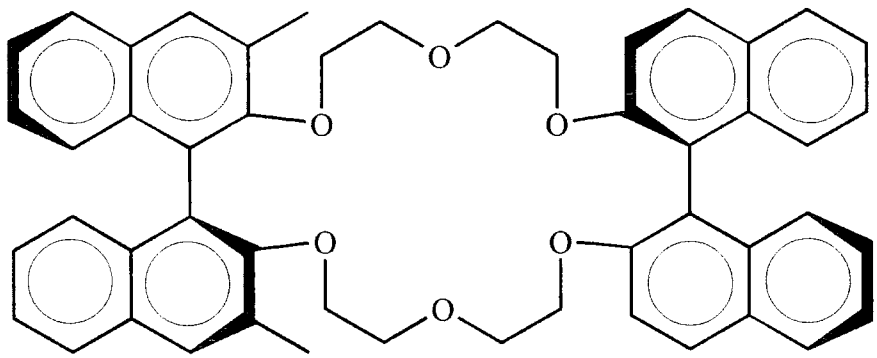

Cram[7]

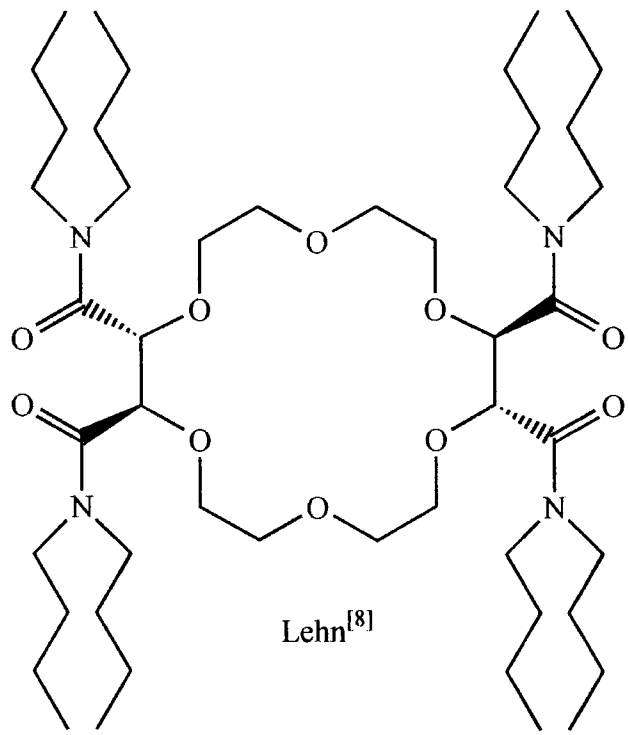

Lehn[8]

Figure 1.2.2.2 Chiral crown ether derivatives.

1.3 Clinical Analysis Electrodes

The area of clinical analysis is concerned with the production of simple diagnostic probes which can be used by an unskilled user, either continuously in an on-line process or discretely as a 'throw away' device. This branch of research is rapidly expanding as the demand increases for more sensitive and selective detection of an ever growing number of clinical analytes[9,10]. Typical areas of interest in clinical analysis are defined in table 1.3.1. Many different electroanalytical techniques have been used to aid the analysis of a given ion[11,12,13]. Of growing importance has been the use of potentiometric and voltammetric electrochemical sensors. These techniques have both been successfully utilised in the areas of clinical analysis and pharmaceutical quality control, with perhaps the two most widely known systems being the determination of blood glucose (voltammetric) and blood calcium levels (potentiometric).

Analytical Application	
Research and Development (pharmacokinetics, metabolism)	
Analysis of raw products (pharmacopoeia monography)	
Analysis of drug formation	
Analysis in biological fluids:	drug therapy monitoring
	drug intoxication
	drug addiction
	doping

Table 1.3.1. Applications to which drug analysis is applied.

1.3.1 Potentiometric Electrochemical Methods

The first application of potentiometric sensors in clinical analysis was the development of the pH electrode for the determination of blood pH. Since then the number of analytes to which these sensors have been applied has grown rapidly[14]. The fundamental process occuring in the most common type of potentiometric sensor (the

polymer membrane-based ion-selective electrode) is a guest-induced selective change in the charge separation across the interface between the polymer membrane and the aqueous sample solution. Hence by the synthesis of highly lipophilic and selective complexing agents, the specificity of these electrodes can be optimised for a given analytical task[15]. This has led to efforts over the last few years being directed to the synthesis of new and more selective ionophores, such as the highly sensitive and selective lithium ionophore synthesised by Parker[16] (figure 1.3.1.1). An electrode based on this ionophore showed a Nernstian gradient (61 mV/decade) with a detection limit of 6.3 x 10^{-6} mol dm^{-3}. The selectivity in a simulated background of clinical cations (1.50 x 10^{-1} mol dm^{-3} NaCl, 4.3 x 10^{-3} mol dm^{-3} KCl, 1.26 x 10^{-3} mol dm^{-3} $CaCl_2$, 0.9 x 10^{-3} mol dm^{-3} $MgCl_2$) was also reported, $-\log K^{pot}_{Li,Clin} = 3.25$.

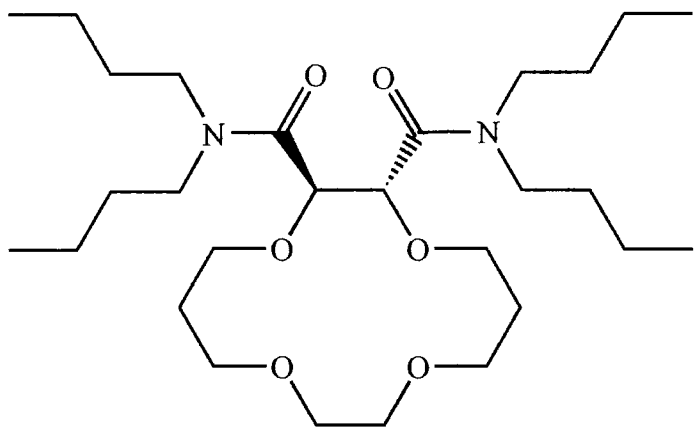

Figure 1.3.1.1 Derivatised 14-crown-4 Lithium Ionophore.

Advances in ionophore technology have been made together with improvements in other areas. The miniaturisation of these sensors has led to the use of more reliable ion-selective field effect transistors (ISFETs)[17,18]. ISFETs have been developed for Ca^{2+}, K^+, Na^+, NH_4^+ and pH, and have been used for in vivo monitoring of Ca^{2+} and K^+. This has led to the production of devices at a lower cost, with greater reproducibility and the potential for multiple sensors on a single chip[19].

A major problem with potentiometric sensors in clinical analysis is the appearance of a shift in the standard potential of the electrode (E^0) when changing from an aqueous electrolyte to a protein containing solution. This shift is due to the induction of a

membrane asymmetry potential in inherently symmetric membranes through a contamination of the membrane surface by proteins[20]. To overcome this problem in clinical analysis, several approaches have been investigated.

1. The alteration of the calibration solutions to ones more closely matching the blood matrix. Work performed by Covington and Kataky[21] took the first steps by matching the calibration matrix in terms of ionic composition, ionic strength and pH. This led to the reduction in the liquid-junction and activity coefficient bias. However, the calibration solutions did not originally contain protein, although this has since been rectified[22].

2. An approach which has been applied for some time in other medical applications involved the surface treatment of a bulk polymer with an outer coating. This may be necessary as conventional materials do not often meet the demands required of them in terms of both their surface and bulk properties[23]. Cosofret and co-workers[24] have applied this approach to ion-selective electrodes by applying a layer of poly-2-hydroxy ethylmethacralate (poly-HEMA) to the blood contacting face of the membrane. Unfortunately the equilibration time of the sensor was quite long (24 hours). However, the electrode response was excellent in whole blood samples, showing very little reduction in the slope of the calibration curve, or any increase in the membrane resistance for a period of up to fourteen days. After this time, the layer of poly-HEMA began to peel away from the bulk PVC.

3. The polymer matrix used in the ion-selective electrode can be substituted for a more biocompatible material[25]. This simple approach was applied by Cosofret[26] and D'Orazio[27]. Both groups replaced the PVC in the polymer membrane by the aliphatic polyurethane TECOFLEX. The polyurethane had been observed previously to show excellent biocompatibility[28]. Indeed both groups successfully showed that this approach led to improvement in the stability of ISEs in the presence of biological media.

4. Recently a novel approach to the problem was proposed by Meyerhoff[29]. It was demonstrated how the emission of low levels of nitric oxide, a potent platelet antiaggregation reagent, resulted in a marked decrease in protein coating for the

electrode. The sensing membrane was composed of three layers, the first and third are cast as normal, the second contained N-N'-dimethylhexanediamine nitric oxide adduct (DMHD/N_2O_2). This adduct is known to generate NO spontaneously in an aqueous environment. In the polymer membrane the release rate of NO from the adduct was reduced, allowing the membrane to be used for several days. Importantly the response characteristics of the electrode were not compromised by the addition of the adduct.

With these developments in reducing the problem of protein interference and the synthesis of better ionophores, the full potential of this type of sensory system for the detection of analytes in whole blood is beginning to be realised.

Whilst ISEs can be used in whole blood, an area to which they are often applied is in the quality control of pharmaceutical preparations. Quality control is relatively straight forward for ISE systems since the concentration of the drug analyte is often quite high (e.g. the standard lidocaine injection solution is 1 % w/v lidocaine hydrochloride in an aqueous background) and the preparations are often aqueous with no protein or other interferents being present.

1.3.2 Voltammetric Electrochemical Methods

The main advantage of potentiometric detection is its high selectivity. This, however, is coupled with a detection range that is limited to approximately 10^{-6} mol dm^{-3}, and many drugs are present in the body at much lower levels. The sensitivity of voltammetric detection had been hindered by the generally low selectivity for a given analyte observed in biological media. The deliberate modification of the electrode surfaces has led to improvements not only in the selective detection of the analyte but also in an increased detection range, through preconcentration[12].

The first application of voltammetric analysis to clinical analysis was the Clark oxygen electrode which was first used to measure dissolved oxygen in blood in 1956. The sensor involves a relatively simple design consisting of a platinum working electrode and a Ag|AgCl reference/counter electrode covered with a Teflon membrane through

which the dissolved oxygen may pass into the electrolyte solution behind the membrane. It was not long before the sensor was modified, and in 1962 the electrode was coated with a further membrane layer which held in place an enzyme, glucose oxidase. The membrane between the electrode and the enzyme allowed the passage of hydrogen peroxide but prevented the passage of potential interferents e.g. ascorbic acid to the electrode surface. The membrane between the glucose oxidase and sample solution allowed the diffusion of the substrate and oxygen to the enzyme. This was originally accomplished by sandwiching the enzyme between a cellulose acetate and a polycarbonate membrane. This constituted the first glucose electrode.

Since this first voltammetric sensor, much research has been done in both simple chemically modified voltammetric sensors and in enzyme linked systems. Work by Murray[30] showed that modification of glassy carbon and graphite surfaces with ethylenediamines via organosilane chemistry was possible as a first step towards assembling electrochemically active centres on the modified surface of the electrode.

Molecules commonly used as ionophores have been applied as surface modifiers to working electrodes in voltammetric analysis. Polymerised calixarenes (figure 1.3.2.1) were applied by Svehla *et al.*[31] to enhance the accumulation of lead(II), copper(II) and mercury(II) ions on a carbon paste electrode prior to anodic stripping. Their results demonstrated the ability of the polymerised surface to preconcentrate these trace metal ions and hence allow their analysis. Unfortunately, the presence of alkali metal ions in the sample solutions was found to have an adverse effect on the electrode response, due to the preferential binding of these ions by the calixarenes.

The idea of preconcentration is not new. Chaney and Baldwin showed that adriamycin, a chemotherapeutic drug, could be preconcentrated onto an unmodified carbon paste electrode[32] allowing a detection limit of 10^{-8} mol dm^{-3} for the drug in urine. The use of a modified electrode surface has the advantage of making the preconcentration more selective, by prohibiting the adsorption of certain species onto the electrode surface.

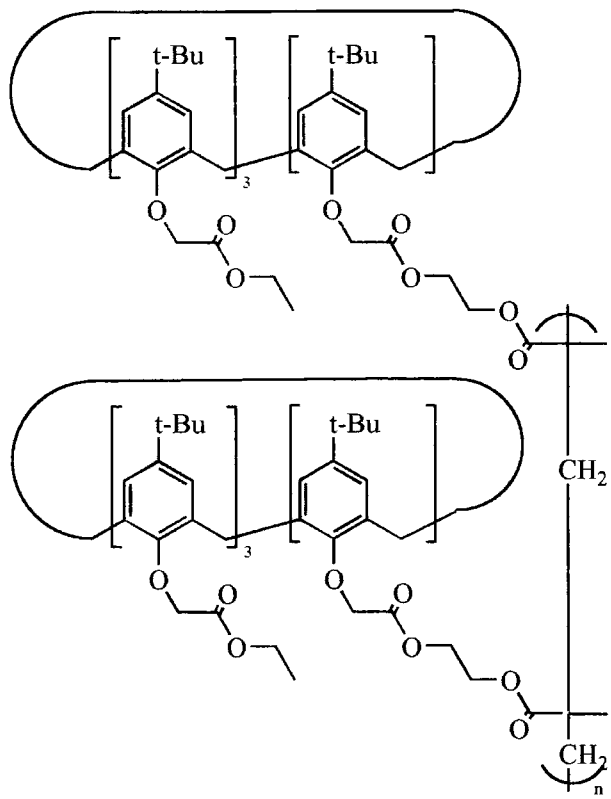

Figure 1.3.2.1 A polymerised calixarene.

Nafion coated carbon paste electrodes have recently been used in the determination of three important β-agonist drugs by Smyth[33]. Nafion, a fluorinated polymer, was chosen as it possesses a large number of anionic sites which reduce the interference from anionic constituents of the sample solution, and help attract the cationic analyte. Work with unmodified electrodes had shown a loss of electrode activity and this was believed to be due to the adsorption of interfering electroactive species from the sample solution. Therefore the Nafion film had two purposes, firstly to prevent the adsorption of interferents onto the carbon paste and secondly as a means of preconcentrating the analytes as required to reach the detection levels needed for biological samples. Using such a Nafion modified electrode, a detection limit of 2.5×10^{-8} mol dm^{-3} salbutamol was achieved.

The utility of a sensor is determined by its selectivity. Hence sensors which combine the high selectivity of a biological element with a physical transducer, can be regarded

as ideal analytical tools for a variety of analytes. Table 1.3.2.1 lists the different biological elements that may be combined with various transducers[34].

Biological Element	Transducer	Measurement
Enzymes	Solid electrodes	Voltammetry
Microorganisms Whole Cells (animal, vegetable)	ISEs GSE FET	Potentiometry
Antibodies	photodiode, photomultiplier (+fibre optic)	Optical
Antigens	Thermister	Calorimetry
	Piezoelectric crystal	Mass Change

Table 1.3.2.1. Sensor components and detection modes. ISE: ion-selective electrode, GSE: Gas-sensing electrode, FET: Field effect transistor.

The combination of an enzyme layer with an electrochemical sensor provides the advantages of specificity of the enzyme system with the sensitivity of voltammetric analysis. The major problem arising from the use of enzymes has been their encapsulation, how to manage it without losing enzymatic activity and without leaching of the enzyme.

The simplest approach is based on membrane entrapment, where the enzyme is held behind a membrane (dialysis membranes are normally used). This approach allows the enzyme to maintain its activity but it can easily leach away. Gel entrapment (using for instance gelatin, starch or polyacrylamide)and cross-linking with a bifunctional agent such as glutaraldehyde have also been used. These methods work fairly well on the whole, although in some cases enzymatic activity can be lost due the cross-linking reaction. Recently enzymes have been immobilised directly onto the electrode surface via adsorption, covalent attachment or entrapment within a polymer membrane cast onto the electrode surface[35,36]. The ability to immobilise an enzyme directly at the electrode surface without affecting its activity has led to the production of sensors with faster response times (fewer rate limiting steps through diffusion). Accompanying the

improved immobilisation techniques, the removal of an oxygen dependence from the commonest enzyme group used, the oxidases, has been achieved by two methods:

i. By the addition of a redox mediator that shuttles electrons between the electrode and the enzyme allowing the rapid reoxidation of the enzyme
ii. Directly wiring the enzyme to the electrode through an electroactive conducting polymer.

The major breakthrough for the mediator approach was the use of ferrocene derivatives. Cass[37] was the first to use the system successfully with 1,1'-dimethylferrocene as the mediator in a glucose sensor. Indeed new glucose sensors using ferrocene and its derivatives are still being reported[38].

Ferrocene derivatives are not the only mediators available. Turner[39] has used tetrathiafulvalene to facilitate electron transfer from the glucose oxidase to a pyrolytic graphite electrode with excellent results. The sensor showed a linear response to glucose over the clinically relevant range ($0 - 2.5 \times 10^{-2}$ mol dm^{-3}), however, the response time was slow (60 s). Another mediator used was benzoquinone. The mediator was held in an α-cyclodextrin polymer film within which the glucose oxidase was attached to the polymer via glutaraldehyde. The mediator is believed to be included within the cyclodextrin cavity[40]. This novel approach produced a glucose sensor which showed a linear response to glucose over the clinically relevant range, and showed little interference from substances such as ascorbic and uric acid.

Much interest has been directed at "wiring" enzymes directly to electrodes since this means the response time of the system may be decreased, and the current drop due to leaching of the mediator or enzyme would be irrelevant. One very interesting sensor employing this technique was described by Heller[41]. The sensor consisted of four layers,

1. The glucose sensing layer.
2. The barrier layer to prevent electrical contact between the sensing layer beneath and the interference-eliminating layer above.
3. The interferent eliminating layer
4. The outer biocompatible layer.

The glucose sensing layer consists of the redox polymer $[(vinylimidazole)Os(bpy)_2Cl]^{+/2+}$, complexed with a genetically engineered glucose oxidase and crosslinked with poly(ethylene glycol) diglycidyl to form an electron-conducting hydrogel. The sensor was designed to measure glucose in the subcutaneous tissue through long term implantation (sensor dimensions 0.125 mm length, 0.25mm diameter). The sensor gave a stable, reproducible and accurate response within 60 s.

Glucose sensors are the most common application of enzyme based voltammetric electrodes due to the excellent properties of glucose oxidase and the high clinical demand for glucose analysis. Other oxidase and oxidoreductase enzymes have been used in sensors. For example, L-lactate oxidase has been immobilised on a platinum electrode to allow the continuous monitoring of lactate in the blood stream or tissue[42].

In clinical analysis the current trend is towards *in vivo* or on-line analysis of specific analytes. This has led to an increased research effort into the miniaturisation of sensor arrays for both potentiometric and voltammetric sensor types. Several approaches have been used. Ion-selective field effect transistors (ISFETs) have always shown the potential to be used in this area, but have suffered from poor encapsulation technology. Recently however this has been improved and 'long term' stability of these sensors has been achieved[43]. Another approach uses thin film technology, where a small flexible sensor can be produced on a polymer backing. This approach has shown itself to be viable for voltammetric enzyme electrodes[44,45].

1.4 Cyclodextrins

Cyclodextrins were first isolated by Villers[46] in 1891 as a degradation product of starch produced by the action of the enzyme glucosyltransferase. They were later characterised as cyclic oligosaccarides in 1904 by Schardinger[47]. Work performed by French[48,49] and others went on to determine the accurate molecular weight of the common cyclodextrins and also to design a route for the synthesis of pure cyclodextrins.

1.4.1 Physical Properties

Cyclodextrins are α-1,4-linked oligosaccarides[50], with a toroidal shape (see figure 1.4.1.2). Each of the chiral glucose units possesses a rigid $^4C_1$ chair conformation (figure 1.4.1.1). The most common cyclodextrins are built up from 6, 7 and 8 glucose units and are known as α-, β-, and γ-cyclodextrins. Table 1.4.1.1 summarises some of the important physical properties of these compounds.

	CYCLODEXTRIN		
	α	β	γ
Number of glucose units	6	7	8
Number of chiral centres	30	35	40
Molecular mass	972.86	1135.01	1297.15
External diameter (pm)	1370-1460	1530-1540	1690-1750
Internal diameter (pm)	470-520	600-650	750-850
Volume of cavity (nm^3)	0.176	0.346	0.510
pK_a of hydroxyl groups		12.1 – 12.6 (all)	
Solubility in water (grams per 100 cm^3, 25°C)	14.50	1.85	23.20
Molarity of saturated solution [M]	0.149	0.016	0.179
Melting and decomposition point (K)	551	572	540

Table 1.4.1.1. Physical properties of cyclodextrins.

The formation of cyclodextrins of fewer than six glucose units is not known. Conformational studies using potential energy calculations performed by Sunderarajan *et al.*[51] showed this to be a consequence of ring strain upon cyclisation. Higher homologues containing up to twelve glucose sub-units have been reported in the literature[52]. These larger macrocyclic ring structures do not form the regular toroidal structure seen in the common 6, 7 and 8 membered cycles due to the absence of the intramolecular hydrogen bonding secondary structure seen in the common cyclodextrins.

As can be seen in figure 1.4.1.2 the preferred C_1 conformation of the glucose units leads to the secondary hydroxyl groups being situated on the wide face and all the primary hydroxyls on the other. The cavity interior is lined by the hydrogen atoms of C(3) and C(5) and the glycosidic oxygen bridges. The consequence of these structural features is the generation of a hydrophobic, Lewis basic, cavity with hydrophilic rims.

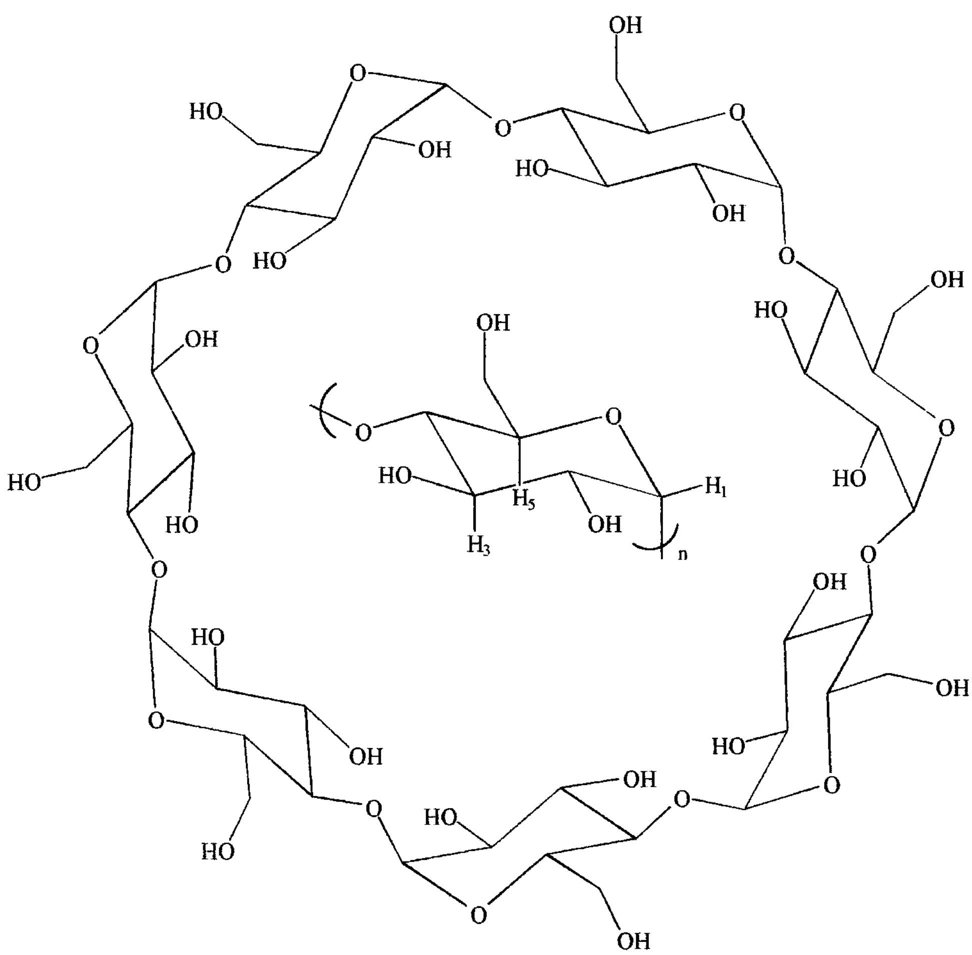

Figure 1.4.1.1. Chemical structure and numbering scheme for β-cyclodextrin.

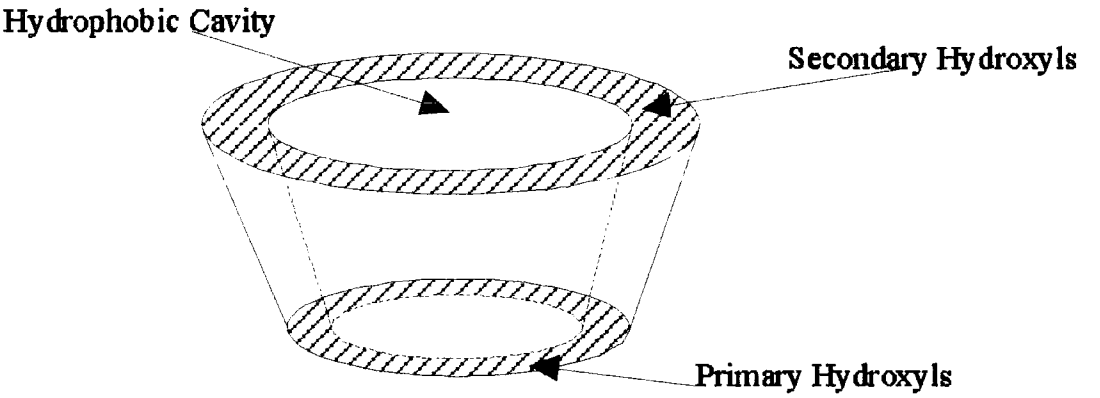

Figure 1.4.1.2. Functional scheme of the cyclodextrin torus.

1.4.2 Intramolecular Hydrogen-bonding

A major feature of cyclodextrin structure relates to their ability to form intramolecular hydrogen bonds. As depicted in figure 1.4.2.1, the C(2) hydroxyl group of one glucose sub-unit can act as a hydrogen bond acceptor for the C(3) OH group of an adjacent glucose unit[53]. The formation of this series of hydrogen bonds around the secondary face rigidifies the macrocycle[51].

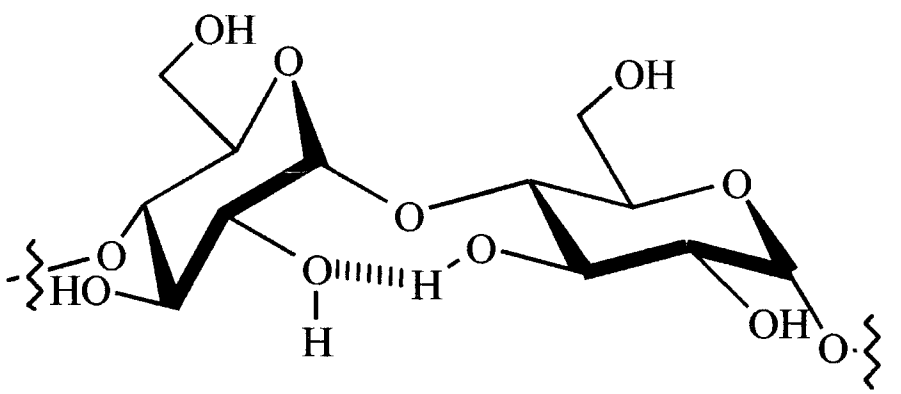

Figure 1.4.2.1. O(2)···HO(3) intramolecular hydrogen bonding in cyclodextrins.

1.4.3 Applications of Cyclodextrins

A wide range of possible guest molecules may be included by cyclodextrins. Due to this, and the fact that complex formation induces changes in the properties of the included substance, cyclodextrins have been used in many different fields of study.

1. Cyclodextrins and their derivatives have been widely employed as the substrate-recognition moieties in artificial enzymes. The cavity of the cyclodextrin acts as a specific discriminating and orientating site. All the reactions catalysed by cyclodextrins proceed via the complexes between them and their substrates, in which a chemical reaction takes place. In most cases, the hydroxyl residues of the cyclodextrin are responsible for the catalytic functions. Large increases in reaction rates have been achieved, since the catalysis occurs intramolecularly in the cyclodextrin-substrate complex[54,55].
2. The capability for changing the physicochemical behaviour of the guest molecule through complexation has received considerable pharmaceutical interest[56,57]. Indeed the advantages of this are numerous and include, the alteration of the drug release rate and solubilisation of sparingly water soluble compounds leading to the increase in the drugs bioavailability. Furthermore, the chemical and photochemical stability of the drugs in their preparation are improved[58] due to the reduction in the rates of hydrolysis and photo decomposition[59].
3. As is discussed in more detail in section 1.7.1, alkylated cyclodextrins are used in HPLC and GLC as both stationary and mobile phases to facilitate enantiodiscrimination[60].
4. In capillary zone electrophoresis (CZE) cyclodextrins are being added as a chiral agent to the background electrolyte to allow the separation of enantiomers[61,62].
5. Derivatised cyclodextrins have also been used in sensors, both fluorescent and electrochemical. The fluorescent sensor relies on the attachment of a chromophore to the cyclodextrin ring. These chromophore-modified cyclodextrins show a change in fluorescence and absorption intensities upon complexation of a guest molecule. Ueno *et al* has designed several systems, one of which had a p-dimethylaminobenzyl moiety attached to an α-cyclodextrin, and was used for the detection of aliphatic alcohols such as n-pentanol[63]. Another system used

N-dansyl-L-leucine as a pendent arm to modify both β- and γ-cyclodextrins. These modified cyclodextrins were used as fluorescent indicators for a series of steroidal compounds[64]. As potentiometric sensors the cyclodextrins were rendered lipophilic by alkylation of either two or three of the hydroxyls groups on each monomer unit. This allowed the cyclodextrins to be used in both ion-selective electrodes[65] and on modified screen printed electrodes[66].

6. Cyclodextrins have also been used as chiral solvating agents (CSA) allowing the determination of enantiomeric purity by NMR[67].

1.5 Cyclodextrin Inclusion Complexes

The most characteristic property of cyclodextrins is their ability to form 1:1 or 2:1 inclusion complexes with a variety of guest molecules, including organic or inorganic compounds of a neutral or ionic nature[60]. Cyclodextrins are capable of forming inclusion complexes with molecules of a size that is compatible with the dimensions of the cavity. It is this geometric factor, rather than chemical factors, which dictates whether a guest molecule will be included in the cyclodextrin cavity[68]. Figure 1.5.1 shows a representation of cyclodextrin inclusion complex formation with p-xylene.

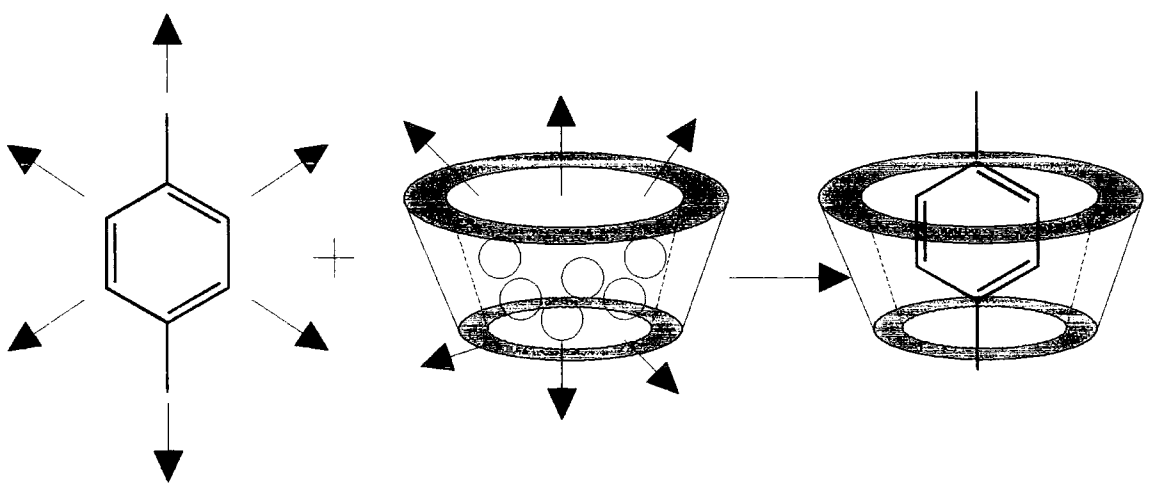

Figure 1.5.1. Schematic illustration of inclusion complexation of p-xylene by a cyclodextrin. The small circles represent the water molecules included in the cyclodextrin cavity.

The inclusion complexes of cyclodextrins with aromatics and various other guest molecules have been widely studied using a variety of techniques such as UV/VIS[57], induced circular dichroism[69], NMR[70] and electrochemical[71] methods.

1.5.1 Factors Contributing to the Free Energy of Binding

The inclusion of a guest molecule into a cyclodextrin cavity involves the substitution of the included water molecules by the less polar guest. This process is an energetically favoured interaction of the relatively nonpolar guest molecule with an imperfectly solvated hydrophobic cavity, and both entropy and enthalpy changes play important roles[72]. The 'driving force' for complexation involves the contribution of various effects whose role depends upon the particular combination of guest and host cyclodextrin. These effects are;

i. substitution of the energetically unfavourable polar-apolar interactions between the included water and the cyclodextrin cavity, and between water and the guest, by the more favoured apolar-apolar interaction between the guest and the cavity, and the polar-polar interaction between bulk water and the released cavity-water molecules
ii. cyclodextrin-ring strain release on complexation
iii. van der Waals interactions
iv. in the case of some guests, hydrogen-bonding between hosts and guest.

Water substitution by a guest molecule of appropriate size, shape and polarity appears universal. Water molecules within the cyclodextrin cavity are incapable of satisfying their tetrahedral hydrogen-bonding capacity unlike those molecules in the bulk. Therefore, those included water molecules may be regarded as being of relatively high energy. The expulsion of these water molecules therefore favours complex formation by a gain in entropy[73] and a favourable change in enthalpy from good hydrogen-bonding of the displaced water to bulk water. The cavity of cyclodextrins larger than γ are so wide that their included water molecules show properties resembling bulk water, consequently the driving force of complexation decreases making these large cyclodextrins slightly weaker complexing agents.

Van der Waals, hydrophobic interactions and hydrogen-bonding all contribute to the favourable enthalpy change upon complexation. Van der Waals forces generally originate from dipole-dipole interactions and are weak. Their energy is proportional to molecular polarisability, which in turn is proportional to molecular refraction. There is a linear correlation between molecular refraction and the dissociation constant of cyclodextrin complexes, implying that van der Waals forces are a major contributor to complexation[73].

The release of ring strain upon complexation is only significant in the case of α-cyclodextrin. This is because the structure of α-cyclodextrin hydrate is distorted due to the existence of two possible intramolecular hydrogen-bonds between adjacent glucose units being open, allowing the inward rotation of one of the glucose units. However, the intramolecular hydrogen-bonds between the C-2 hydroxyl group of one glucose unit and the C-3 hydroxyl (acting as the proton donor) of an adjacent glucose unit are all formed in both β- and γ-cyclodextrins giving them 7 and 8 intramolecular hydrogen bonds respectively.

1.6 Alkylated Cyclodextrins

The selective derivatisation of cyclodextrin molecules has become an active area of research[60,74], spurred on by the need to alter the inclusion ability and solubility characteristics of the native cyclodextrin. One branch of this research led to alkylated cyclodextrins[75].

1.6.1 Inclusion complexes of alkylated cyclodextrin

The inherent chirality of cyclodextrin molecules allows them to form diastereomeric complexes following inclusion of a chiral guest. This led in turn to attempts to use cyclodextrins as reagents for chiral resolution since the diastereoisomers possess different free energy values which may aid the separation of the pair of enantiomers. This has been investigated in two different approaches: the use of cyclodextrins in chiral stationary phases and as highly soluble modified cyclodextrins as mobile phase additives. As stationary phases, the native cyclodextrins often showed poor

resolution[69], possibly due to the rigid symmetry of the cavity. This led to the investigation of functionalised cyclodextrins in which the hydroxyl groups were acylated or alkylated. The benefits of functionalisation included an increase in the lipophilicity of the cyclodextrins, making them suitable for use in chromatographic applications and in solvent polymer membranes. In addition functionalisation led to a distortion of the cavity by removal of some of the intramolecular hydrogen bonds. It was hoped that the distortion of the cavity would led to greater enantioselectivity and to some extent this has been born out by experimental results[76]. The interruption of the intramolecular hydrogen bonding leads to a more flexible structure which then allows greater chiral discrimination. This reduction in the pre-organisation of the host allows closer host-guest interactions. Recent molecular modelling studies on the complexes of α-pinene with permethylated α- and β-cyclodextrins performed by Black *et al.*[77] showed that changes in the host cyclodextrin structure did occur, allowing a better accommodation or 'induced fit' of the guest molecule.

1.6.2 Chiral recognition through induced fit

Alkylated cyclodextrins have been used as the host molecule in a wide variety of applications which require the separation of enantiomers. Without the hydrogen bonding to rigidly define the structure, the molecules are more flexible.. Good examples of this are seen in the complex between per-O-methyl-α-cyclodextrin and mandelic acid[78] and in the complex of 2-chloropropionate with 3-acetyl-2,6-dipentyl-β-cyclodextrin[79]. It was noted that in the presence of (R)-mandelate, the cyclodextrin cavity was substantially less symmetrical (and somewhat elliptical in nature) compared to the complex with the (S)-enantiomer. Another difference, and probably the most important in determining the enantiomer selectivity, is the orientation of the mandelate aromatic ring within the cavity. With the (S)-enantiomer the ring is parallel to the z-axis of the cavity, whereas in the case of the (R)-enantiomer the phenyl ring is inclined by approximately 20^0 to the z-axis within the cavity. The inclination allows the formation of hydrogen bonds between the carboxylic acid group and the host. The cyclodextrin host derivative is therefore capable of recognising the chirality of the guest mandelic acid.

1.7 Applications of lipophilic cyclodextrins

The improved ability of modified cyclodextrins to discriminate between enantiomers, and their enhanced lipophilicity, has led to their application in a wide variety of analytical techniques[60,80].

1.7.1 Chromatography

The use of cyclodextrins in many branches of chromatography has proved to be successful. In liquid chromatography modified cyclodextrin bonded stationary phases have been demonstrated to be effective at separating enantiomers. Also highly soluble modified cyclodextrins have been used as mobile phase additives in reverse phase HPLC systems. In gas chromatography both immobilised cyclodextrins, their derivatives and cyclodextrin polymers have been used as stationary phases. Alkylated cyclodextrins have played a major role in this area of separation[81,82], indeed they have acted as enantioselective hosts for the separation of alkene enantiomers [77,83] (figure 1.7.1.1).

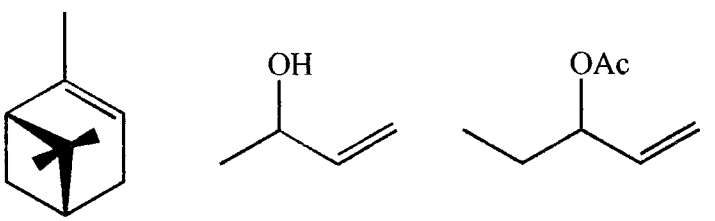

Figure 1.7.1.1 Enantiomeric alkenes studied.

Cyclodextrins have also become increasingly used in capillary zone electrophoresis, either as an additive to the stationary phase[84], or as part of the stationary phase. Guttman *et al* incorporated the cyclodextrin into a polyacryamide gel and this system showed an excellent separation of dansylated aminoacids. The ability to separate enantiomers was also demonstrated when the aqueous-soluble cyclodextrin 2,6 dimethyl-β-cyclodextrin was added to the electrolyte background[61,62] of a CZE experiment.

1.7.2 Cyclodextrins in Electrochemical devices

The lipophilicity of alkylated cyclodextrins allows them to be included in ion-selective electrode membranes. Bates and coworkers[85] used 'poly'octyl-α-cyclodextrin as an ionophore in a sensor for ephedrine. The results showed, unsurprisingly, a difference in response of the electrode to the two enantiomers, with the (+) enantiomer being bound preferentially, and showing improved slopes and limits of detection. Cyclodextrins have also been used in voltammetric experiments, notably in the sub-picomolar detection of acetylcholine by Kataky[66]. Most other studies using cyclodextrins in this area have been involved in the investigation of their inclusion complexes, and the effect these complexes have upon the electrochemical characteristics of the included analyte[86].

1.8 Investigation of Molecular Recognition by Cyclodextrins

Cyclodextrins are capable of differentiating between structurally related and enantiomeric species. To investigate this phenomenon the techniques of mass spectrometry and nuclear magnetic resonance spectroscopy have been widely used.

1.8.1 Mass Spectrometry

The development within the last decade of several new ionisation techniques and inlet systems has led to an increased number of applications of mass spectrometry. These new 'soft' ionisation techniques include electrospray (ES), fast atom bombardment (FAB), plasmaspray (PS) and thermospray (TSP). These developments have allowed mass spectrometry to be applied to high molecular weight, involatile macromolecules such as proteins, enzymes and, of particular interest here, to cyclodextrins. These soft methods permit ionisation without high temperatures or high field gradient[87], allowing the ionisation of involatile molecules without immediate fragmentation. Hence detection of the molecular ion may be undertaken.

Electrospray soft ionisation technique has been used widely. Here the soft ionisation is explained by an ion evaporation mechanism. The sample is sprayed using the high

electric field between the capillary and the counter electrode to produce highly charged droplets. Desolvation of these droplets either by the drying gas or heat reduces their size. At a certain critical size, the repulsion between the charged entities in the droplet exceeds the surface tension and ions are emitted. This technique has been used successfully for cyclodextrin complexes, for example in characterising the 1:1 complexes of 2-hydroxypropyl-β-cyclodextrin[88] with the enantiomers of phenylalanine methyl ester, propranolol and tryptophan methyl ester. It has also been applied in the investigation of the interactions between 2,6 diethanolamine-β-cyclodextrin and the drugs glybenclamide and furosemide[89].

1.8.2 Nuclear Magnetic Resonance

The majority of cyclodextrin applications require the formation of a complex in solution. The application of NMR techniques to the investigation of complexation with cyclodextrins and their derivatives is central to the understanding of these structures and the dynamics of complexation[90].

In 1970 Demarco and Thakkar[91] demonstrated that the aromatic moiety of a guest molecule was included within the cyclodextrin cavity. It was observed that the protons located on the inner face of the cyclodextrin cavity, H(3) and H(5), were subject to anisotropic shielding by the aromatic ring, shifting the resonances to higher frequency. The exterior protons were unaffected.

The advent of Fourier transform NMR and the development of reliable superconducting magnets allowed more detailed investigations to be performed. The full assignment of per-O-methyl-β-cyclodextrin using 2D correlation techniques was published in 1983[92]. This led to the study of cyclodextrin complexes in the attempt to track down the important host-guest interactions which led to recognition. Perly and Djedaini[70] applied a variety of high resolution NMR techniques to the investigation of the complexes of steroids with β-cyclodextrins. They showed categorically that β-cyclodextrins formed true inclusion complexes with steroids such as prednisolane because only the chemical shifts of protons located in the hydrophobic cavity were affected by complexation. Indeed the study went on to show that the inclusion

stoichiometries and binding constants could be fully rationalised by considering the nature and position of substituents on the steroidal skeleton.

Research by Li and Purdy[93] showed that the substitution pattern on an aromatic moiety included within the cavity dictates the guest orientation within the cavity. The complexes of ephedrine with α-, β-cyclodextrins and their derivatives have been studied in an effort to ascertain the effect of varying the cavity size and alkylation pattern[77,86] as well as allowing the determination of the binding constants. The investigations showed, as expected, that the aromatic moiety was included within the hydrophobic cavity, and that any enantiomer discrimination observed was due to the relative orientation of the chiral side chain in relation to the secondary hydroxyl rim. This leads to discrimination as only one enantiomer is able to form stabilising hydrogen bonds to the peripheral hydroxyls of the host.

1.9 References

1. Morf W. E., The principles of ion-selective electrodes and membrane transport, vol. 2, Elsevier, Oxford, 1981
2. Sutherland I. O., *Chem. Soc. Rev.*, 1986, **15**, 63-91
3. Cram D. J., *Angew. Chem. Int. Ed. Engl.*, 1988, **27**, 1009-1020
4. Obasjima K., *Yakugaku Zasshi*, 1995, **115**(6), 431-445
5. Spichiger U. E., Freiner D., Bakker E., Rosatzin T., Simon W., *Sensors & Actuators B*, 1993, **11**, 263-271
6. Odashima K., Naganawa R., Radecka H., Kataoka M., Kimura E., Koike T., Tohda K., Tange M., Furuta H., Sessler J. L., Yagi K., Umezawa Y., *Supramol. Chem.*, 1994, **4**(2), 101-113
7. Peacock S. C., Cram D. J., *J. Chem. Soc., Chem. Commun.*, 1976, 282-284
8. Bussmann W., Lehn J-M., Oesch U., Plumere P., Simon W., *Helv. Chim. Acta*, 1981, **64**, 657-661
9. Yim H-S., Kibbert C. E., Ma S-C., Kliza D. M., Lin D., Park S-B., Torre C. E., Meyerhoff M. E., *Biosensors & Bioelectron.*, 1993, **8**, 1-38
10. Guidelines for Providing Quality Stat Laboratory Services, AACC Press, 1987
11. Kauffmann J-M., Vire J-C., *Anal. Chim. Acta*, 1993, **273**, 329-334
12. Wang J., *Anal. Chem.*, 1995, **67**(12), 487R-492R
13. Pungor E., Feher Zs., Nagy G., Linder E., Toth K., *Anal. Proc.*, 1982, 79-82
14. ed. Thomas J. D. R., Membrane Electrodes in Drug-Substances Analysis, Cosofret V. V., Pergamon Press, 1982
15. Bakker E., Meruva R. K., Pretsch E., Meyerhoff M. E., *Anal. Chem.*, 1994, **66**, 3021-3030
16. Faulkner S., Kataky R., Parker D., Teasdale A., *J. Chem. Soc., Perkin Trans. 2*, 1995, 1761-1769
17. Bergveld P., *Sensors & Actuators A*, 1996, **56**, 65-73
18. Galan-Vidal C. A., Munoz J., Dominguez C., Alegrat S., *Trend Anal. Chem.*, 1995, **14**(5), 225-231
19. Pinkerton T. C., Lawson B. L., *Clin. Chem.*, 1982, **28**(9), 1946-1955
20. Durselen L. F. J., Wegmann D., May K., Oesch U., Simon W., *Anal. Chem.*, 1988, **60**, 1455-1458

21. Covington A. K., Kataky R., *J. Chem. Soc., Faraday Trans.*, 1993, **89**(2), 369-376
22. Maas B., Sprokholt R., Maas A., Fogh-Anderson N., *Scand. J. Clin. Lab. Invest.*, 1996, **56**, suppl 224, 179-186
23. Ikada Y., *Biomaterials*, 1994, **15**(10), 725-744
24. [24] Cosofret V. V., Erdosy M., Anderson J. M., *Anal. Lett.*, 1994, **27**(15), 3039-3063
25. Park B. S., Chung S., Cha G. S., Kim H. D., *Bull. Koren Chem. Soc.*, 1995, **16**(11), 1033-1036
26. Linder E., Cosofret V. V., Ufer S., Buck R. P., Kao W. I., Neuman M. R., Anderson J. M., *J. Biomed. Mat. Res.*, 1994, **28**, 591-601
27. D'Orazio P., Bowers Jr. G. N., *Clin. Chem.*, 1992, **38**(7), 1332-1339
28. Szycher M., Reed A. M., Siciliano A. A., J. *Biomater. Appl.*, 1988, **3**(2), 297-402
29. Espadas-Torre C., Oklejas V., Mowery K., Meyerhoff M. E., *J. Am. Chem. Soc.*, 1997, **119**, 2321-2322
30. Elliott C. M., Muray R. W., *Anal. Chem.*, 1976, **48**(8), 1247-1254
31. Arrigan D. W. M., Svehla G., Harris S. J., McKervey M. A., *Electroanalysis*, 1994, **6**, 97-1056
32. Chaney Jr. E. N., Baldwin R. P., *Anal. Chem.*, 1982, **54**, 2556-2560
33. Boyd D., Rodriguez J. R. B., Ordieres A. J. M., Blanco P. T., Smyth M. R., *Analyst*, 1994, **119**, 1979-1984
34. Kauffman J. M., Guilbault C. G., Enzyme Electrode Biosensors: Theory and Applications, Bioanalytical Applications of Enzymes, vol. 36, John Wiley & Sons Inc., London, 1992
35. Scheller F. W., Schubert F., Renneberg R., Muller H-G., Janchen M., Weise H., *Biosensors*, 1995, **1**, 135-160
36. Gorton L., *Electroanalysis*, 1995, **7**(1), 24-45
37. Cass A. E. G., Davis G., Francis G. D., Hill A. O., Aston W. J., Higgins I. J., Piotkin E. V., Scott L. D. L., Turner A. P. F., *Anal. Chem.*, 1984, **56**, 667-671
38. Nishida K., Sakakida M., Ichinose K., Uemur A., Uehara M., Kajiwara K., Miyata T., Shichiri M., Ishihara K., Nakabayashi N., *Med. Progress Tech.*, 1995, **21**, 91-103
39. Turner A. P. F., Hendry S. P., Cardosi M. F., *Biotech '87*, **1**(3), 125-137
40. Kutner W., Wu H., Kadish K. M., *Electroanalysis*, 1994, **6**, 934-944
41. Csoregi E., Quinn C. P., Schmidtke D. W., Lindquist S-E., Pishko M. V., Ye L., Katakis I., Hubbell J. A., Heller A., *Anal. Chem.*, 1994, **66**, 3131-3138

42. Baker D. A., Gough D. A., *Anal. Chem.*, 1995, **67**, 1536-1540
43. Reinhoudt D. N., *Sensors & Actuators B*, 1995, **24-25**, 197-200
44. Urban G., Jobs T., Keplinger F., Ashaher E., Tilado O., Fasching R., Kohl F., *Biosensors & Bioelectron.*, 1992, **7**, 733-739
45. Borchart M., Dumschat C., Camman K., Knoll M., *Sensors & Actuators B*, 1995, **24-25**, 721-723
46. Villers A., *Compt. Rend. Acad. Sci. (Paris)*, 1891, **112**, 536-539
47. Schardinger F., *Wein. Klin. Wochenschi*, 1904, **17**, 207-210
48. French D., Rundle R. E., *J. Am. Chem. Soc.*, 1942, **64**, 1651-1653
49. French D., Levine M. L., Pazur J. H., Norberg E., *J. Am. Chem. Soc.*, 1949, **71**, 353-356
50. Bender H., *Carbohydr. Res.*, 1978, **65**, 85-97
51. Sundararajan P. R., Rao V. S. R., *Carbohydr. Res.*, 1970, **13**, 351-358
52. Pulley A. O., French D., *Biochem. Biophys. Res. Commun.*, 1961, **5**, 11-15
53. Steiner T., Saenger W., *J. Am. Chem. Soc.*, 1992, **114**, 10146-10154
54. Saenger W., *Angew. Chem. Int. Ed. Engl.*, 1980, **19**, 344-362
55. ed. Szeitli J., Isa T., Cyclodextrins in Comprehensive Supramolecular Chemistry, ed. Atwood J. L., MacNicol J. E. D., Voglte F., vol. 3, chapter 12, Pergamon, Oxford, 1996
56. Valsami C. N., Macheras P. E., Koupparis M. A., *J. Pharm. Sci.*, 1990, **79**(12), 1087-1094
57. Chowdhury M., Basu R., *Ind. J. Chem.*, 1996, **35A**, 901-902
58. Brewster M. E., Horia M. S., Simpkins J. W., Bodor N., *Pharm. Res.*, 1991, **8**(6), 792-795
59. ed. Szeitli J., Isa T., Cyclodextrins in Comprehensive Supramolecular Chemistry, ed. Atwood J. L., MacNicol J. E. D., Voglte F., vol. 3, chapter 14, Pergamon, Oxford, 1996
60. Li S., Purdy W. C., *Chem. Rev.*, 1992, **92**, 1457-1470
61. Fanali S., Chrom., 1989, 21, 441-446
62. Nishi H., Kowusenya Y., Miyamoto T., Sato T., *J. Chromatogr.*, 1994, **659**, 449-457
63. Hamasaki K., Ueno A., Toda F., *J. Chem. Soc., Chem. Commun.*, 1993, 331-333

64. Ikeda H., Nakamura M., Ise N., Oguma N., Nakamura A., Ikeda T., Toda F., Ueno A., *J. Am. Chem. Soc.*, 1996, **118**, 10980-10988

65. Parker D., Kataky R., Kelly P. M., Palmer S., *Pure & Appl. Chem.*, 1996, **68**(6), 1219-1223

66. Kataky R., Parker D., *Analyst*, 1996, **121**, 1829-1834

67. Uccello-Barretta G., Balzano F., Caporusso A. M., Iodice A., Salvadori P., *J. Org. Chem.*, 1995, **60**, 2227-2231

68. Alvira E., *Chem. Phys. Lett.*, 1997, **267**, 221-228

69. Mularz E. A., Cline-Love L. J., Petersheim M., *Anal. Chem.*, 1988, **60**, 2751-2755

70. Djedaini F., Perly B., *J. Pharm. Sci.*, 1991, **80**(12), 1147-1161

71. Godinez L. A., Lin J., Munoz M. M., Coleman A. W., Kaifer A. E., *Electroanalysis*, 1996, **8**(11), 1072-1074

72. Lewis E. A., Hansen L. D., *J. Chem. Soc., Perkin Trans. 2*, 1973, **2**, 2081-2085

73. Van Elten R. L., Clowes G. A., Sabastian J. F., Bender M. L., *J. Am. Chem. Soc.*, 1967, **89**, 3253-3262

74. ed. Szeitli J., Isa T., Cyclodextrins in Comprehensive Supramolecular Chemistry, ed. Atwood J. L., MacNicol J. E. D., Voglte F., vol. 3, chapter 4, Pergamon, Oxford, 1996

75. Croft A. P., Bartsch R. A., *Tetrahedron*, 1983, **39**(9), 1417-1474

76. Holzgrabe U., Mallwitz H., Branch S. K., Jefferies T. M., Wiese M., *Chirality*, 1997, **9**, 211-219

77. Black D. R., Parker C. G., Zimmerman S. S., Lee M. L., *J. Comput. Chem.*, 1996, **17**(8), 931-939

78. Harata K., Uekama K., Otagiri M., Hirayama F., *Bull. Chem. Soc. Jpn.*, 1987, **60**, 497-502

79. Kohler J. E. H., Hohla M., Richters M., Konig W. A., *Chem. Ber.*, 1994, **127**, 119-126

80. Szejlti J., *Supramol. Chem.*, 1995, **6**, 217-223

81. Konig W. A., Lutz S., Hagen M., Krebber R., Wenz G., Baldenius K., Ehlers J., Dieck H. T., *J. High Res. Chromatogr.*, 1989, **12**, 35-39

82. Konig W. A., Krebber R., Wenz G., *J. High Res. Chromatogr.*, 1989, **12**, 641-644

83. Lipkowitz K. B., Pearl G., Coner B., Peterson M. A., *J. Am. Chem. Soc.*, 1997, **119**, 600-610

84. Guttman A., Paulus A., Cohen S., Grinberg N., Karger B. L., *J. Chrom.*, 1988, **20**, 41-52

85. Bates P. S., Kataky R., Parker D., *J. Chem. Soc., Perkin Trans. 2*, 1994, 669-675

86. Bersier P. M., Beersier J., Klingert B., *Electroanalysis*, 1991, **3**, 443-455

87. Clench M. R., A Comparison of Thermospray, Plasmaspray, Electrospray and Dymanic FAB, V. G. Monographs in Mass Spectrometry, 1992, No. 3

88. Haskins N. J., Saunders M. R., Camilleri P., *Rapid Commun. Mass Spectrom.*, 1994, **8**, 423-426

89. Selva A., Redenti E., Ventura P., Zanol M., Casetta B., *J. Mass Spectrom.*, 1996, **31**, 1364-1370

90. ed. Wilcox C. S., Schneider H. J., Durr H., Frontiers in Supramolecular Organic Chemistry and Photochemistry, V. C. H., Weinheim, 1991

91. Demarco P. V., Thakkar A. L., J. *Chem. Soc., Chem. Commun.*, 1970, 2-4

92. Johnson J. R., Shankland V., Sadler I. H., *Tetrahedron*, 1985, **41**, 3147-3152

93. Li S., Purdy W. C., *Anal. Chem.*, 1992, **64**, 1405-1412

Chapter Two

Detection of Local Anaesthetics

2.1 Introduction

A brief introduction to local anaesthetics is presented (section 2.1.1), followed by the methods that have been used to determine the concentration of local anaesthetics in both clinical samples and drug preparation control (section 2.1.2). Section 2.2 contains the experimental procedure followed. The results for the local anaesthetics studied are presented and discussed in section 2.3.

2.1.1 Local Anaesthetics

Local anaesthetics were first used by the Viennese ophthalmologist Carl Koller when he used cocaine to produce a reversible corneal anaesthesia by dropping cocaine solution into the eye. The use of cocaine as an anaesthetic rapidly spread and within a few years was being used widely. However it was not until 1905 that a less dangerous synthetic substitute, procaine, was discovered[1].

Local anaesthetic molecules consist of an aromatic moiety linked via an ester or amide group to a basic side chain (except benzocaine, which is considered an atypical local anaesthetic, as it has no basic side chain). The molecules are all weak bases with pK_a values in the range 8 – 9 (lidocaine 8.2, bupivacaine 8.1, the exception is benzocaine 2.5) so that they are partially ionized at physiological pH. This fact is important as only the neutral form can pass through the nerve sheath and axon membrane to reach the correct binding site (situated on the inside of the sodium channel) where the protonated form binds. Local anaesthetics in plasma are bound by proteins, to a greater or lesser extent, and α_1-acid glycoprotein is the main protein to which local anaesthetics bind (along with other basic drugs). This means that the total drug concentration in plasma consists of two forms, 'bound' and 'free'. Such behaviour is similar to the problem of 'bound and 'free' calcium measurements, where ion-selective electrodes have proven well suited to measurement of the 'free' cationic fraction.

2.1.1.1 Lidocaine Hydrochloride

Lidocaine hydrochloride was synthesised in 1943 by Lofgren and was first used in 1948 as a local anaesthetic. Lidocaine acts as not only an effective local anaesthetic but also a class 1b antidysrhythmic drug. The normal therapeutic plasma range is 1.0 – 5.0 mg/l (4×10^{-6} to 2×10^{-6} mol dm^{-3}), although in some patients concentrations of up to 8.0 mg/l (2.0×10^{-5} mol dm^{-3}) may be required to prevent ventrical arrhythmias[1].
The most widely used detection technique is HPLC with an UV detector.

2.1.1.2 Bupivacaine Hydrochloride

Bupivacaine hydrochloride is a long acting local anaesthetic and is used for nerve blocks in general, including epidural anesthesia and post-surgical pain relief. It is administered in the range 1.0×10^{-4} to 7.0×10^{-5} mol dm^{-3} depending on the type of nerve block required. The preferred analytical method is GLC with a nitrogen-phosphorus detector[2], with a limit of detection of 1mg/l (3×10^{-6} mol dm^{-3}).

2.1.2 Detection of Local Anaesthetics

There are many methods used for the detection of local anaesthetics and these can be grouped under three main headings, colorimetric, chromatographic (GLC and HPLC) and electrochemical.

2.1.2.1 Colorimetric

This technique requires the local anaesthetic to have an absorption band separated from that produced by any other constituent of the analyte sample. A few colorimetric methods for lidocaine have been reported, and one of the more recent was devised by Crux *et al.*[3] who measured the absorption at 271 nm in illicit drug samples. This method has also been used to determine levels of local anaesthetics in pharmaceutical preparations. Saleh *et al.*[4] described such a method involving the use of haematoxylin reagent in the presence of boric acid to give a red-violet chromogen. The method could

be applied to many types of preparation. However, the assay time was excessive, being in excess of 30 minutes.

2.1.2.2 Gas Liquid Chromatography (GLC)

This method has the sensitivity to monitor a large range of drugs in plasma, provided the drugs are volatile and thermally stable at temperatures up to 200 °C. Whilst many papers have been published on the determination of lidocaine and bupivacaine in plasma, they all require a lengthy centrifuge step to extract the analytes into an organic phase. This adds considerable time to the analysis. A wide variety of detectors have been used in conjunction with the GLC detection of local anaesthetics; flame ionisation[5], nitrogen-phosphorus[6,7] and surface ionisation detection[8,9,10] have all been described in the literature. By using an appropriate detector with a capillary column to provide a high degree of separation, complex mixtures can be separated and individual constituents detected. This high degree of separation allows not only the primary analyte to be detected but also the drug metabolites that may also be pharmacologically active[5]. Whilst this method does provide high detection limits, it is relatively slow.

2.1.2.3 High Performance Liquid Chromatography (HPLC)

As with GLC, a complex mixture of components can be separated based on their individual physiochemical properties, and the individual components then eluted and detected. Nevertheless, any biological sample still requires pre-treatment to remove proteins from the sample as they can accumulate on the separating column and lead to clogging and consequently a decrease in chromatographic performance. Many groups have worked to develop systems where the biological sample could be injected directly. Systems including column switching and specialised packing materials (e.g. the use of restricted access reverse phase material) have been developed. One such material described by Pinkerton[11], contained a glycolpropyl-bonded surface that was nonadsorptive to proteins and a polypeptide phase that would separate the analytes. Yu *et al.*[12] have combined the ideas of column switching and specialised packing to produce a HPLC system for bupivacaine.

The most common type of HPLC method uses reverse-phase separation. This has the advantage relatively of more rapid separation and analysis of the analyte and its metabolites[13] than normal phase separation, due to the weak surface energies of the non-polar support and the polar nature of the mobile phase.

Detection by HPLC of lidocaine, bupivacaine and their metabolites has been described using mainly UV[14,15,16,17], though a voltammetric detector has been used for the detection of lidocaine[18]. Both GLC and HPLC gave similar detection limits of 1μg/ml (3.7×10^{-6} mol dm^{-3}) for lidocaine and 10 ng/ml (3.7×10^{-8} mol dm^{-3}) for bupivacaine, but analysis times are shorter with HLPC.

2.1.2.4 Electrochemical Detection

The use of ISEs as a means of determining levels of clinically relevant analytes has, in principle, several advantages over chromatographic methods. The potential advantages of using ISEs are their ability to monitor selectively and continuously the levels of a particular ion in solution, even whole blood or serum, without the need for a separation step. In addition, they have uses in drug quality control where reliable, quick and accurate methods are required.

Several ISEs for both lidocaine[19,20,21] and bupivacaine[22,23] have been fabricated. All the electrodes produced were based on the ion-pair principle with either lidocaine or bupivacaine complexed to a bulky anion in the membrane phase. To date no neutral ionophore based systems have been studied. All the electrodes produced Nernstian gradients. However very few interference studies were carried out, also no protein interference effects were studied. The lack of such detailed studies can be explained by the authors desire to use these electrode systems for drug preparation control, where the drug normally is in an aqueous sample.

2.2 Experimental

The local anaesthetics used in this study were the hydrochloride salts of lidocaine and bupivacaine;

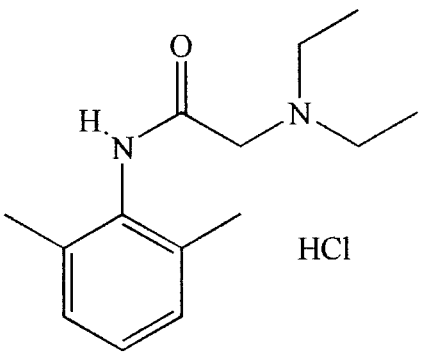

Lidocaine Hydrochloride

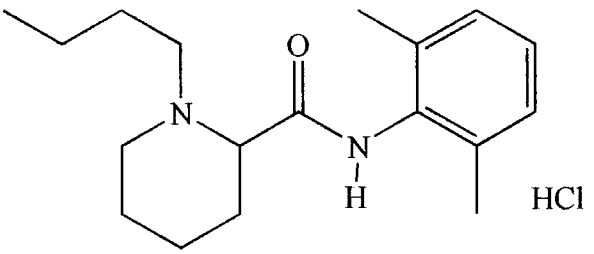

Bupivacaine Hydrochloride

2.2.1 Lidocaine Hydrochloride

2.2.1.1 Potentiometric Calibrations

All measurements were performed using constant volume dilution (section 5.1.2).
The electroactive membranes used were,

1) 2,3,6 Trioctyl-β-cyclodextrin (1.2 %), *o*NPOE (65.6 %), PVC (32.8 %) and TKB (0.4 %)
2) 2,3,6 Trioctyl-β-cyclodextrin (1.2 %), *o*NPOE (65.6 %), Tecoflex SG 80 (32.8 %) and TKB (0.4 %)

The membranes were conditioned in 1 x 10^{-3} mol dm^{-3} lidocaine hydrochloride for 12 h prior to use. The initial solution was 1 x 10^{-1} mol dm^{-3} lidocaine hydrochloride, and the diluent solution was de-ionized water.
Lidocaine hydrochloride was supplied by Sigma (Poole, Dorset, UK).

2.2.1.2 Interference Experiments

All measurements were made using continuous volume dilution, the selectivity coefficients were determined using the fixed interferent method (section 5.1.3). The membranes used were of the same composition as used in the calibration measurements.

The interferents used in this work were glycine, L-histidine, nicotinamide, vitamin B_1, and simulated clinical background consisting of 1.45 x 10^{-1} mol dm^{-3} sodium chloride, 4.3 x 10^{-3} mol dm^{-3} potassium chloride and 1.26 x 10^{-3} mol dm^{-3} calcium chloride.
The initial solutions consisted of 1 x 10^{-1} mol dm^{-3} lidocaine hydrochloride along with the interferent. The interferent solutions were;

1) 'clinical background'
2) 1 x 10^{-2} mol dm^{-3} glycine + 'clinical background'
3) 1 x 10^{-2} mol dm^{-3} nicotinamide hydrochloride + 'clinical background'
4) 1 x 10^{-3} mol dm^{-3} nicotinamide hydrochloride + 'clinical background'
5) 1 x 10^{-2} mol dm^{-3} vitamin B_1 + 'clinical background'
6) 1 x 10^{-2} L-histidine + 'clinical background'

All solutions were prepared using de-ionized water.

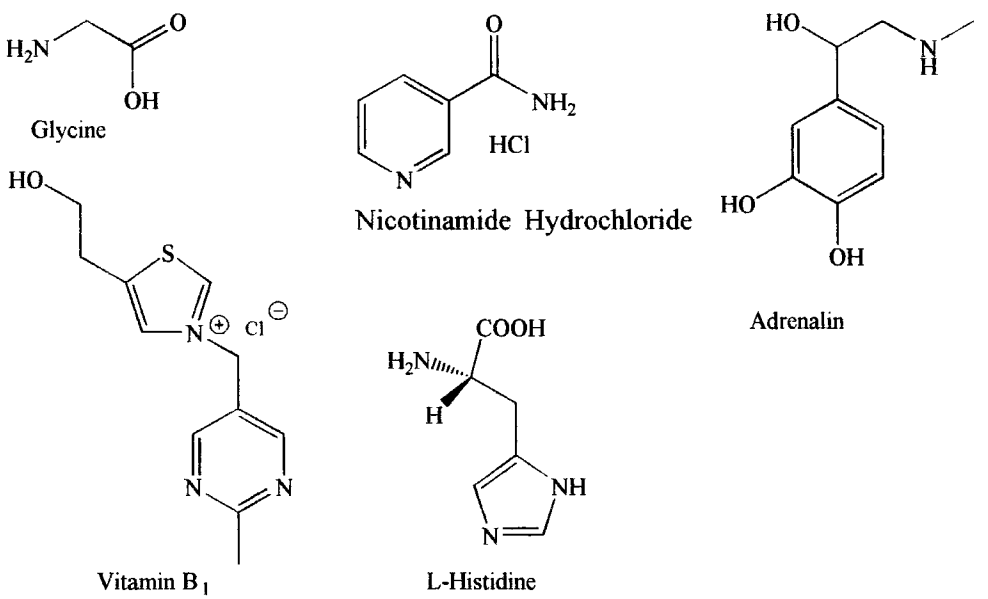

Figure 2.2.1.2. Structures of the organic interferents used in the study.

Sodium chloride, potassium chloride and calcium chloride were of analytical grade obtained from Merck (Poole, Dorset, UK). Glycine and L-histidine were obtained from Sigma (Poole, Dorset, UK), Vitamin B_1 and nicotinamide hydrochloride were obtained from Fluka (Buchs, Switzerland).

2.2.1.3 Protein Interference Dip Test

The membranes used were;

1) 2,3,6 Trioctyl-β-cyclodextrin (1.2 %), PVC (32.8 %), *o*NPOE (65.6 %), TKB (0.4 %).
2) 2,3,6 Trioctyl-β-cyclodextrin (1.2 %), TECOFLEX SG 80 (32.8 %), *o*NPOE (65.6 %), TKB (0.4 %).

The membranes were mounted as described later. The membrane was conditioned in a solution of 1 x 10^{-3} mol dm^{-3} lidocaine hydrochloride and 'clinical background'.
The experiment was carried out as described in section 5.1.5

2.2.1.4 Flow Injection Analysis

2.2.1.4.1 Calibration Experiments

The membranes used in this section of the work were;

1) 2,6 Didodecyl-β-cyclodextrin (1.2 %), *o*NPOE (65.6 %), PVC (32.8 %), and KTClPB (0.4 %)
2) 2,6 Didodecyl-β-cyclodextrin (1.2 %), DOS (65.6 %), Tecoflex SG 80 (32.8 %), and KTClPB (0.4 %)

The di-substituted cyclodextrin was used because results obtained by Dr. Ritu Kataky had shown that this ionophore led to better electrode response characteristics. The electrodes were conditioned in 1 x 10^{-3} mol dm^{-3} lidocaine hydrochloride for 12 h prior to use.

The equipment was set-up as described in section 5.1.4. The carrier solution was 1 x 10^{-3} mol dm^{-3} lidocaine hydrochloride with 1 x 10^{-1} mol dm^{-3} sodium chloride.
The analyte samples were prepared in half decade intervals by serial dilution.
All solutions were made-up using de-ionized water.

2.2.1.4.2 Protein Interference Experiments

Bovine Serum Albumin (BSA)

The membranes, carrier solution and reference solution used were the same as in the calibration experiments (section 2.2.1.4.1).

The analyte sample solutions were prepared in the concentration range 1 x 10^{-1} mol dm^{-3} to 1 x 10^{-6} mol dm^{-3} in half decade intervals by serial dilution. Each sample contained a background of 1 x 10^{-1} mol dm^{-3} sodium chloride and 40 g/l BSA (supplied by Sigma, Poole, Dorset, UK).

α_1-acid glycoprotein (AAG)

The membrane used in this study was 2,6 didodecyl-β-cyclodextrin (1.2 %), Tecoflex SG 80 (32.8 %), DOS (65.6 %), KTClPB (0.4 %).

The carrier and the reference solution were the same as in the calibration. The analyte sample solutions were prepared in the concentration range 1 x 10^{-1} mol dm^{-3} to 1 x 10^{-6} mol dm^{-3} in half decade intervals by serial dilution. Each sample contained a background of 1 x 10^{-1} mol dm^{-3} sodium chloride and 0.55 g/l AAG (supplied by Sigma, Poole, Dorset, UK).

Human Serum

Blood was taken from willing subjects at Dryburn Hospital (Durham); this was then centrifuged leaving serum. No anti-coagulants were added to the serum, as the serum was used within 12 h of the blood being taken.

The membrane used was 2,6 didodecyl-β-cyclodextrin (1.2 %), Tecoflex SG 80 (32.8 %), DOS (65.6 %), KTClPB (0.4 %).

A series of spiked human serum samples were made up by serial dilution these were, 1×10^{-2}, 5×10^{-3}, 1×10^{-4}, 1×10^{-5}, 1×10^{-6}, 5×10^{-6} and 1×10^{-7} mol dm^{-3}. The carrier solution used was 1×10^{-3} mol dm^{-3} lidocaine hydrochloride with a simulated 'clinical background' (1.45×10^{-1} mol dm^{-3} NaCl, 4.3×10^{-3} mol dm^{-3} KCl and 1.26×10^{-3} mol dm^{-3} $CaCl_2$). Before the human serum samples were used a reference curve was produced (between 1×10^{-1} and 1×10^{-6} mol dm^{-3}) where the lidocaine samples contained the 'clinical background'. The human serum samples were injected into the system with no washing between injections to remove any adsorbed protein.

To observe the effects of cleaning the membrane between serum injections two experiments were performed on the 1×10^{-2} mol dm^{-3} lidocaine hydrochloride/human serum sample;

1) Injection of the serum samples with no attempt to wash between injections.
2) Between analyte injections, a Pepsin solution (5 % pepsin in 0.1×10^{-1} mol dm^{-3} Hydrochloric acid) was injected through the sample loop and into the detector cell.

2.2.2 Bupivacaine Hydrochloride

2.2.2.1 Potentiometric Calibrations

All measurements were performed using constant volume dilution.
The electroactive membranes used were;

1) 2,3,6 Trioctyl-β-cyclodextrin (1.2 %), *o*NPOE (65.6 %), PVC (32.8 %) and TKB (0.4 %)
2) 2,3,6 Trioctyl-β-cyclodextrin (1.2 %), *o*NPOE (65.6 %), Tecoflex SG 80 (32.8 %) and TKB (0.4 %)

The membranes were conditioned in 1 x 10^{-3} mol dm^{-3} bupivacaine hydrochloride for 12 h prior to use. The initial solution was 1 x 10^{-2} mol dm^{-3} bupivacaine hydrochloride, and the diluent solution was de-ionized water.
The bupivacaine hydrochloride was supplied by Sigma (Poole, Dorset, UK).

2.2.2.2 Interference Experiments

All measurements were made using the continuous volume dilution, the selectivity coefficients were determined using the fixed interferent method (section 5.1.3). The membranes used were of the same composition as used in the calibration measurements. The interferents used in this work were glycine, L-histidine, nicotinamide, vitamin B_1, adrenaline, and simulated 'clinical background'. The simulated 'clinical background' consisting of 1.45 x 10^{-1} mol dm^{-3} sodium chloride, 4.3 x 10^{-3} mol dm^{-3} potassium chloride and 1.26 x 10^{-3} mol dm^{-3} calcium chloride.
The initial solutions consisted of 1 x 10^{-2} mol dm^{-3} bupivacaine hydrochloride along with the interferent. The interferent solutions were;

1) 'clinical background'
2) 1 x 10^{-2} mol dm^{-3} glycine + 'clinical background'
3) 1 x 10^{-2} mol dm^{-3} nicotinamide hydrochloride + 'clinical background'
4) 1 x 10^{-3} mol dm^{-3} nicotinamide hydrochloride + 'clinical background'
5) 1 x 10^{-2} mol dm^{-3} vitamin B_1 + 'clinical background'
6) 1 x 10^{-2} L-histidine + 'clinical background'
7) 2.7 x 10^{-2} mol dm^{-3} adrenaline + 'clinical background'

All the solutions were prepared using de-ionized water.
Sodium chloride, potassium chloride and calcium chloride were of analytical grade obtained from Merck (Poole, Dorset, UK). Glycine, L-histidine and adrenaline were obtained from Sigma (Poole, Dorset, UK), Vitamin B_1 and nicotinamide hydrochloride were obtained from Fluka (Buchs, Switzerland).

2.2.2.3 Protein Interference Dip Test

The membranes used were;

3) 2,3,6 Trioctyl-β-cyclodextrin (1.2 %), PVC (32.8 %), *o*NPOE (65.6 %), TKB (0.4 %).
4) 2,3,6 Trioctyl-β-cyclodextrin (1.2 %), TECOFLEX SG 80 (32.8 %), *o*NPOE (65.6 %), TKB (0.4 %).

The membranes were mounted as described earlier. The membrane was conditioned in a solution of 1 x 10^{-3} mol dm^{-3} bupivacaine hydrochloride and 'clinical background'. The experiment was carried out as described in section 5.1.5.

2.3 Results and Discussion

2.3.1 Lidocaine Hydrochloride

2.3.1.1 Potentiometric Calibrations

Initially in order to identify the most suitable functionalized cyclodextrin for use in ion-selective electrodes for this class of compounds, lipophilic α-, β- and γ-cyclodextrins were evaluated as ionophores in potentiometric sensors for procaine hydrochloride. 2,3,6 Trioctyl-α-cyclodextrin gave no response to the ion. 2,6 dioctyl-γ-cyclodextrin showed a sub Nernstian response, with a slope of only 42.5 mV/decade. Use of 2,6 didodecyl-β-cyclodextrin gave rise to only a slightly sub-Nernstian response (slope 50.0 mV/decade), which improved to an ideal Nernstian response in the presence of a simulated 'clinical background' of cations[24].

Following on from this work it was decided to investigate further the response to lidocaine hydrochloride using 2,3,6 trioctyl-β-cyclodextrin as the ionophore.
In addition the effect of using TECOFLEX SG 80 as the membrane matrix instead of PVC was evaluated. Such a study was of direct interest in assessing the suitability of each matrix in the assay of serum samples. In blood or serum samples there are usually problems with protein interference. Polyurethanes (e.g. TECOFLEX) have been used by several research groups in an attempt to reduce the shift in the measured potential due to the non-specific adsorption of proteins on the membrane surface[25,26]. Therefore, it was of interest to study the electrode response when TECOFLEX was used as the matrix in the calibration experiments.

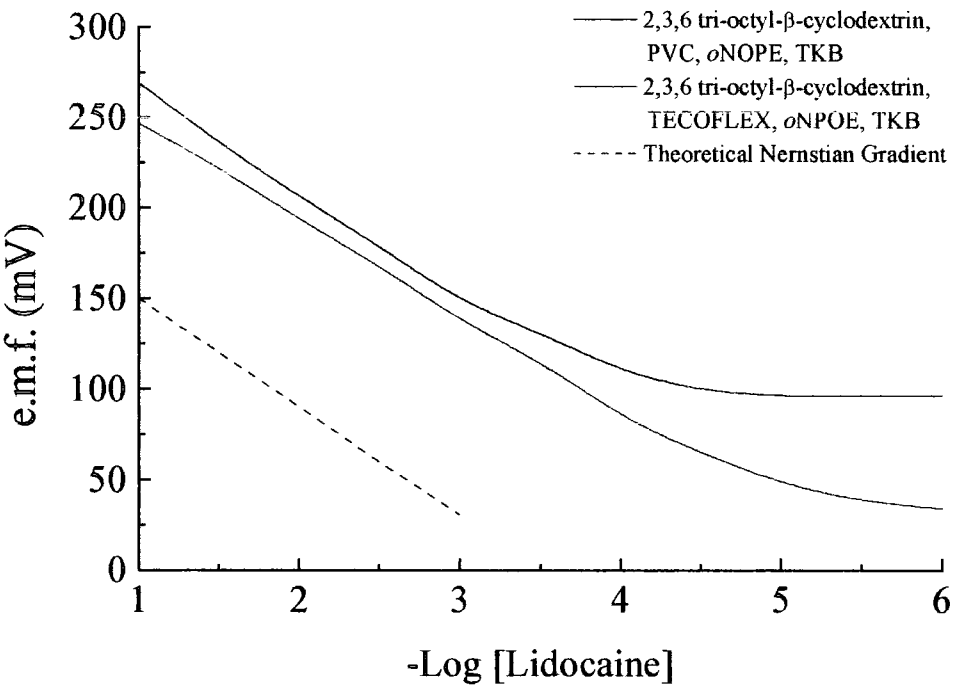

Figure. 2.3.1.1.1 Lidocaine Calibrations using both PVC and TECOFLEX membrane matrices at 298 K.

The results from the calibration in deionized water (Figure 2.3.1.1.1 and Table 2.3.1.1.1) show the response characteristics of the 2,3,6 trioctyl-β-cyclodextrin based electrodes. The results using a PVC matrix showed an excellent Nernstian gradient, while using the TECOFLEX polymer the response was slightly sub-Nernstian at 298 K.

Membrane Matrix	**Gradient (mV/decade)**	**Limit of detection (mol dm^{-3})**
PVC	59.1	1.6×10^{-4}
TECOFLEX SG 80	54.2	8.7×10^{-6}

Table. 2.3.1.1.1. Calibration data. Each membrane contains 2,3,6 trioctyl-β-cyclodextrin, *o*NPOE and TKB.

The results obtained from the calibrations are comparable with those obtained by various other groups[18,19.20.21]. However, as mentioned earlier, these electrodes were all based on an ion-pair membrane system, so that these lipophilic cyclodextrin-based sensors were the first neutral ionophores used for the detection of lidocaine.

2.3.1.2 Potentiometric Interferent Studies

The interference effect of various cationic species found in serum was studied (Figures 2.3.1.2.1 and 2.3.1.2.2). The simulated 'clinical background' contained 1.45 x 10^{-1} mol dm^{-3} NaCl, 4.3 x 10^{-3} mol dm^{-3} KCl and 1.26 x 10^{-3} mol dm^{-3} $CaCl_2$. The concentrations of these ions were chosen to fall within the normal physiological range observed. The other interferents used, glycine (1.46 x 10^{-4} – 3.52 x 10^{-4} mol dm^{-3}), histidine (7.3 x 10^{-5} – 1.25 x 10^{-4} mol dm^{-3}), vitamin B_1 (1.2 x 10^{-8} – 5.9 x 10^{-8} mol dm^{-3}) and nicotinamide (3.3 x 10^{-5} – 7.4 x 10^{-5} mol dm^{-3}) were all chosen to allow comparison between this study and others performed on the same analyte. The physiological ranges for these compounds are given in brackets. The concentration chosen for these interferents was arbitrarily set at 1 x 10^{-2} or 1 x 10^{-3} mol dm^{-3}, depending upon the solubility of the interferent.

In the presence of a simulated 'clinical background' of Na^+, K^+ and Ca^{2+} the responses of both electrodes were Nernstian with good selectivity coefficients ($-\log K_{ij}^{pot}$, overall ~ 3.0), and good limits of detection (-Log [Lidocaine] ≥ 3.3). This is consistent with what is known about cyclodextrins, i.e. that the hydrophobic nature of the cyclodextrin cavity will include the aryl moiety and/or the amine portion of the lidocaine preventing any interference from the hydrophilic alkali and alkaline earth cations[27,28].

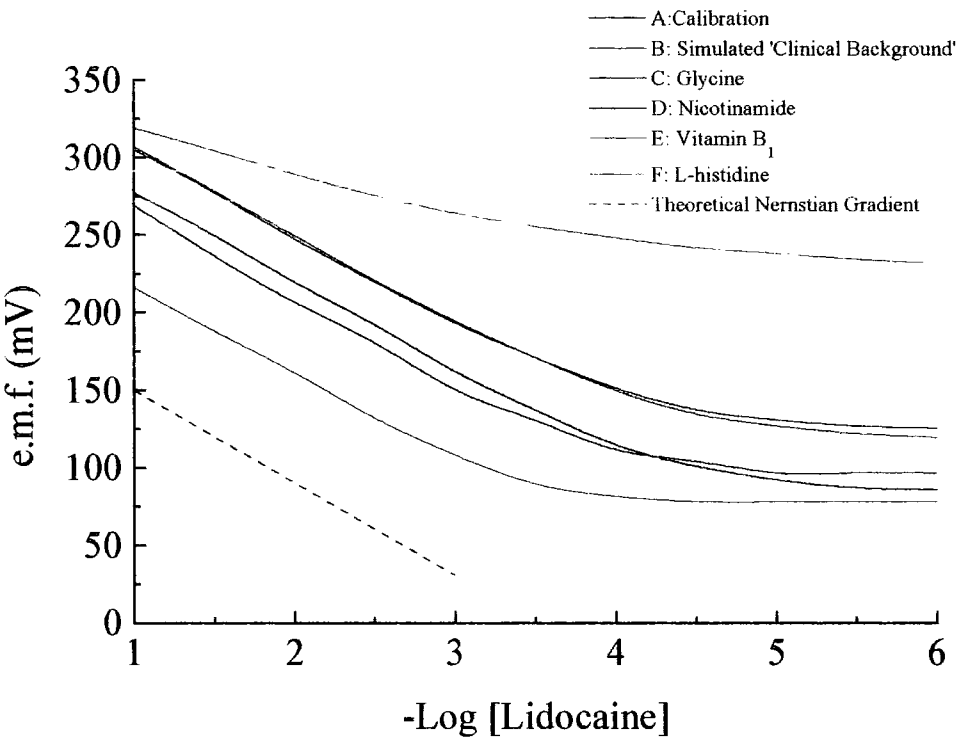

Figure 2.3.1.3.1. Response Curves for Calibration and interferents for the PVC membrane. A: aqueous, B: clinical Interference; C: 1 x 10^{-2} mol dm^{-3} Glycine; D: 1 x 10^{-3} mol dm^{-3} Nicotinamide; E: 1 x 10^{-2} mol dm^{-3} Vitamin B_1; F: 1 x 10^{-2} mol dm^{-3} L-histidine.

Membrane Matrix	Interferent	Gradient (mV/ decade)	Limit of detection (mol dm^{-3})	- Log K_{ij}^{pot}
PVC	'clinical background'	58.0	6.5×10^{-5}	4.0
	Vitamin B_1	56.4	3.6×10^{-4}	2.4
	L-histidine	41.7	9.1×10^{-4}	2.0
TECOFLEX	'clinical background'	55.7	4.8×10^{-4}	2.5
	Vitamin B_1	56.8	7.6×10^{-4}	2.1
	L-histidine	67.4	3.6×10^{-3}	1.4

Table 2.3.1.2.1. Potentiometric results for lidocaine detection in the presence of cationic interferent species.

The interference from various cationic organic species on the electrode response was studied for lidocaine (table 2.3.1.2.1). Selectivity coefficients were calculated for vitamin B_1 and L-histidine. These two molecules have pK_a values of 4.8 and 9.2 (for vitamin B_1), and 2.2, 6.17 and 9.28 (for L-histidine) and hence are ionic at the physiological pH (pH 7.4) and at the pH of the analyte solutions pH ~ 6.0). For the other organic interferents used i.e. glycine, nicotinamide and adrenaline (relevant pK_a values > 8) selectivity coefficients were not calculated as the organic interferent was not ionic at the pH the investigations were performed at. The interferents are primarily non-ionic at physiological pH, so that any effect on the electrode response would be due to blockage of the ionophore or electrode fouling rather than any competition between the interferent and lidocaine for charge induced membrane transport.

The major interferent for lidocaine was L-histidine which reduced the slope of the PVC electrode to 41.7 mV/decade (limit of detection 9.1×10^{-4} mol dm^{-3}). With the TECOFLEX membrane an increase in the slope to 67.4 mV/decade was observed (limit of detection 3.6×10^{-3} mol dm^{-3}). Nicotinamide also interfered, and produced a continuous base line drift for 2 to 3 h. The drift was not evident when the concentration of nicotinamide background was reduced to 1×10^{-3} mol dm^{-3}.

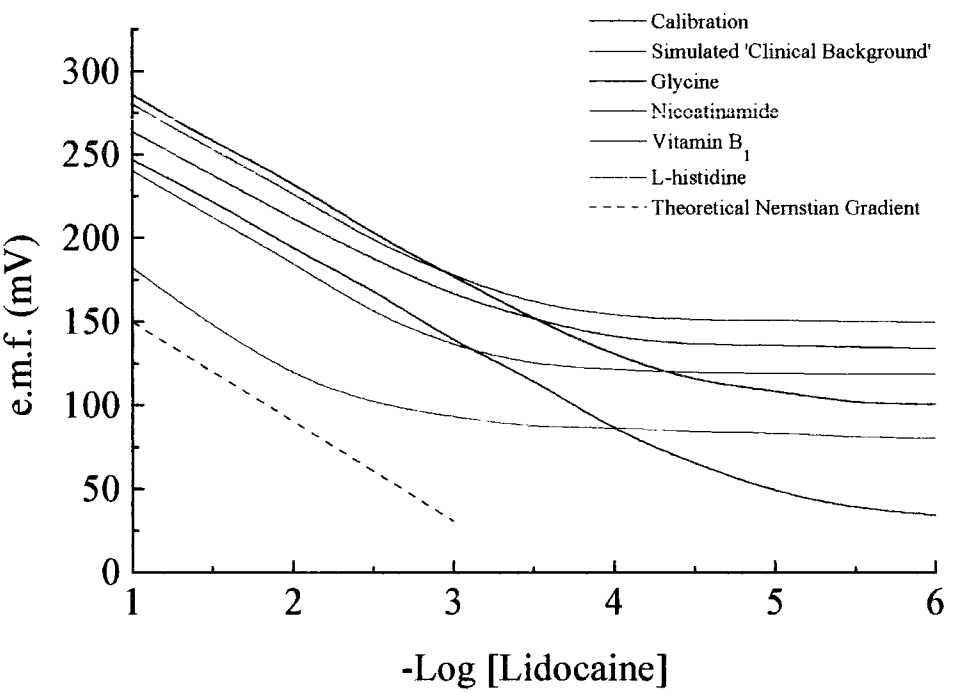

Figure 2.3.1.3.2. Response Curves for Calibration and interferents for the TECOFLEX SG 80 membrane. A: aqueous, B: clinical Interference; C: 1 x 10^{-2} mol dm^{-3} Glycine; D: 1 x 10^{-3} mol dm^{-3} Nicotinamide; E: 1 x 10^{-2} mol dm^{-3} Vitamin B_1; F: 1 x 10^{-2} mol dm^{-3} L-histidine.

The results from the interference experiments indicate that the major interferents are those molecules of similar size and structure to the primary analyte i.e. L-histidine and nicotinamide. The interaction of lidocaine with the cyclodextrin is probably via inclusion of the aryl moiety with hydrogen bonding interactions between either the protonated amino group or the amido –NH with the glycosidic oxygen or the ether oxygens on the side chains. Given such a mode of binding between lidocaine and the cyclodextrin it is not surprising that the major interferents were aryl species with pendant amide or amine groups. However the physiological levels of these interferents is considerably lower than used in the interference studies, 7.3 x 10^{-5} – 1.25 x 10^{-4} mol dm^{-3} and 3.3 x 10^{-5} – 7.4 x 10^{-5} mol dm^{-3} respectively for histidine and nicotinamide. Therefore in a clinical situation the interference for these molecules can be expected to be significantly lower.

2.3.1.3 Protein Interference

The effect of switching PVC and TECOFLEX based lidocaine selective electrodes between the aqueous electrolyte (containing simulated 'clinical background') and the electrolyte solution (which contained added protein) produced three sets of data. These corresponded to the presence of Bovine serum albumin (BSA), α_1-acid glycoprotein (AAG) and Pooled human serum (HS) respectively as described previously in section 5.1.5. Each of the three data sets comprises two further sets of data, corresponding to aqueous and protein containing solutions for the PVC and TECOFLEX membranes.

2.3.1.3.1 Bovine Serum Albumin (BSA) Interference

After the initial exposure to BSA, the recorded potential dropped (Figure. 2.3.1.3.1.1. pts 1 and 2) for both the PVC- and TECOFLEX-based electrodes.

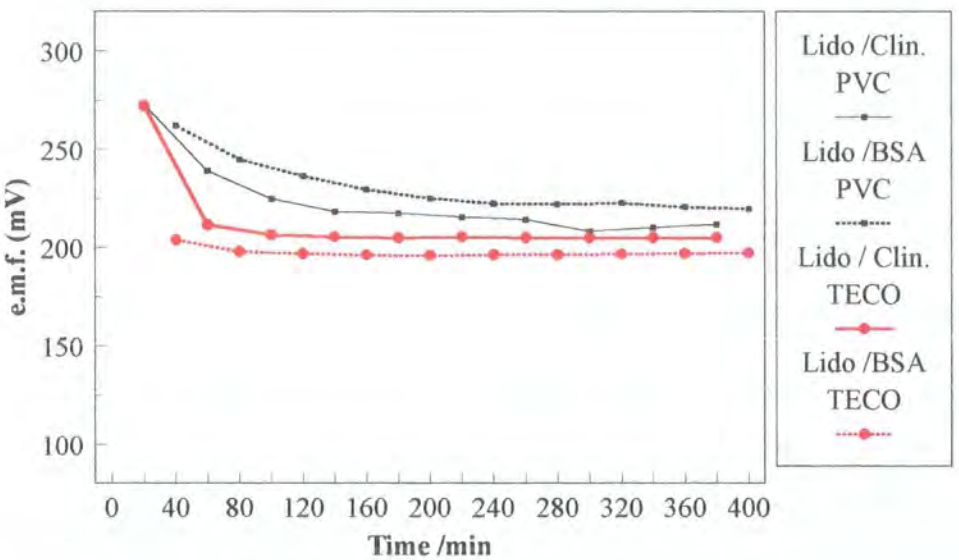

Figure 2.3.1.3.1.1. The potentiometric response for both PVC and TECOFLEX based membrane electrodes in the presence of 40 g/l BSA.

After this initial exposure to BSA, the TECOFLEX membrane returned to its original $E^0_{internal}$ value in the aqueous sample (containing simulated 'clinical background'). This result is consistent with the results obtained by other groups, which have shown that

TECOFLEX-based membranes produce a small, reproducible "asymmetry potential" for calcium ion-selective electrodes[25,26].

The PVC-based membrane however, did not show the same reproducibility in its $E^{0}_{internal}$ values after exposure to the BSA. Indeed the results showed a degree of scatter. Again, this is consistent with work published on calcium ion-selective electrodes by Simon[29] and D'Orazio[25].

2.3.1.3.2 Interference from α_1-acid glycoprotein (AAG)

Drugs in whole blood and serum are well known to bind to proteins. This protein binding can be extensive and the relevant proportions of bound drug can have profound effects on the therapeutic availability of the drug in the body, as only the free fraction may cross biological membranes[30]. The most common of the plasma proteins to bind drugs are albumin and α_1-acid glycoprotein (the so called acute phase or 'stress' protein). On the whole it is the more acidic drugs (e.g. barbiturates) that bind to albumin, while basic drugs (e.g. local anaesthetics) bind to AAG[31]. With approximately 65 % of lidocaine being bound by AAG, this percentage can increase as the concentration of AAG present in serum increases, for example after surgery or myocardial infarction.

The measurements performed used 0.55 g/l AAG in a 'clinical background' of Na^+, K^+ and Ca^{2+}. The results show (Figure 2.3.1.3.2.1) that the effect of AAG on inducing a shift in the $E^{0}_{internal}$ was very small for both electrodes at the concentrations of analyte and AAG used.

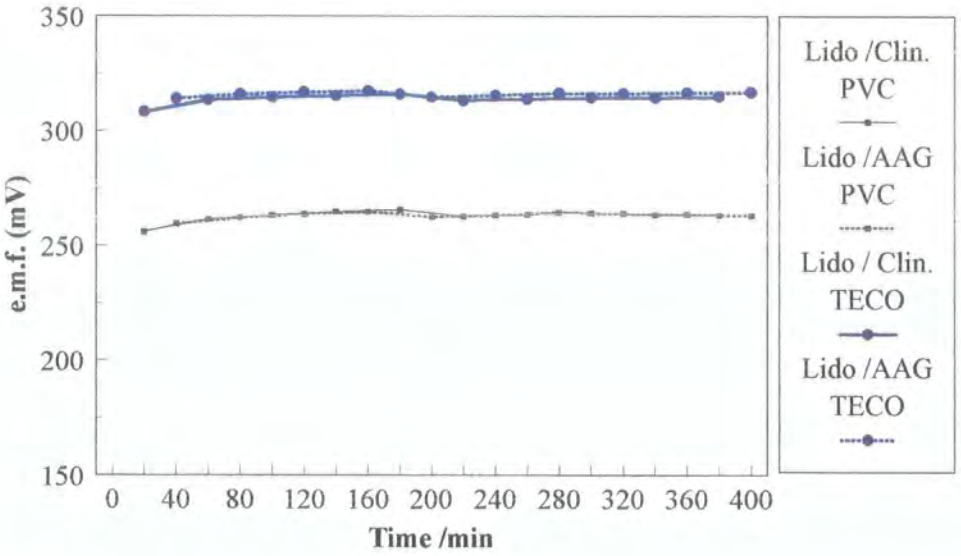

Figure 2.3.1.3.2.1. Potentiometric Response for both PVC and TECOFLEX based membranes with α_1-acid glycoprotein interference.

2.3.1.3.3 Pooled Human Serum (HS) Interference

Since one use of this sensor was to be to monitor levels of lidocaine in serum, this experiment was carried out to observe the shift in potential induced by pooled human serum.

The results obtained (Figure. 2.3.1.3.3.1) show a similar trend to that observed for the BSA interference. The main difference was that the induced $E^0_{internal}$ shift when the electrodes were transferred between the aqueous and protein based solution (approximately 20 mV) was larger than was observed in the presence of BSA only (approximately 8 mV).

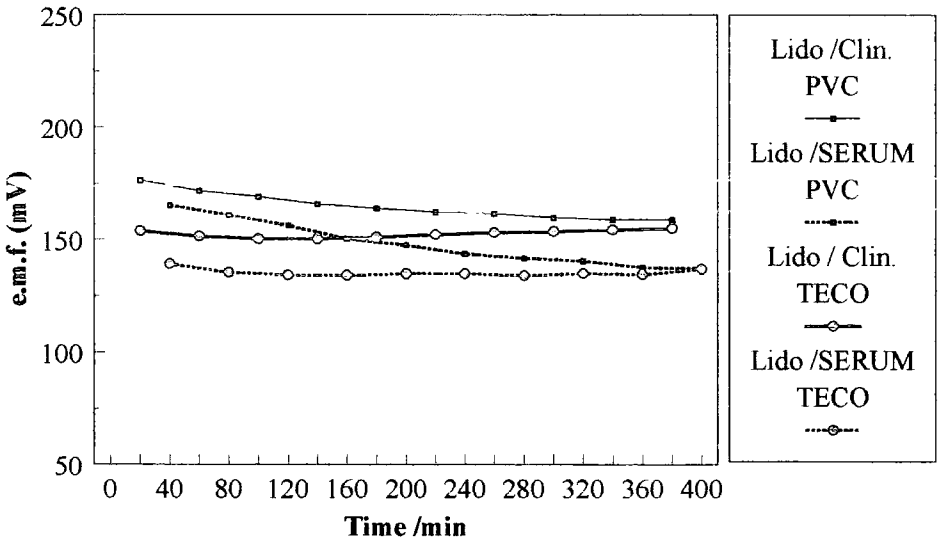

Figure 2.3.1.3.3.1. Potentiometric Results for both PVC and TECOFLEX based ISEs with pooled human serum.

2.3.1.4 Flow Injection Analysis

The experimental work was performed using the equipment described in section 5.1.4. Most routine determinations of clinical analytes are performed using this technique due to its inherent advantages of a high sample throughput and the ease of automation.

The results are broken down into two sections, the first section relates to the calibration experiments. Three membranes were studied to examine the effect of membrane matrix material (PVC or TECOFLEX) and plasticizer (*o*NPOE or DOS). The second section was concerned with the effect of protein on the response curves for lidocaine. It was envisaged that protein interference would be reduced compared with the dip-test method due to the short contact time between the protein-containing sample and the ion-sensing membrane. This has been the case for both work on both potassium[32] and calcium[26] which has been published, and in each case, the protein interference effect was shown to be small.

2.3.1.4.1 FIA Calibration

The electrode characteristics of three electroactive membranes were compared:

1. 2,6 Didodecyl-β-cyclodextrin, PVC, *o*NPOE, KTClPB
2. 2,6 Didodecyl-β-cyclodextrin, TECOFLEX SG 80, *o*NPOE, KTClPB
3. 2,6 Didodecyl-β-cyclodextrin, TECOFLEX SG 80, DOS, KTClPB

A comparison of the calibration and interference results for both 2,3,6 trioctyl-β-cyclodextrin and 2,6 didodecyl-β-cyclodextrin showed that the 2,6 didodecyl-β-cyclodextrin gave the better response to lidocaine. In the calibration curves shown below, the average peak heights for each concentration point are the average of the peak to baseline potential for at least five successive injections of analyte solution.

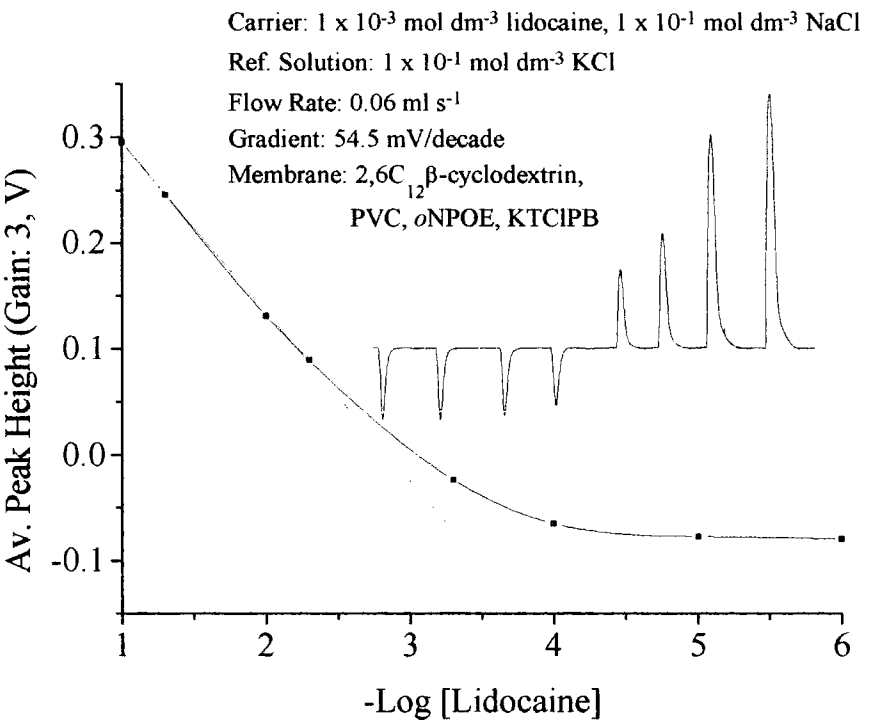

Figure 2.3.1.4.1a. Calibration with PVC based membrane.

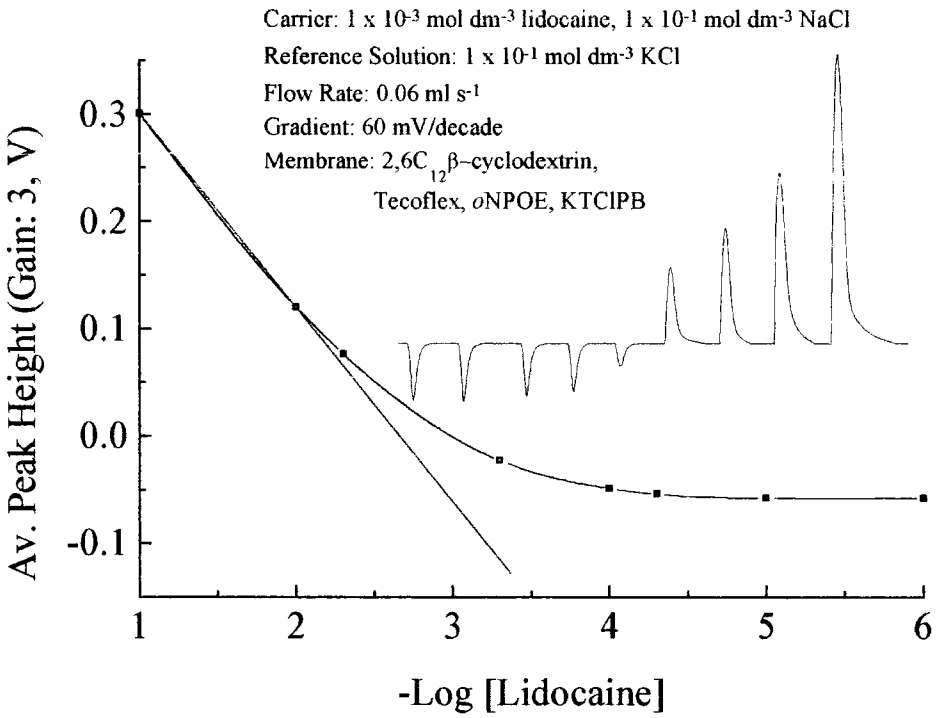

Figure 2.3.1.4.1b. Calibration using TECOFLEX, *o*NPOE based membrane.

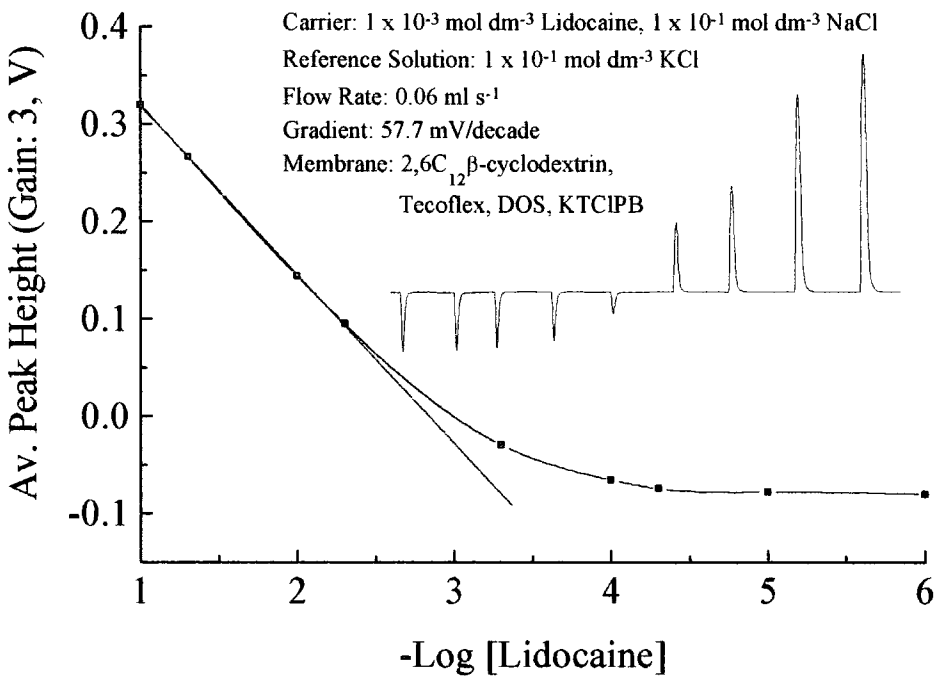

Figure 2.3.1.4.1c. Calibration using TECOFLEX, DOS based membrane.

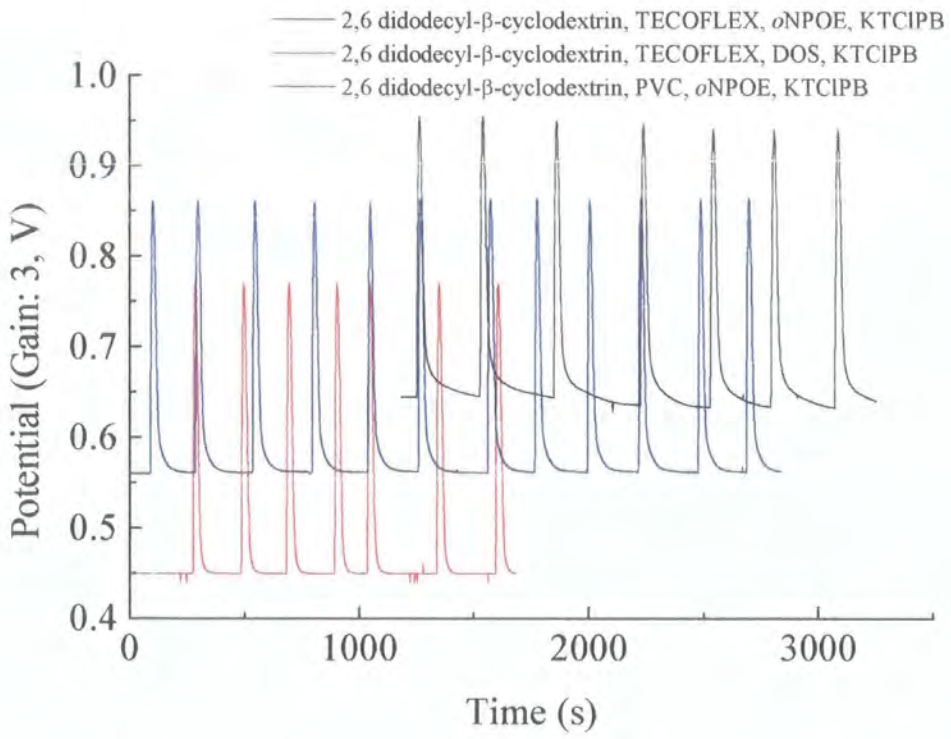

Figure 2.3.1.4.1d Comparison of response traces for an analyte sample of 1×10^{-1} mol dm^{-3} lidocaine.

The results from the calibrations are illustrated in Figures 2.3.1.4.1a, b, and c. The TECOFLEX-based membranes produced Nernstian gradients, whereas the PVC-based membrane was slightly sub-Nernstian in its response whilst the DOS based membrane appeared to give the most stable baseline and consistent peak height. Of the three membranes studied the TECOFLEX-*o*NPOE was the most sensitive towards the analyte (figure 2.3.1.4.1d). However, the peak-response was not ideal and a tailing of the peak and drift in the baseline was observed. The tailing produced meant that if this membrane was to be used in an FIA analyser for lidocaine, the time between injections would have to be longer.

2.3.1.4.2 FIA studies of Protein Interference

2.3.1.4.2.1 Effect of BSA Interference

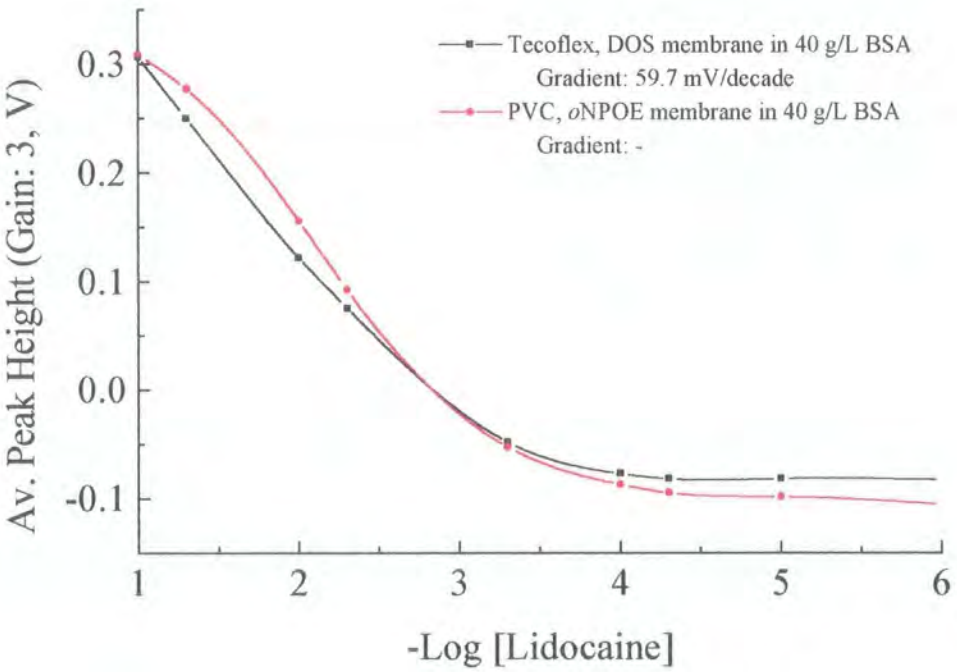

Figure 2.3.1.4.2.1a BSA interference on PVC and TECOFLEX membranes.

Both the PVC and TECOFLEX membranes were tested with analyte solutions containing 40 g/l BSA and the results are shown in figure 2.3.1.4.2.1a. These experiments showed that the TECOFLEX membrane maintained the Nernstian response in the presence of protein, whilst the PVC-based electrode produced a non-Nernstian response curve. Figure 2.3.1.4.2.1b shows the response traces both for PVC and TECOFLEX based membranes in the presence of 40 g/l BSA, the analyte concentration was 5 x 10^{-4} mol dm^{-3} lidocaine. The figure clearly shows the instability of the PVC baseline, and irreproducibility of the peak height.

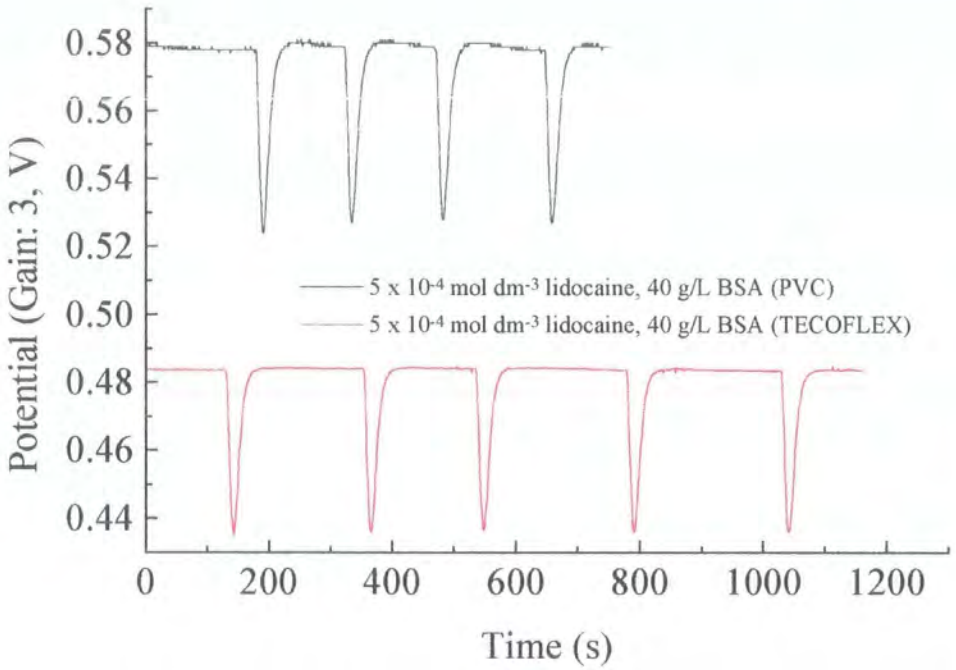

Figure 2.3.1.4.2b. Comparison of PVC and TECOFLEX based ISEs towards an analyte solution of 5 x 10^{-4} mol dm^{-3} lidocaine with 40 g/l BSA.

It was also of interest to study the variation of the recorded potential with time. Such a drift in the baseline or variation in the peak height would indicate that the protein present in the samples may be inducing an 'asymmetry potential'. A comparison between the response traces for 1 x 10^{-4} mol dm^{-3} lidocaine with and without BSA is given in figure 2.3.1.4.2.1c.

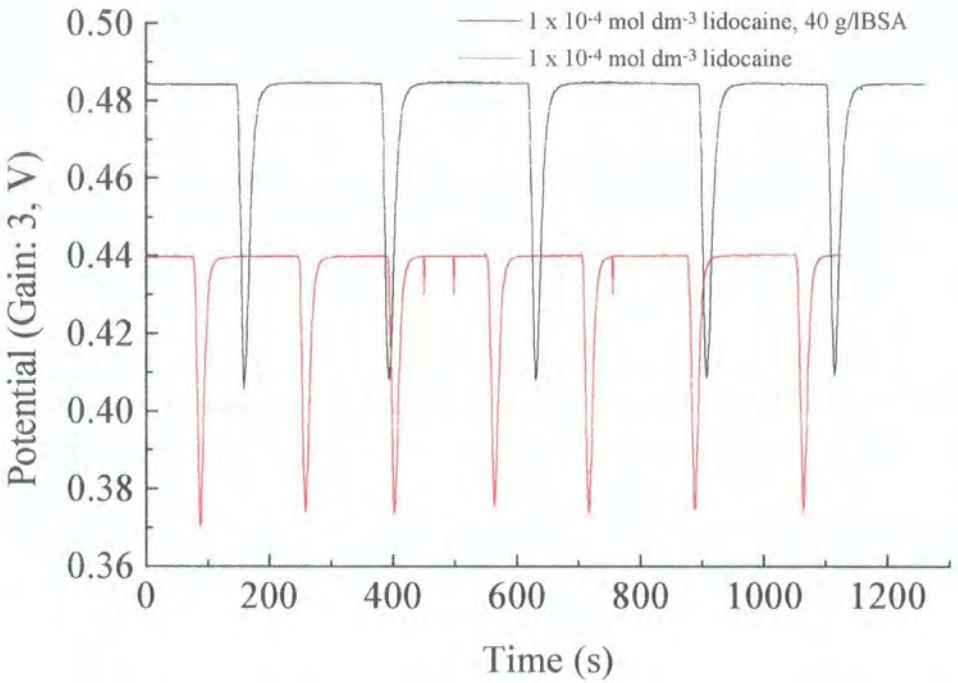

Figure 2.3.1.4.2.1c. Comparison of the response traces for 1 x 10^{-4} mol dm^{-3} lidocaine and 1 x 10^{-4} mol dm^{-3} lidocaine, 40 g/l BSA, both in a background of 1 x 10^{-1} mol dm^{-3} NaCl. Membrane composition: 2,6 Didodecyl-β-cyclodextrin, TECOFLEX, DOS, KTClPB.

This study shows clearly that upon each injection of the BSA containing sample there was no variation in the baseline or peak potential caused by protein adsorption onto the membrane.

2.3.1.4.2.2 Interference from α_1-acid glycoprotein

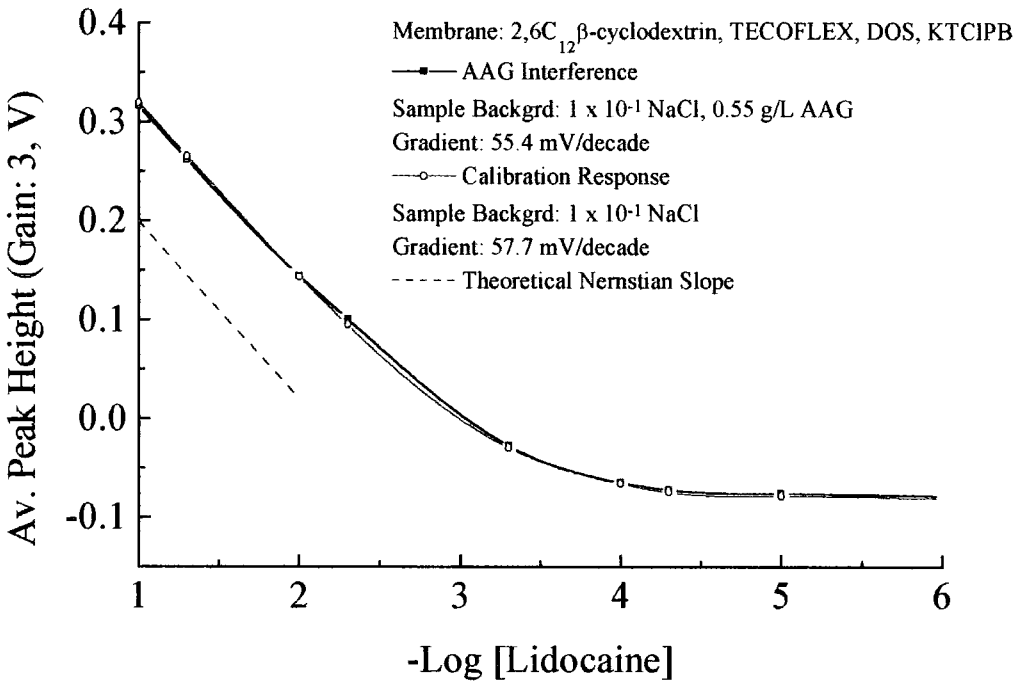

Figure 2.3.1.4.2.2a. Response to lidocaine in the presence of 0.55 g/l AAG, compared with the calibration response.

The effects of α_1-acid glycoprotein on the response of the TECOFLEX-DOS-based membrane were investigated. Figure 2.3.1.4.2.2a shows a comparison between the response curves for the calibration and solutions containing 0.55 g/l AAG. The gradient is only reduced slightly (55.4 mV/decade from 57.7 mV/decade).

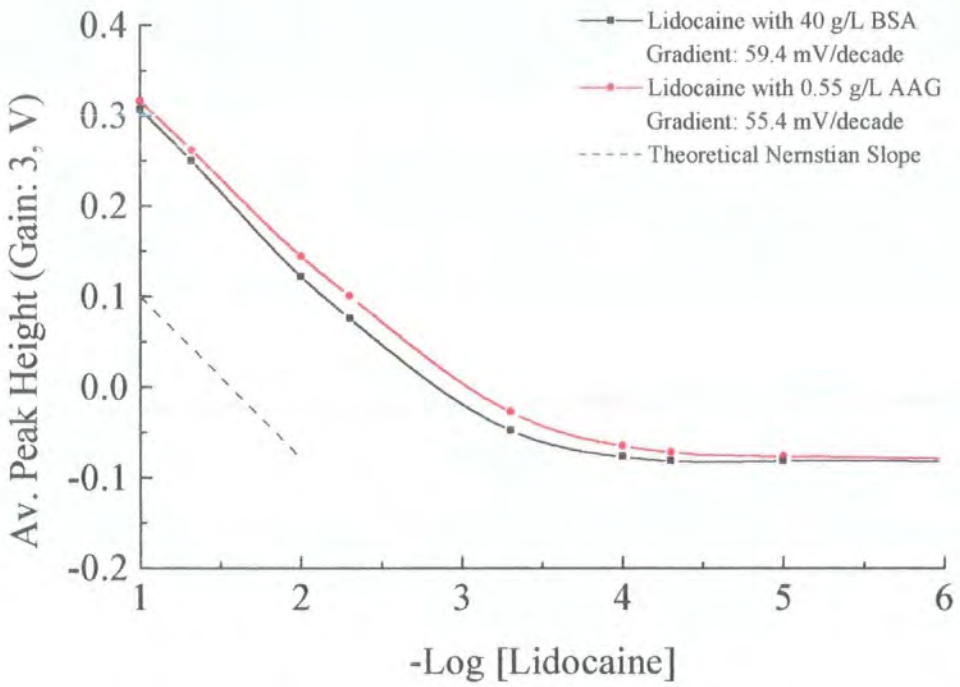

Figure 2.3.1.4.2.2b Comparison of lidocaine response in the presence of BSA and AAG.

A comparison was then made between the response curves for analyte solutions containing 40g/l BSA and 0.55 g/l AAG. Both types of protein had little effect on the electrode as the electrode was able to maintain a Nernstian response (calibration gradient: 57.7 mV/decade, BSA interference gradient: 59.4 mV/decade, AAG interference gradient: 55.4 mV/decade). Furthermore, the electrodes in both BSA and AAG solutions produced a steady baseline (figure 2.3.1.4.2.2c), with no drift evident, implying that the protein was not 'adhering' to the electrode surface and hence not inducing a membrane 'asymmetry potential'.

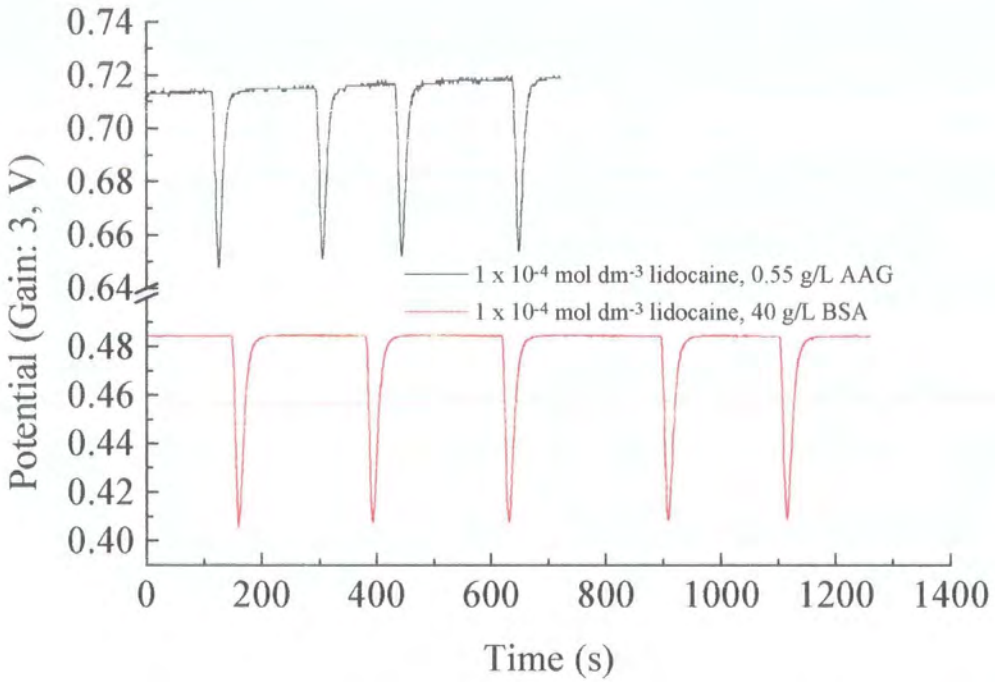

Figure 2.3.1.4.2.2c Comparison of responses for an analyte sample of 1 x 10^{-4} mol dm^{-3} lidocaine with BSA and AAG.

2.3.1.4.2.3 Effect of Human Serum

Samples of human serum were obtained from healthy adult volunteers – including the author. Before the doped human serum samples were injected into the FIA, a response curve was produced using lidocaine samples containing a simulated 'clinical background' (i.e. containing 1.45 x 10^{-1} mol dm^{-3} NaCl, 4.6 x 10^{-3} mol dm^{-3} KCl and 1.26 x 10^{-3} mol dm^{-3} $CaCl_2$). The 'clinical background' was added to the initial solutions as it may be considered as a simple calibration matrix for the blood serum samples. The resulting response curve can be considered a simple reference curve similar to those commonly used in clinical analysis, to which response of the doped human serum samples can be compared. However, the reference solutions only contained sodium, potassium and calcium, and did not, as more complex analytical reference solutions do, correct for pH, ionic strength and protein content[33,34].

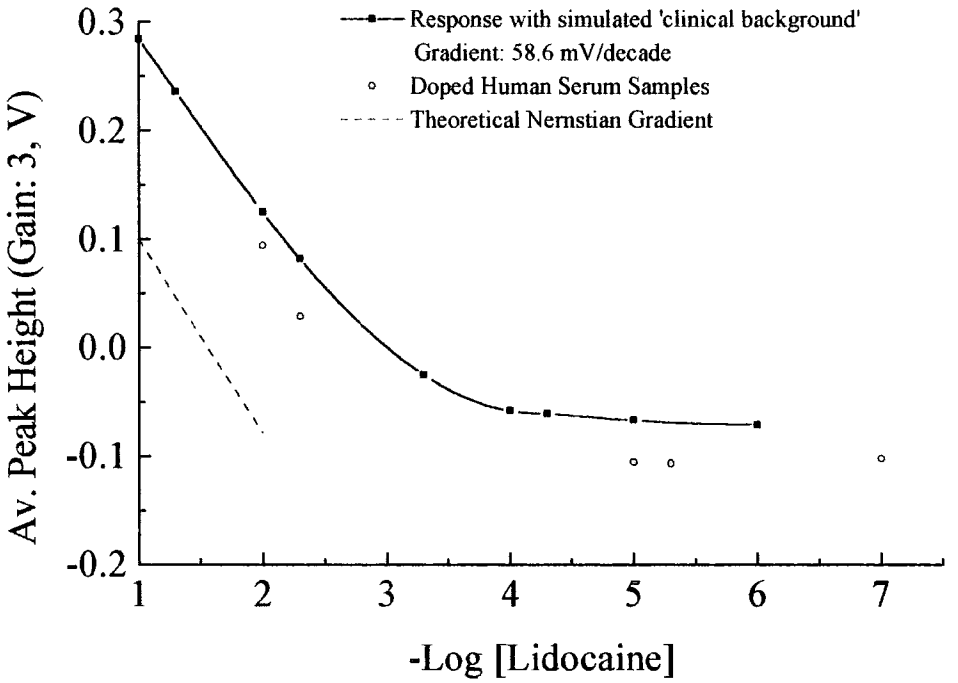

Figure 2.3.1.4.2.3a. A response curve for lidocaine solutions in presence of simulated 'clinical background' and doped human serum samples.

The response in the presence of the simulated 'clinical background' gave an excellent gradient (58.6 mV/decade) with a good overall selectivity coefficient (-log $K^{pot}_{lido.clin}$ = 2.7, overall) showing again that charge dense cations do not interfere with the response of the electrode. As can be seen from figure 2.3.1.4.2.3a the response of each doped human serum sample is offset from the calibration curve by 13 ± 3 mV. This suggests that the 'calibration matrix' is not ideal and that a more realistic calibration solution should be used. The offset was probably due to a protein induced 'asymmetry potential'.

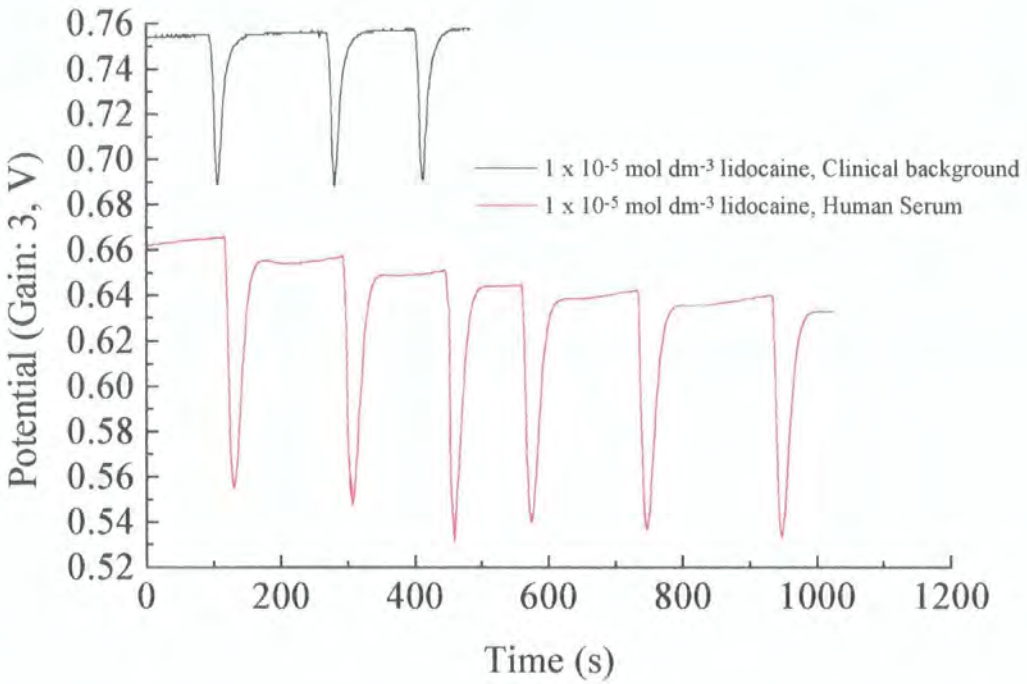

Figure 2.3.1.4.2.3b. Comparison between responses obtained for 1 x 10^{-5} mol dm^{-3} lidocaine in a background of simulated 'clinical background' and in human serum.

This is consistent with the results obtained from the dip-test protein studies discussed earlier. These dip-test results also showed that the asymmetry is greater than that observed with BSA alone (see figure 2.3.1.4.2.3c). Therefore, in addition to the albumin some other serum constituent is also affecting the results.

The results shown in figure 2.3.1.4.2.3b are the responses for solutions of 1 x 10^{-5} mol dm^{-3} lidocaine with either a background of 'clinical cations' or in human serum. The figure shows that, although the peak to baseline potential remained constant, the baseline was drifting.

As the electrodes were adsorbing proteins from the serum samples, the effect of washing the system through with a solution known to remove protein from electrodes was investigated. A 5% solution of pepsin in 0.1 M hydrochloric acid was used for this purpose. The pepsin solution was injected alternately with the human serum samples. The effect of using the pepsin solution is shown in figure 2.3.1.4.2.3d. The pepsin solution appeared to have a significant effect in reducing the drift in the baseline, which is most easily seen by comparison with the response curve when the system was not washed with the pepsin solution.

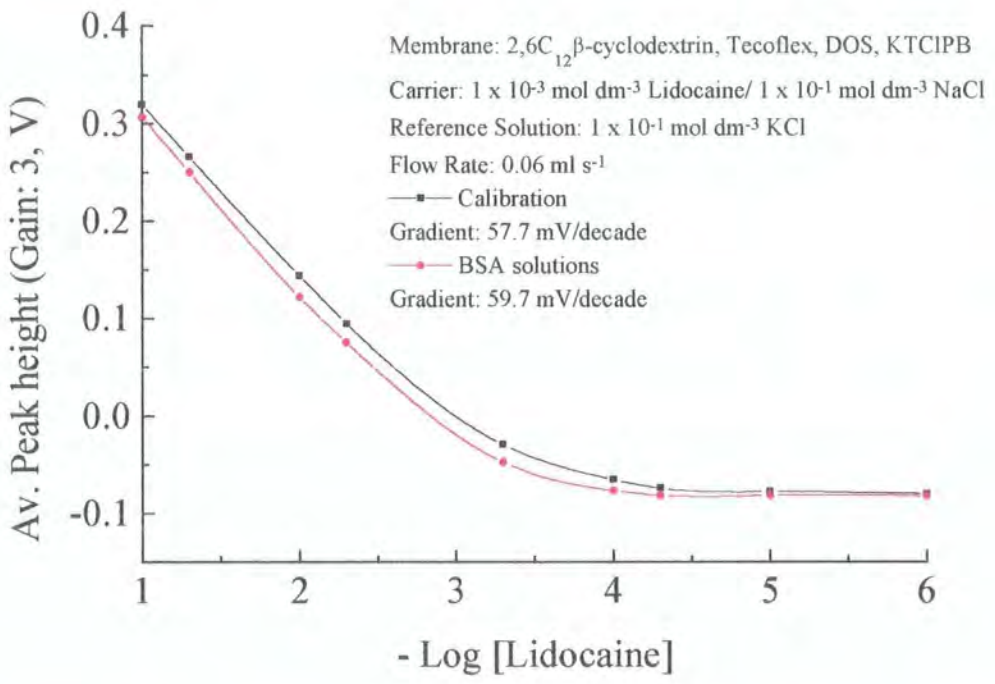

Figure 2.3.1.4.2.3c. Comparison of the Response curves for the calibration solutions and those containing 40 g/l BSA.

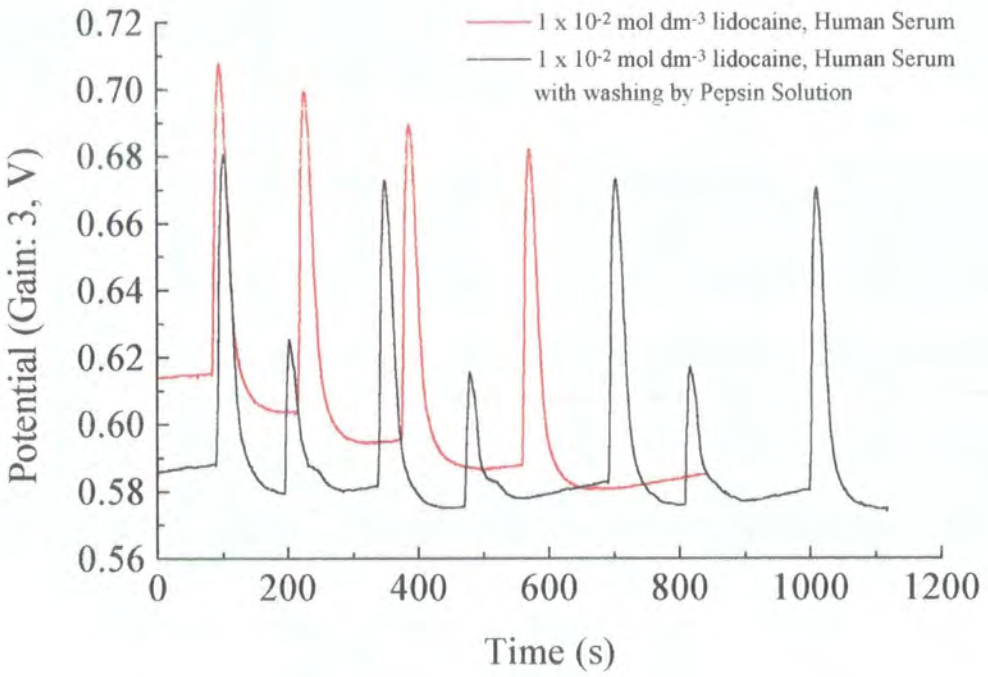

Figure 2.3.1.4.2.3d. Traces for 1 x 10^{-2} mol dm^{-3} lidocaine in human serum, with and without washing between injections with pepsin solution.

2.3.2 Bupivacaine Hydrochloride

2.3.2.1 Potentiometric Calibrations

The results from the calibrations in deionized water are shown in Figure 2.3.2.1.1 and Table 2.3.2.1.1. They reveal that both electrodes showed Nernstian response to bupivacaine, and gave excellent limits of detection.

The results compare favourably with those obtained by Shoukry *et al.*[22], whose sensor was based on ion-pair formation between tetraphenylborate ions and bupivacaine cations in a PVC membrane. This electrode showed a Nernstian response (58.2 mV/decade) and a detection limit of 2×10^{-4} mol dm^{-3}.

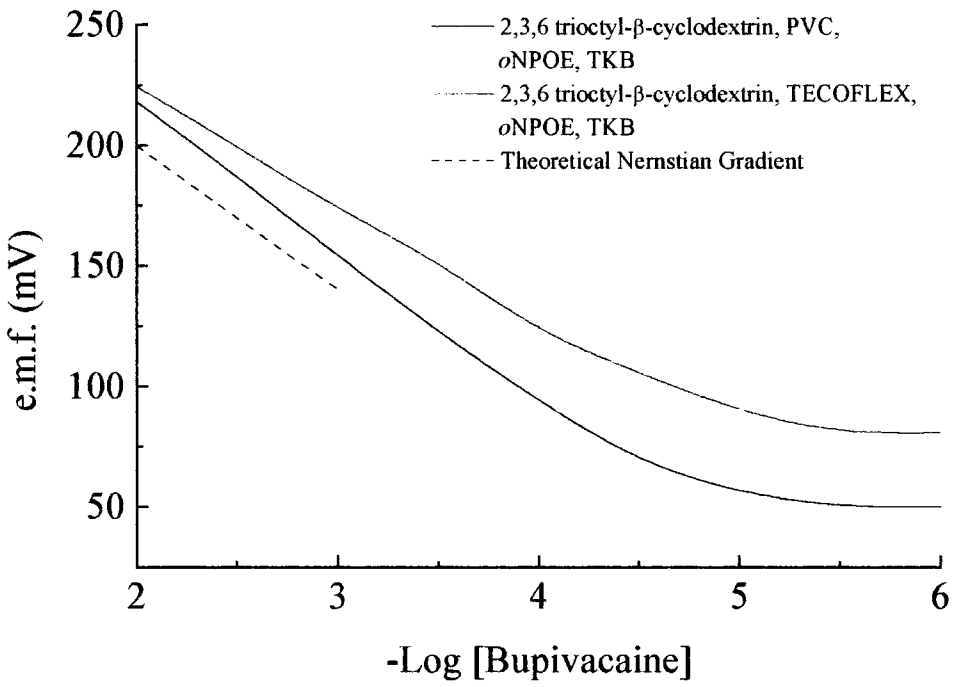

Figure 2.3.2.1.1 Bupivacaine Calibration performed at 298 K. Comparison of TEOFLEX- and PVC-based membranes.

Membrane Matrix	Gradient (mV/ decade)	Limit of Detection (mol dm^{-3})
PVC	57.2	1.2×10^{-5}
TECOFLEX SG 80	56.5	4.9×10^{-5}

Table 2.3.2.1.1. Calibration Data. Each membrane contains 2,3,6 trioctyl-β-cyclodextrin, *o*NPOE and TKB.

2.3.2.2 Interferent Experiments

The interference effect of various cationic species found in serum was studied (Figures 2.3.2.2.1, 2.3.2.2.2 and table 2.3.2.2.1), by examining the response characteristics of both PVC and TECOFLEX based bupivacaine sensitive electrodes. The simulated 'clinical background' contained 1.45×10^{-1} mol dm^{-3} NaCl, 4.3×10^{-3} mol dm^{-3} KCl and 1.26×10^{-3} mol dm^{-3} $CaCl_2$. The concentration values, as before, were all chosen to fall within the normal physiological range observed for these ions. The other interferents used, glycine ($1.46 \times 10^{-4} - 3.52 \times 10^{-4}$ mol dm^{-3}), histidine ($7.3 \times 10^{-5} - 1.25 \times 10^{-4}$ mol dm^{-3}), vitamin B_1 ($1.2 \times 10^{-8} - 5.9 \times 10^{-8}$ mol dm^{-3}), nicotinamide ($3.3 \times 10^{-5} - 7.4 \times 10^{-5}$ mol dm^{-3}) and adrenaline (2.7×10^{-6} mol dm^{-3}) were all chosen to allow comparison between this study and others performed on the same analyte. The physiological ranges for these compounds are given in brackets. With the exception of adrenaline, the concentration shown is that routinely used in bupivacaine injections. The concentration chosen for these interferents was arbitrarily set at 1×10^{-2} or 1×10^{-3}, mol dm^{-3} depending upon the solubility of the interferent.

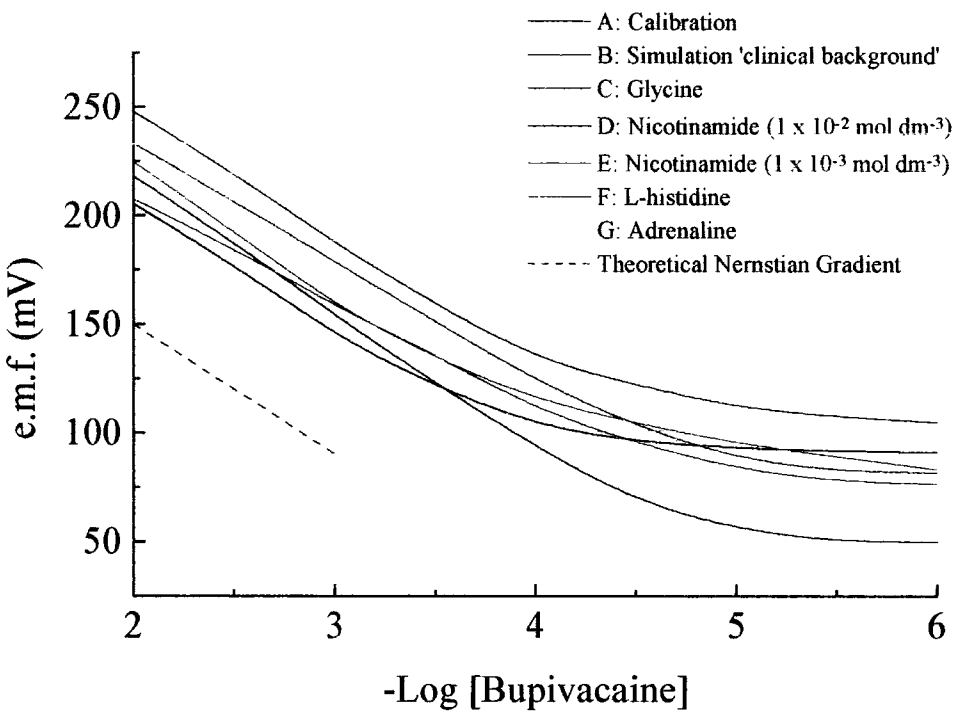

Figure 2.3.2.2.1. Response Curves for Calibration and interferents for the PVC membrane. A: aqueous, B: clinical Interference; C: 1 x 10^{-2} mol dm^{-3} Glycine; D: 1 x 10^{-3} mol dm^{-3} Nicotinamide; E: 1 x 10^{-3} mol dm^{-3} Nicotinamide; F: 1 x 10^{-2} mol dm^{-3} L-histidine; G: 2.7 x 10^{-6} mol dm^{-3} Adrenaline.

In the simulated 'clinical background' the response from both the electrodes was maintained. As before excellent selectivity coefficients (-Log K_{ij}^{pot}, overall $\geq$ 4) were observed, with very good limits of detection and slopes.

With the 'organic' interferents, selectivity coefficients were only calculated for the solution of L-histidine in 'clinical background' as this was the only interferent that was ionic at the pH used (pH ~ 6). Any interference from the other molecules would have to arise from blockage of the ionophore cavity or electrode fouling.

The results show that major interferents for bupivacaine were nicotinamide and vitamin B_1. Since neither of the interferents are charged at the pH in question the interference cannot occur though competition between the analyte and these interferents for charge induced membrane transport. The interference is probably due to the vitamin B_1 and

nicotinamide hindering the uptake of bupivacaine by blocking the cyclodextrin cavity. However, the physiological levels of these interferents are considerably lower than those used in the interference studies ($3.3 \times 10^{-5} - 7.4 \times 10^{-5}$ and $1.2 \times 10^{-8} - 5.9 \times 10^{-8}$ mol dm^{-3} respectively for nicotinamide and vitamin B_1). Therefore in a clinical situation the interference from these molecules can be expected to be significantly lower.

Membrane Matrix	**Interferent**	**Gradient (mVdecade)**	**Limit of Detection (mol dm^{-3})**	**-Log K_{ij}^{pot}**
PVC	**'Clinical background'**	53.9	1.6×10^{-5}	4.0
	L-histidine	60.4	6.0×10^{-5}	2.8
TECOFLEX	**'Clinical background'**	56.3	1.9×10^{-5}	3.9
	L-histidine	61.7	2.1×10^{-4}	2.7

Table 2.3.2.2.1. Potentiometric results for bupivacaine detection in the presence of cationic interferent species.

The effect of the interferents upon the response of the electrodes studied was less pronounced than that reported previously by other groups[22]. The use of an alkylated cyclodextrin has also reduced the interference from the charge dense cations of Na^+ and K^+ compared with those from the ion-pair electrode (- Log K_{Bup,Na^+}^{pot} = 1.6, - Log K_{Bup,K^+}^{pot} = 1.9)[22].

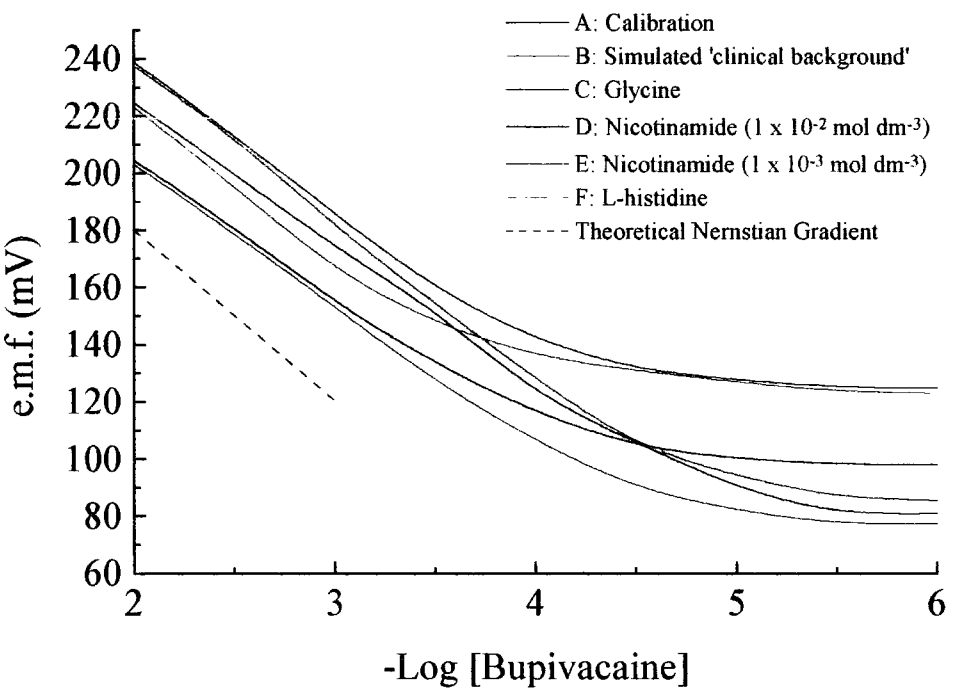

Figure 2.3.2.2.2. Response Curves for Calibration and interferents for the TECOFLEX membrane. A: aqueous, B: clinical Interference; C: 1 x 10^{-2} mol dm^{-3} Glycine; D: 1 x 10^{-3} mol dm^{-3} Nicotinamide; E: 1 x 10^{-3} mol dm^{-3} Nicotinamide; F: 1 x 10^{-2} mol dm^{-3} L-histidine.

2.3.2.3 Protein Interference

Switching the PVC and TECOFLEX based bupivacaine selective electrodes between the aqueous electrolyte (containing the simulated 'clinical background') and an electrolyte solution containing added protein produced three sets of data. These sets corresponded to the presence of bovine serum albumin (40 g/l), α_1-acid glycoprotein (0.55 g/l) and pooled human serum respectively as described in section 5.1.5. Each of the three data sets comprised two further sets of data, corresponding to aqueous and protein containing solutions for the PVC and TECOFLEX membranes.

2.3.2.3.1 Effect of Bovine Serum Albumin

For both the PVC and TECOFLEX based membranes, an initial drop in potential was observed after the first exposure of the membranes to protein (pts 1 and 2 in Figure 2.3.2.3.1.1). After this initial exposure to protein, the TECOFLEX-based membrane (in the aqueous solutions containing simulated 'clinical background') returned to its original $E^{0}_{internal}$ potential. Each successive exposure to the protein led to a small and reproducible protein induced shift (asymmetry potential 6 mV). The PVC based electrode however showed a varying protein induced potential shift, the magnitude of which was highly variable, 8 ± 3 mV.

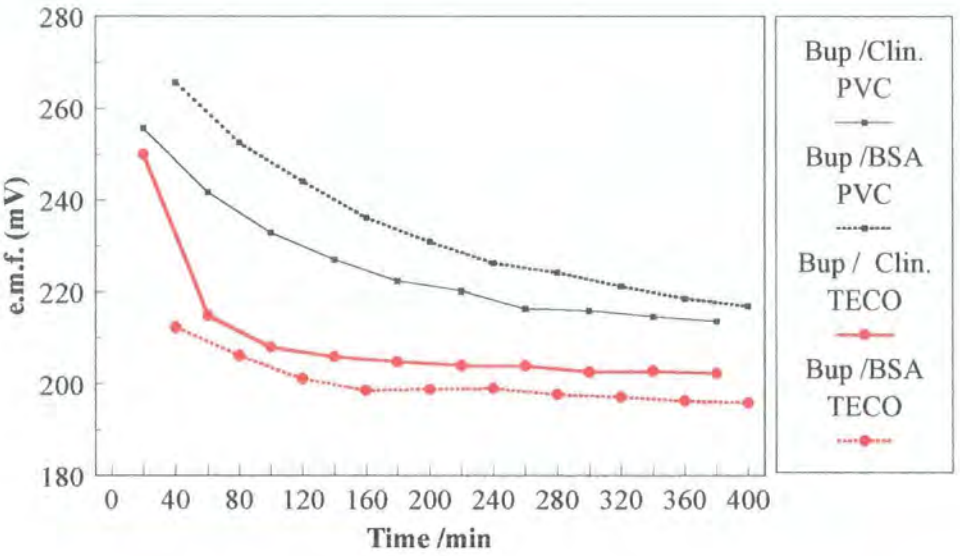

Figure 2.3.2.3.1.1. Potential Response results for both PVC and TECOFLEX based bupivacaine selective electrodes with bovine serum albumin interference.

These results are consistent with those reported by D'Orazio[24] who has compared the response characteristics of PVC- and TECOFLEX-based calcium electrodes. His work showed that the protein induced "asymmetry potential" was much smaller and more reproducible for a TECOFLEX-based ion-selective electrode than a PVC one.

Since it is known that basic drugs, like bupivacaine, do not bind albumin, it is likely that any potential differences between the results for the aqueous and the protein containing solution must be due to the nature of the matrix material.

2.3.2.3.2 Interference Effect of α_1-acid glycoprotein

The protein to which basic drugs, such as bupivacaine, bind is α_1-acid glycoprotein. An experiment was performed to observe if any difference in potential could be observed due to protein binding of the analyte, bupivacaine. The results from this experiment are illustrated in Figure 2.3.2.3.2.1.

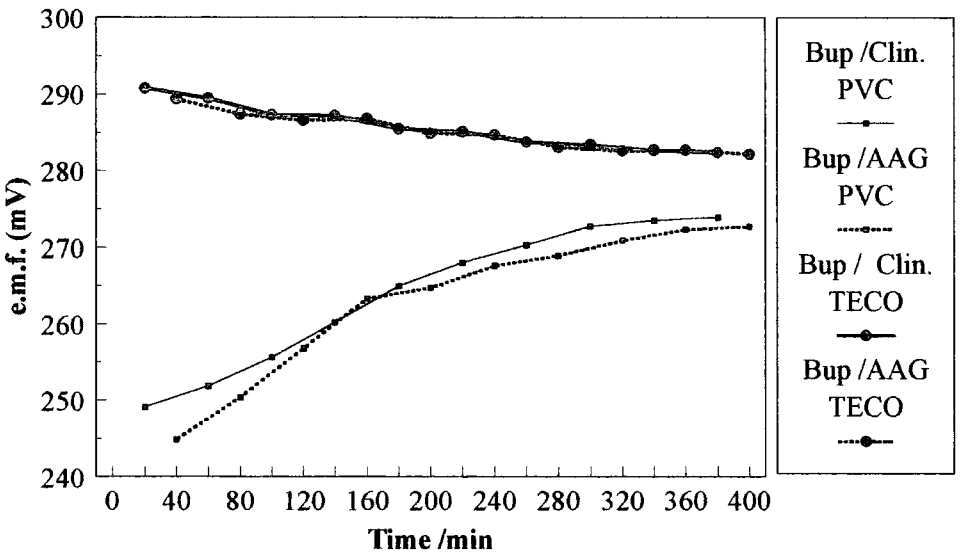

Figure 2.3.2.3.2.1. Potential Response for PVC and TECOFLEX based bupivacaine selective electrodes with α_1-acid glycoprotein Interference.

Both the PVC and TECOFLEX based membranes gave rise a shift in $E^0_{internal}$ values, after each successive exposure to the α_1-acid glycoprotein. The effect was more pronounced for the PVC membrane. This systematic shift in the $E^0_{internal}$ for the PVC electrode is again probably due to protein adsorption on the electrode. PVC has a less polar surface than TECOFLEX so it is more prone to protein binding than TECOFLEX. Protein binding to the PVC surface may cause an increase in the apparent resistance of the system and therefore affect the measured potential. The lack of any change in the TECOFLEX potential suggests that this protein was not binding to the surface.

2.3.2.3.3 Potential Response Effect of Pooled Human Serum

A similar trend to that found for BSA interference was observed (figure 2.3.2.3.3.1). The TECOFLEX-based membrane consistently returned to its initial $E^0_{internal}$ after each exposure to the protein solution, although the induced "asymmetry potential" was larger (asymmetry potential - human serum: 20 mV, bovine serum albumin: 6 mV). With the PVC electrode, the results again revealed a scatter in the $E^0_{internal}$ recovery after protein exposure and again the "asymmetry potential" was larger. In each case the larger "asymmetry potential" is probably due to the strong binding of bupivacaine with the plasma proteins (though not with albumin)[35]. This stronger binding is due to its lipophilicity, (distribution coefficient, octanol/water, log $P_{Bupivacaine}$: 2.5, log $P_{Lidocaine}$: 0.6) which is significantly higher than that of lidocaine.

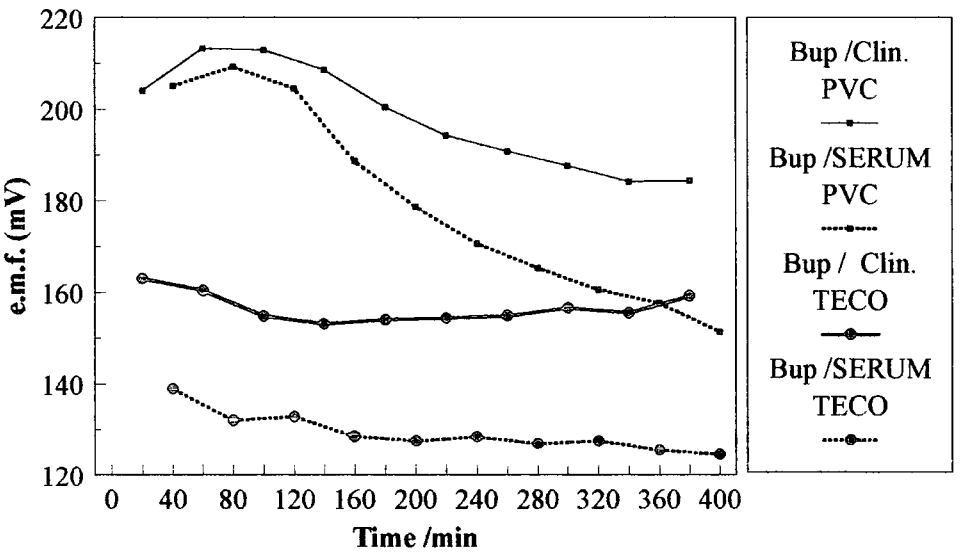

Figure 2.3.2.3.3.1. Potential Response for PVC and TECOFLEX based bupivacaine selective electrodes with pooled human serum interference.

2.3.3 Summary

Host guest complexation between cyclodextrins and local anaesthetics has been studied previously[36,37]. The cyclodextrin derivatives 2,6 didodecyl- and 2,3,6 trioctyl-β-cyclodextrin were the first neutral ionophores reported for local anaesthetics. The study performed showed that they may be used as ionophores for the hydrochlorides of local anaesthetics. Electrode response parameters were maintained in the presence of serum levels of Na^+, K^+ and Ca^{2+} and several organic cationic species. The adverse effect on sensitivity observed for the lidocaine electrode, (induced by the presence of 1 x 10^{-2} mol dm^{-3} histidine and 1 x 10^{-3} mol dm^{-3} nicotinamide), and the bupivacaine selective electrode (with 1 x 10^{-2} mol dm^{-3} vitamin B_1) will probably be reduced significantly at the much lower levels of these interferents in serum.

The study showed the TECOFLEX based electroactive membranes to be preferable to PVC based membranes for measurements in protein containing solutions. The drift induced by the protein on baseline potentials and peak height reproducibility in the FIA experiments was substantially smaller with TECOFLEX rather than PVC as the membrane matrix.

Flow injection analysis is a particularly suitable technique for the rapid analysis of samples of small volume. The combination with ion-selective electrodes has previously been shown to confer the advantages of increased sensitivity, decreased chemical interference, fast response time and good reproducibility of results[38] to an analysis system. The experimental results show that the determination of lidocaine in protein containing samples can be achieved by the combination of FIA, with a TECOFLEX based ion-selective polymer-membrane. This means that a lidocaine analysis in 'real' clinical samples could be achieved.

2.4 References

1. Rang H. P., Dale M. M., Ritter J. M., Pharmacology. 3rd ed. Churchill Livingstone, London, 1995, ch. 34
2. ed. Dollery C., Therapeutic Drugs. Churchill Livingstone, London, 1991
3. Cruz A., Lopez-Rivadulla M., Bermejo A. M., Sanchez I., Fernandez P., *Anal. Lett.*, 1995, **27**(14), 2663-2675
4. Saleh G. A., Askal H. F., *Anal. Lett.*, 1995, **28**(15), 2663-2671
5. DiFazio C. A., Brown R. E., *Anesthesiology* 1971, **34**(1), 86-88
6. Adjepon-Yamoah K. K., Prescott L. F., *J. Pharm. Pharmac.*, 1974, **26**, 889-893
7. Lesko L. J., Ericson J., *J. Chromatogr., Biomed. Applic.*, 1980, **182**, 226-231
8. Hawkins J. D., Bridges R. R., Jennison T. A., *Ther. Drug Monit.*, 1982, **4**, 103-106
9. Hattori H., Yamamoto S., Yamada T., Suzuki O., *J. Chromatogr., Biomed. Applic.*, 1991, **564**, 278-282
10. Arimoto H., Shiomi K., Fujii T., *J. High Res. Chromatogr.*, 1991, **14**, 672-675
11. Hagestain I. H., Pinkerton T. C., *Anal. Chem.*, 1985, **57**, 1757-1763
12. Yu Z., Abdel-Rehim M., Westerlund D., *J. Chromatogr., Biomed. Applic.* 1994, **654**, 221-230
13. Mould G. P., Marks V., Mechanisms of Drugs in Anaesthesia. 2nd ed. Edward Arnold, London, 1993, ch. 10
14. Lindberg R. L. P., Kanto J. H., Phlajamaki K. K., *J. Chromatogr., Biomed. Applic.*, 1992, **383**, 357-364
15. Kastrissios H., Hung M., Triggs E. J., *J. Chromatogr., Biomed. Applic.*, 1992, **577**, 103-107
16. Murillo I., Costa J., Salva P., *J. Liq. Chromatogr.*, 1993, **16**(16), 3509-3514
17. Tam M. K., Tawfik S. R., Ke J., Coutts R. T., Gray M. R., Wyse D. G., *J. Chromatogr., Biomed. Applic.*, 1987, **423**, 199-206
18. Halbert M. K., Baldwin R. O., *J. Chromatogr., Biomed. Applic.*, 1984, **306**, 269-277
19. Ionescu M. S., Abrutis A. A., Radulescu N., Baiulescu G. E., Cosofret V. V., *Analyst*, 1985, **110**, 929-931
20. Hassam S. S. M., Ahmed M. A., *J. Assoc. Off. Anal. Chem.*, 1986, **69**(4), 618-621
21. Kureichuk A. S., Pantsurkin V. I., Ptukha E. V., Potemkin K. D., *Zhurnal Analiticheskoi Khimii*, 1990, **45**(3), 569-574

22. Satake H., Miyata T., Kanishina S., *Bull. Chem. Soc. Jpn.*, 1991, **64**, 3029-3034
23. Shoukry A. F., Issa Y. M., El-Shiekh R., Zareh M., *Anal. Lett.*, 1991, **24**(9), 1581-1590
24. Kataky R., Palmer S., *Electroanalysis*, 1996, **8**(6), 585-590
25. D'Orazio P., Bowers Jr. G. N., *Clin. Chem.*, 1992, 38(7), 1332-1339
26. Park S. B., Chung S., Cha G. S., Kim H. D., *Bull. Korean Chem. Soc.*, 1995, **16**(11)1033-1037
27. Kataky R., Parker D., Kelly P. M., *Scand. J. Clin. Lab. Invest.*, 1995, **55**, 409-419
28. Parker D., Kataky R., Kelly P. M., Palmer S., *Pure & Appl. Chem.*, 1996, **68**(6), 1219-1223
29. Durselen L. F. J., Wegmann D., May K., Oesch U., Simon W., *Anal. Chem.*, 1988, **60**, 1455-1459
30. Wood M., *Anesthesiology*, 1991, **75**, 721-723
31. ed. Hall C. J., Feldman S. A., PAton W., Scurr S., Mechanisms of Drugs in Anesthesia. 2nd ed., Edward Arnold, London, 1993, ch. 5
32. Jemey J., Toth K., Lindner E., Pungor E., *Microchem. J.*, 1992, **45**, 232-247
33. Covingtion A. K., Kataky R., *J. Chem. Soc. Faraday Trans.*, 1993, **89**(2), 369-376
34. Maas B., Sprokholt R., Maas A., Fogh-Anderson N., *Scand. J. Clin. Lab. Invest.*, 1996, **56**, suppl 224, 179-186
35. Tucker G. T., Boyes R. N., Bridenbough P. O., Moore D. C., *Anesthesiology*, 1970, **33**(3), 287-303
36. Dollo G., Le Corre P., Chevanne F., Le Verge R., *Int. J. Pharm.*, 1996, **136**, 165-174
37. Takisawa N., Shirahama K., Tanaka I., *Colloid Polym. Sci.*, 1993, **271**, 499-506
38. Toth K., Fucsko J., Lindner E., Feher Zs., Pungor E., *Anal. Chem. Acta*, 1986, **179**, 359-370

Chapter Three

The Potentiometric and Amperometric Detection of Antidepressants

3.1 Introduction

The chapter contains an introduction to some of the properties of tricyclic antidepressants (section 3.1.1). The analytical methods which have been applied to the detection of antidepressants are discussed (section 3.1.2). The experimental studies performed are described in section 3.2. The results from the potentiometric and amperometric experiments are presented and discussed in section 3.3.

3.1.1 Antidepressants

The tricylic antidepressants imipramine, desipramine and trimipramine are some of the most important antidepressant drugs in current clinical use. The first of them, imipramine was discovered by Kuhn in the 1950's.

The tricyclic antidepressants are all lipophilic and relatively strong bases, as shown by their high pK_a values (imipramine 9.4, desipramine 10.2, trimipramine is the exception 7.72). As with many basic drugs, this class of compound bind to plasma proteins, in particular α_1-acid glycoprotein (AAG). This can lead to problems as the levels of this protein can vary depending on the condition of the patient, for example, inflammatory disease which increases the levels of AAG[1].

Their primary mode of action as antidepressants is believed to be inhibition of the uptake of catecholamines (specifically noradrenaline) by the nerve terminals. This may occur via competition for the carrier protein that forms part of the membrane transport system.

Their relatively low concentration in physiological fluids (therapeutic concentration ~ 10^{-7} to 10^{-8} mol dm^{-3}) is indicative of their effectiveness. Levels above this range lead to adverse effects; seizures, unconsciousness, cardiac arrhythmia and respiratory depression[2]. Their low concentration and the large number of metabolites formed by the tricyclic antidepressants means that any detection method should be both sensitive and selective. Bearing this in mind, the current preferred detection method for most tricyclic antidepressants is HPLC[1,3].

3.1.2 Detection of Antidepressants

Various rather tedious methods for the measurement of tricyclic antidepressants are currently used[4]. A common theme amongst the majority of these is the need for the drugs to be extracted from the biological matrix before analysis. The methods used have included spectrophotometric techniques, gas-liquid chromatography (GLC), high-performance liquid chromatography (HPLC) and radioimmunoassay (RIA). Some electrochemical methods have also been described since they have the ability to determine analyte concentrations directly in whole blood, serum or urine without any extraction steps.

3.1.2.1 Spectrophotometric Techniques

Spectrophotometric techniques were among the first methods used to detect these molecules. However, the specificity of the methods described was poor, with the metabolites of the parent drug causing a significant level of interference. However, a recent flow injection chemiluminescence detection method described by Townshead[5] showed both excellent detection limits for imipramine (5×10^{-7} mol dm^{-3}) and low interference was observed from constituents of human urine (e.g. uric acid).

3.1.2.2 Gas-liquid Chromatography

Gas chromatography is the most widely used method for detection of tricyclic antidepressants, indeed GC-coupled with nitrogen detection[6] is the preferred method of analysis for imipramine, desipramine and trimipramine hydrochlorides. Limits of detection are of 5, 1 and 0.5 μg/l (1.6×10^{-8}, 3.3×10^{-9} and 1.5×10^{-9} mol dm^{-3}) for imipramine, desipramine and trimipramine respectively. If mass spectrometric analysis is used instead of nitrogen detection, the detection limits can be improved by three orders of magnitude[7]. However, the methods do require the time consuming extraction of the analyte from the plasma phase into a volatile solvent. The advantage of this technique over spectrophotometry is its ability to separate the metabolites from the parent drug because of their difference retention times on a capillary column.

Therefore, not only the parent drug but also the metabolites are detected, some of which also have antidepressant activity.

3.1.2.3 High-performance Liquid Chromatography (HPLC)

This method has also been applied to the detection of most tricyclic antidepressants. The preferred methodology involves use of a reverse phase, column to improve the column efficiency, coupled to a UV or amperometric detector. When using an amperometric detector detection limits of 1.6×10^{-8} and 1.7×10^{-8} mol dm^{-3} have been reported for imipramine and desipramine respectively[8]. However, extraction of the analyte from the plasma matrix is still required[9].

3.1.2.4 Radioimmunoassay

Radioimmunoassay techniques have the advantages of high sensitivity and rapid analysis for small volumes of plasma (<0.5 ml), without the need for extraction of the analyte from the plasma[10]. A major problem is the lack of availability of tritium-labelled tracers with high specific activity, and the inherent cost of these radiolabelled molecules.

3.1.2.5 Electrochemical Analysis

As mentioned above (section 3.1.1), the use of ISEs to monitor levels of clinically relevant analytes has several advantages over chromatographic methods. ISEs can monitor the concentrations of the required drug continuously, if necessary. In addition the concentration in whole blood can be measured, removing the requirement to separate the analyte from the blood matrix.

Both potentiometric and amperometric methods of detection have been described. Potentiometric ion-exchange membrane electrodes have been devised by Cosofret[11] and Hopkala[12]. These ISEs however showed slightly sub-Nernstian gradients with detection limits of 5×10^{-6} and 6×10^{-5} mol dm^{-3} respectively. In both cases, the electrodes gave modest selectivities over organic and inorganic cationic species such as Vitamins B_1 and B_6, ephedrine, K^+, Ca^{2+} and Mg^{2+}.

Amperometric detection of pharmaceuticals has been used widely and several methods have been proposed for the detection of tricyclic compounds[13] since they are easily oxidised via a two step, three electron ECE process[14]. An amperometric detection scheme was reported by Wang[15], in which differential pulse voltammetry was used, following interfacial accumulation at either glassy carbon or carbon paste electrodes. With a four minute preconcentration time, detection limits of 1.5 x 10^{-8} mol dm^{-3} imipramine, 1.7 x 10^{-8} mol dm^{-3} desipramine and 1.4 x 10^{-8} mol dm^{-3} trimipramine were achieved. Biryol *et al.*[16] used poly(*N*-vinylimidazole)-modified carbon paste electrodes to determine imipramine (and amitriptyline) hydrochlorides. They met with only moderate success, achieving detection limits of approximately 10^{-5} mol dm^{-3} for both analytes. Khodari reported a sensor for trimipramine[17] using a lipid-modified carbon paste electrode. The hydrophobic nature of the electrode surface enhances the preconcentration of trimipramine with respect to an unmodified electrode. The resulting sensor showed a detection limit of 1 x 10^{-9} mol dm^{-3} trimipramine with no interference from uric acid (known to interact with carbon electrode surfaces).

3.2 Experimental

3.2.1 Imipramine Hydrochloride

3.2.1.1 Potentiometric Experimental

3.2.1.1.1 Calibration.

The membranes used were;

1) 2,6 Didodecyl-α-cyclodextrin (1.2 %), PVC (32.8 %), *o*NPOE (65.6 %), TKB (0.4 %).
2) 2,6 Didodecyl-β-cyclodextrin (1.2 %), PVC (32.8 %), *o*NPOE (65.6 %), TKB (0.4 %).
3) 2,3,6 Trioctyl-γ-cyclodextrin (1.2 %), PVC (32.8 %), *o*NPOE (65.6 %), TKB (0.4 %).
4) 2,6 Didodecyl-γ-cyclodextrin (1.2 %), PVC (32.8 %), *o*NPOE (65.6 %), TKB (0.4 %).

All the calibration experiments were carried out using the CVD method described in section 5.1.2. The electrodes were conditioned in 1 x 10^{-3} mol dm^{-3} imipramine hydrochloride for 12 h prior to use. The initial analyte solution used in the CVD was 1 x 10^{-1} mol dm^{-3} imipramine hydrochloride.
Imipramine hydrochloride was supplied by Sigma (Poole, Dorset, UK).

3.2.1.1.2 Effect of interferents on Electrode response

All measurements were performed using the constant volume dilution method (as described in section 5.1.2), the selectivity coefficients were determined using the mixed solution method (section 5.1.3).

The membranes were of the same composition as used in the calibration experiments. The interferents used were glycine, nicotinamide hydrochloride, L-histidine and 'clinical background' cations. The initial solution used consisted of 1 x 10^{-1} mol dm^{-3} imipramine hydrochloride in the presence of the required interferent. The concentration of the interferents was;

1) 'Clinical background' cations
2) 1 x 10^{-2} mol dm^{-3} Glycine with 'clinical background' cations
3) 1 x 10^{-2} mol dm^{-3} Nicotinamide with 'clinical background' cations
4) 1 x 10^{-2} mol dm^{-3} L-Histidine with ''clinical background' cations

The 'clinical background' consisted of 1.45 x 10^{-1} mol dm^{-3} NaCl, 4.3 x 10^{-3} KCl and 1.26 x 10^{-3} $CaCl_2$.

All solutions were prepared using de-ionised water.

3.2.1.2 Amperometry Experimental

3.2.1.2.1 Effect of Conditioning Potential

The working electrode of a screen printed electrode was coated with 1 μl aliquot of a solution comprising of 5 % 2,6 didodecyl-α-cyclodextrin, 40 % TECOFLEX SG80, 55.4 % *o*NPOE, 0.6 % TKB in THF. Before use, the solvent was allowed to evaporate slowly, and the electrode was soaked for 1 h in an analyte solution prior to beginning any experiments.

The analyte solutions studied were of two concentrations 1 x 10^{-3} and 1 x 10^{-4} mol dm^{-3} imipramine hydrochloride in 0.05 mol dm^{-3}, pH 7 phosphate buffer.

The voltammograms were recorded using the square wave voltammetry technique. The initial conditions used were,

Conditioning Potential: -
Equilibrium Time: 80 s
Frequency: 5 Hz
Scan Increment: 2 mV
Pulse Amplitude: 2.5 x 10^{-2} V
Voltage Range: 0 to +0.75 V

Subsequently, the method of detection was optimised by introducing conditioning potentials of +0.57 V for 20s followed by –0.2 V for 30s.

3.2.1.2.2 Calibration using Square Wave Voltammetry

A screen printed electrode was coated as described in the previous section. The equipment was configured as described in section 5.2.1). The modified electrode used was soaked for 1 h in analyte solution prior to use. The square wave voltammograms were recorded using the optimised conditions described previously.

The imipramine hydrochloride solutions used were prepared by serial dilution from 1 x 10^{-3} to 1 x 10^{-9} mol dm^{-3} in a background of 0.05 mol dm^{-3}, pH 7 phosphate buffer.

The experimental conditions detailed above were subsequently used in the investigation of desipramine and trimipramine.

3.2.1.2.3 Exhaustive Electrolysis

Exhaustive electrolysis was performed only on an imipramine solution to give information on the nature of the analyte oxidation. This was performed using the MF-1056 electrolysis cell described later (section 5.2.2). The technique used was controlled potential coulometry, the conditions used were;

Initial Potential: +0.57 V
Time: 16 h

After the electrolysis, a square wave voltammogram was recorded using the conditions described in the previous section. The solution utilised was 1 x10^{-4} mol dm^{-3} imipramine hydrochloride in phosphate buffer.

3.2.1.2.4 Effect of cyclodextrin on response

The effect of the alkylated α-, β- and γ-cyclodextrins on the electrode response was studied using desipramine. Glassy carbon electrodes were modified in two ways:

Approximately 1 µl of 1 x 10^{-2} mol dm^{-3} cyclodextrin in acetonitrile was deposited on a clean glassy carbon surface and the solvent allowed to evaporate. The cyclodextrins used were the didodecyl substituted α-, β- and γ-cyclodextrins.
A Membrane comprising of 5 % cyclodextrin, 40 % TECOFLEX SG 80, 55.4 % *o*NPOE and 0.6 % TKB in THF was deposited on a clean glassy carbon electrode surface and the THF allowed to evaporate. The cyclodextrin used was either 2,6 didodecyl-α-cyclodextrin or 2,6 didodecyl-γ-cyclodextrin.

The cyclic voltammograms were produced using the experimental configuration described in section 5.2.1. The conditions used were, scan rate 200 mV/s, scan increment 2mV, voltage range +0.2 to +1.0 V.

Before each experiment the electrode was allowed to soak for 1 h prior to the beginning of a run.

The analyte solution was 1 x 10^{-3} mol dm^{-3} desipramine hydrochloride in 0.05 mol dm^{-3}, pH 7 phosphate buffer. The phosphate buffer was supplied by BDH (Poole, Dorset).

3.2.1.2.5 pH Dependence

A screen printed electrode was modified as described in the previous section.
The pH of a 1 x 10^{-4} mol dm^{-3} trimipramine hydrochloride solution in phosphate buffer was adjusted over the pH range 6 to 9.

Over this range, the electrode response was studied using the square wave voltammetry method with the optimised conditions described in section 3.2.1.2.1.

3.3 Results and Discussion

The detection of imipramine, desipramine and trimipramine hydrochlorides were studied by both potentiometric and voltammetric methods.

3.3.1 Potentiometric Methods of Analysis

The potentiometric analysis used Philips body electrodes incorporating a polymer membranes described previously in section 3.2.

3.3.1.1 Calibration Results and Discussion

Calibration experiments using the constant volume dilution method were performed for all the antidepressants. The electrodes incorporating the alkylated cyclodextrins responded well to the presence of imipramine hydrochloride (see figure 3.3.1.1 and table 3.3.1.1), with Nernstian responses and good limits of detection (~ 10^{-5} mol dm^{-3}). A comparison of the responses from electrodes incorporating the di- and tri-alkylated γ-cyclodextrins revealed little or no difference in response due to the change in alkylation pattern. This behaviour has been observed previously for guanidine and other achiral guest molecules[18] in which the presence of the free hydroxyl had little effect on the binding of the guests. Such behaviour implies that these molecules are not involved in a hydrogen-bonding interaction with the 3-position. Instead the binding to the cyclodextrin may involve N-H donation to the 2,6-ring oxygens.

The calibration data for all the electrodes compare favourably with those obtained by the Cosofret[11] and Hopkala[12] groups. The results obtained by incorporating cyclodextrins into the electrodes gave better slopes than those reported previously by other groups[11,12] (gradients 53.3 and 51.0 mV/decade respectively for Cosofret *et al.* and Hopkala *et al.*) where the sensing was based on ion-pair association between imipramine and a lipophilic anion (e.g. dinonylnaphthalenesulphonate). The limits of detection obtained were comparable to those obtained by Hopkala (~ 10^{-5} mol dm^{-3}),

but, they were a decade lower than those reported by Cosofret with the imipramine-dinonylnaphthlane sulphonic acid ion-pair[11].

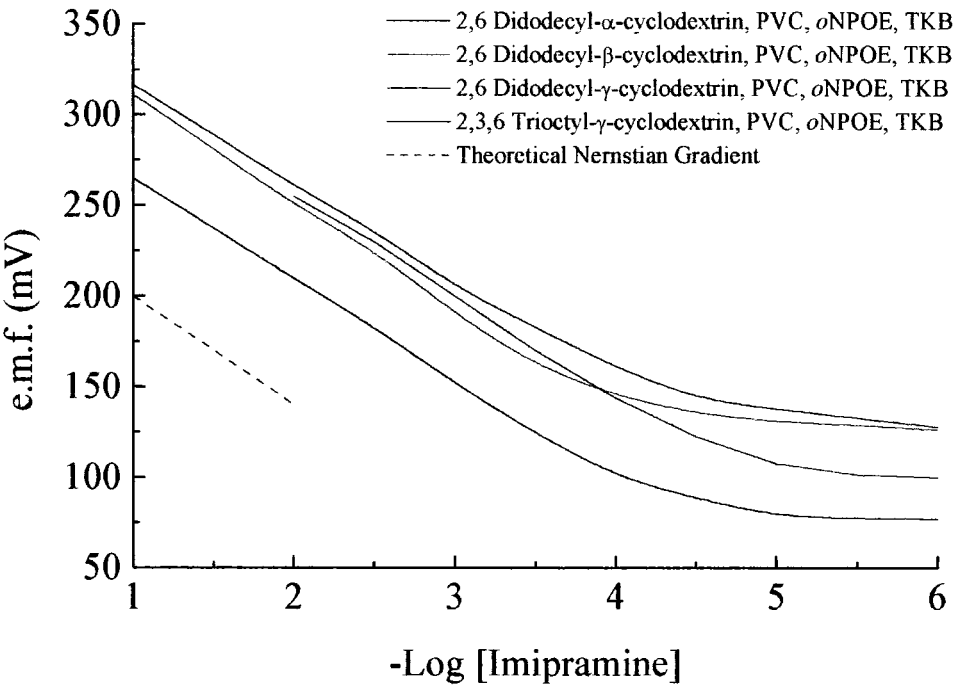

Figure 3.3.1.1. Electrode response curves for imipramine sensitive electrodes.

Ionophore	Gradient (mV/decade)	Limit of Detection (mol dm^{-3})
$2,6C_{12}\alpha CD$	54.5	2.6×10^{-5}
$2,6C_{12}\beta CD$	59.9	6.4×10^{-5}
$2,6C_{12}\gamma CD$	54.2	1.0×10^{-5}
$2,3,6C_{8}\gamma CD$	56.1	5.0×10^{-5}

Table 3.3.1.1 Imipramine Calibration Results at 298 K.

Electrodes incorporating alkylated cyclodextrins all produced excellent calibration results for the determination of desipramine hydrochloride, and gave good Nernstian

gradients and excellent limits of detection (~ 10^{-5} mol dm^{-3}). The results for the calibration are shown in figure 3.3.1.2. and table 3.3.1.2.

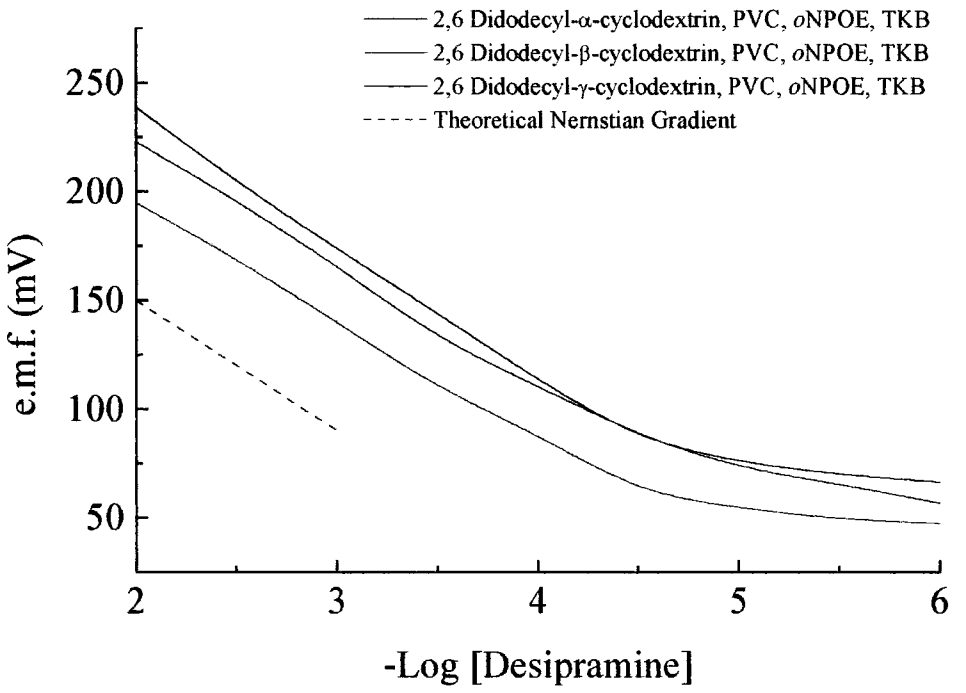

Figure 3.3.1.2. Desipramine Calibration results.

Ionophore	Gradient (mV/decade)	Limit of Detection (mol dm^{-3})
2,6C_{12}αCD	60.0	9.9 x 10^{-6}
2,6C_{12}βCD	54.5	1.6 x 10^{-5}
2,6C_{12}γCD	59.6	9.5 x 10^{-6}

Table 3.3.1.2. Desipramine Calibration Results at 298 K.

The calibration experiments performed using electrodes incorporating 2,6 didodecyl-α-, β- and γ-cyclodextrins as the ionophore for the detection of trimipramine hydrochloride produced the results shown in figure 3.3.1.3. and table 3.3.1.3. The results revealed excellent limits of detection and Nernstian gradients for both the α- and γ-cyclodextrins,

with a slightly sub-Nernstian gradient for the electrode incorporating 2,6 didodecyl-β-cyclodextrin.

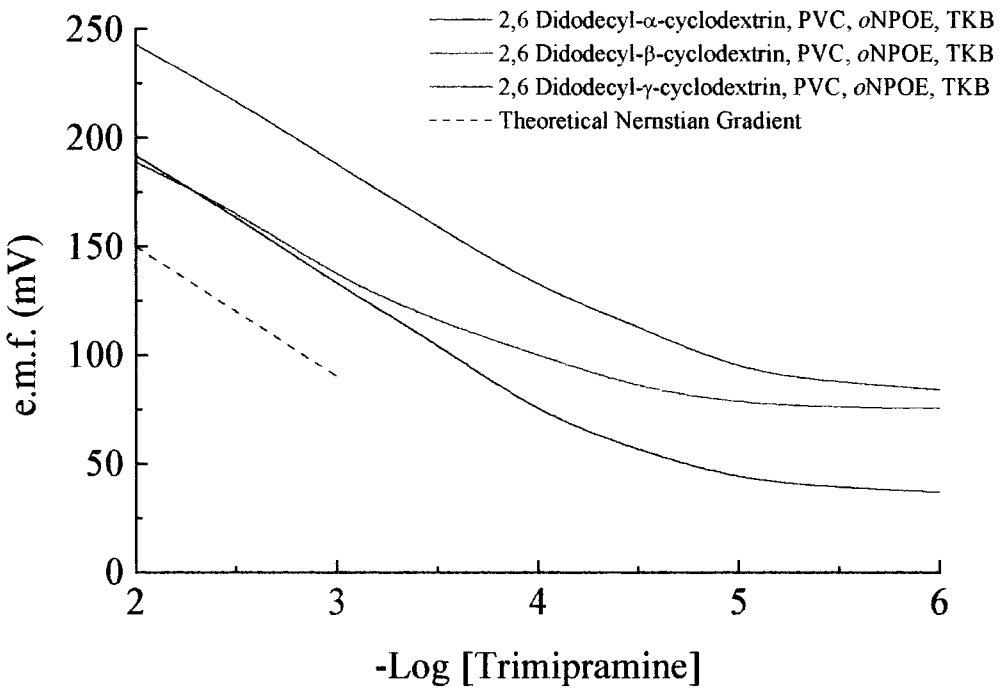

Figure 3.3.1.3. Electrode response curves for trimipramine sensitive electrodes.

Ionophore	**Gradient (mV/decade)**	**Limit of Detection (mol dm^{-3})**
$2,6C_{12}\alpha CD$	60.3	2.7×10^{-5}
$2,6C_{12}\beta CD$	47.5	4.2×10^{-5}
$2,6C_{12}\gamma CD$	57.0	1.4×10^{-5}

Table 3.3.1.3 Calibration Results for trimipramine sensitive electrode incorporating various alkylated cyclodextrin ionophores at 298 K.

3.3.1.2 Interference Studies

The interference from a variety of species found in serum on the electrode response characteristics of imipramine, desipramine and trimipramine hydrochloride sensitive electrodes was studied. The simulated 'clinical background' contained 1.45 x 10^{-1} mol dm^{-3} NaCl, 4.3 x 10^{-3} mol dm^{-3} KCl and 1.26 x 10^{-3} mol dm^{-3} $CaCl_2$ which correspond to values within the normal physiological range observed for these ions. The concentration of all other interferents (glycine, histidine and nicotinamide) was arbitrarily set at 1 x 10^{-2} mol dm^{-3}. It must be noted however that the normal physiological range of these molecules is almost 100 times lower, glycine (1.46 x 10^{-4} – 3.52 x 10^{-4} mol dm^{-3}), histidine (7.3 x 10^{-5} – 1.25 x 10^{-4} mol dm^{-3}), and nicotinamide (3.3 x 10^{-5} – 7.4 x 10^{-5} mol dm^{-3}).

The results of the electrode response from the interference studies for imipramine hydrochloride are shown in table 3.3.1.2.1. In the presence of serum levels of Na^+, K^+ and Ca^{2+} the limit of detection was unaffected. Also Nernstian response was maintained and excellent selectivity coefficients (-log K_{ij}^{Pot}, overall $\geq$ 3.6) were observed. This is consistent with the known characteristics of cyclodextrin inclusion complexes[19]. The hydrophobic nature of the cyclodextrin cavity precludes the inclusion of the charge dense cations such as those present in the serum background. The cyclodextrin prefers to include the hydrophobic, charge diffuse head group of the tricyclic molecule.

The interference from various likely interfering species on the electrode response was studied for the imipramine electrodes incorporating the alkylated cyclodextrins (table 3.3.1.2.1). With an interferent concentration of 1 x 10^{-2} mol dm^{-3} in the presence of the serum background, no interference was noted for glycine. However, the presence of both nicotinamide and L-histidine resulted in reduced gradients and poor selectivity when 2,6 didodecyl-α-cyclodextrin was the ionophore. The results have not been reported in terms of selectivity coefficients for nicotinamide since it was primarily non-ionic at the experimental pH (~ 6) and in the physiological pH (~7.4). The interference may be related to competitive inclusion in the cyclodextrin cavity. However, since the interferent is not fully ionised it can not compete with imipramine for charge induced membrane transport.

The results from desipramine electrode studies with both organic and inorganic cationic interferent molecules are shown in table 3.3.1.2.2. In the presence of serum levels of Na^+, K^+ and Ca^{2+}, the electrode response remained excellent. The limit of detection was unaffected, as was the Nernstian gradient. The selectivity coefficient for each of the electrodes studied was also good (-log K_{ij}^{Pot}, overall $\geq$ 3.6). When the organic interferents were present (glycine, nicotinamide and L-histidine) along with the serum levels of Na^+, K^+ and Ca^{2+}, the response of the electrodes was, on the whole, unaffected. For both glycine and L-histidine, their presence had effect on either the limit of detection or the gradient. With nicotinamide, the electrodes incorporating 2,6 didodecyl-α- and γ-cyclodextrin showed no interference. However, the electrode incorporating 2,6 didodecyl-β-cyclodextrin showed a significant reduction in the gradient. This may be due to competitive binding between the nicotinamide and desipramine analyte for the cyclodextrin cavity.

The effect of interferents on the trimipramine sensitive electrode are tabulated in table 3.3.1.2.3. The effect of the serum background on the electrode response was minimal, with excellent selectivity coefficients being recorded (-log K_{ij}^{Pot}, overall $\geq$ 3.7). In the presence of 1 x10^{-2} mol dm^{-3} glycine and nicotinamide (both with a background of serum cations), the response of the electrodes were unaffected with Nernstian gradients and limits of detection being maintained. However, studying the effect of L-histidine on the trimipramine electrode response was not possible due to the formation of a white precipitate.

	2,6C_{12}αCD			2,6C_{12}βCD			2,6C_{12}γCD		
Medium	**Gradient (mV/decade)**	**LD (–log c)**	**-log K_{ij}^{pot}**	**Gradient (mV/decade)**	**LD (–log c)**	**-log K_{ij}^{pot}**	**Gradient (mV/decade)**	**LD (–log c)**	**-log K_{ij}^{pot}**
aqueous	54.5	4.6	-	59.9	4.2	-	58.1	4.6	-
'clinical'	62.1	3.8	3.0	61.8	3.7	2.9	55.6	3.3	2.5
glycine+clin	54.5	3.9	-	54.1	4.1	-	58.8	4.2	-
L-histidine+clin	48.9	2.2	1.4	22.0	3.8	3.1	-	-	-
nicotinamide+clin	51.8	3.2	-	44.0	3.7	-	-	-	-

Table 3.3.1.2.1. Response in the presence of interferents for imipramine selective electrodes at 298 K.

a) clinical: 1.45×10^{-1} mol dm^{-3} NaCl, 4.3×10^{-3} mol dm^{-3} KCl, 1.26×10^{-3} mol dm^{-3} $CaCl_2$

b) LD = limit of Detection

c) –log c = -log [Imipramine]

	2,6C_{12}αCD			2,6C_{12}βCD			2,6C_{12}γCD		
Medium	**Gradient (mV/decade)**	**LD (–log c)**	**-log K_{ij}^{pot}**	**Gradient (mV/decade)**	**LD (–log c)**	**-log K_{ij}^{pot}**	**Gradient (mV/decade)**	**LD (–log c)**	**-log K_{ij}^{pot}**
aqueous	60.0	5.0	-	54.5	4.8	-	59.6	5.0	-
'clinical'	61.7	5.2	4.3	60.9	4.4	3.6	58.4	4.9	4.3
Glycine+clin	63.2	4.6	-	59.9	4.4	-	60.7	4.8	-
L-histidine+clin	59.6	4.0	3.2	60.1	4.1	4.5	59.4	4.2	3.9
nicotinamide+clin	62.3	4.6	-	44.6	5.2	-	57.9	4.7	-

Table 3.3.1.2.2. Interference results for the desipramine electrodes at 298 K.

a) clinical: 1.45×10^{-1} mol dm^{-3} NaCl, 4.3×10^{-3} mol dm^{-3} KCl, 1.26×10^{-3} mol dm^{-3} $CaCl_2$

b) LD = Limit of Detection

c) –log c = -log [Desipramine]

	2,6C$_{12}$αCD			2,6C$_{12}$βCD			2,6C$_{12}$γCD		
Medium	**Gradient (mV/decade)**	**LD (–log c)**	**-log K_{ij}^{pot}**	**Gradient (mV/decade)**	**LD (–log c)**	**-log K_{ij}^{pot}**	**Gradient (mV/decade)**	**LD (–log c)**	**-log K_{ij}^{pot}**
aqueous	60.3	4.6	-	47.5	4.4	-	57.0	4.8	-
'clinical'	64.2	4.6	3.75	53.8	5.2	4.3	51.5	5.6	4.8
glycine+clin.	63.0	4.3	-	60.3	4.6	-	63.2	4.8	-
L-histidine+clin	white ppt formed			white ppt formed			white ppt formed		
nicotinamide+clin	64.1	4.3	-	57.5	4.6	-	61.3	4.7	-

Table 3.3.1.2.3. Interference results for the trimipramine electrodes at 298 K.

a) clinical: 1.45×10^{-1} mol dm^{-3} NaCl, 4.3×10^{-3} mol dm^{-3} KCl, 1.26×10^{-3} mol dm^{-3} $CaCl_2$

b) LD = Limit of Detection

c) –log c = -log [Trimipramine]

3.3.1.3 Summary

From the results obtained for imipramine, desipramine and trimipramine hydrochlorides some general conclusions may be drawn.

The initial electrode potentials (E^0_{Init}) from the aqueous calibrations for imipramine and desipramine hydrochloride were in the order: $2,6C_{12}\alpha>2,6C_{12}\beta>2,6C_{12}\gamma=2,3,6C_8\gamma$ whereas for trimipramine the (E^0_{Init}) order was: $2,6C_{12}\gamma>2,6C_{12}\alpha>2,6C_{12}\beta$.

Such trends suggest that the Gibbs free energy of binding ($\Delta G=-nFE$) associated with the inclusion of the hydrophobic side chains of imipramine and desipramine hydrochloride in the α- and β-cyclodextrin cavities is more favourable than that of the bulkier side chain of trimipramine hydrochloride. The bulkier trimethylated side chain of trimipramine appears be more strongly bound by the larger γ-cyclodextrin cavity. An alternative hypothesis could be that due to the increased size of the γ-cyclodextrin cavity, the tricyclic moiety itself may be included rather than the less bulky side chain.

The results presented constitute the first detection method using neutral ionophores for any of these tricyclic antidepressants. The electrode response is sufficient to determine the levels of these drugs in pharmaceutical preparations (e.g. for drug quality control). However the limits of detection are not sufficiently low to allow the assay of the drugs in plasma samples, unless the dependence of potential on -log [analyte] in the non-linear region of the calibration graph can be determined. This method has been reported previously by Kereichuk[20] and used in the detection of lidocaine.

3.3.2 Amperometric Detection

Amperometric detection has the inherent advantage of a superior detection limit with respect to potentiometric detection (~ 10^{-10} mol dm^{-3} compared to ~ 10^{-6} mol dm^{-3}). Also, the tricyclic electron rich aryl moiety of these molecules appears ideal for oxidation. Indeed previous work by Bard, Faulkner and Ledwith[14] reported a two step, three electron ECE mechanism for the oxidation of these molecules.

3.3.2.1 pH Dependence

The pH of a solution containing 1 x10^{-4} mol dm^{-3} trimipramine hydrochloride in phosphate buffer was adjusted over the pH range 6-9, and the peak current was recorded for the peak at +0.18 V. The results of these studies are shown in figure 3.3.2.1.1.

It can be seen that the response of the electrode rapidly decreases both above and below pH 7. The reduced response in acidic media is consistent with the mechanism proposed by Ambrose *et al.*[21]. They showed that the oxidation of similar tricyclic compounds was via an ECE (electrochemical-chemical-electrochemical) mechanism (figure 3.3.2.1.2).

$$O_1 + n_1 e \leftrightarrow R_1$$
$$2R_1 \xrightarrow{k} O_2$$
$$O_2 + n_2 e \leftrightarrow R_2$$

Figure 3.3.2.1.2 ECE Mechanism.

We can clearly see in the scheme (scheme 3.3.2.4) that the rate of the chemical coupling step would be reduced as the acidity of the analyte solution increased, due to the involvement of protons in that step.

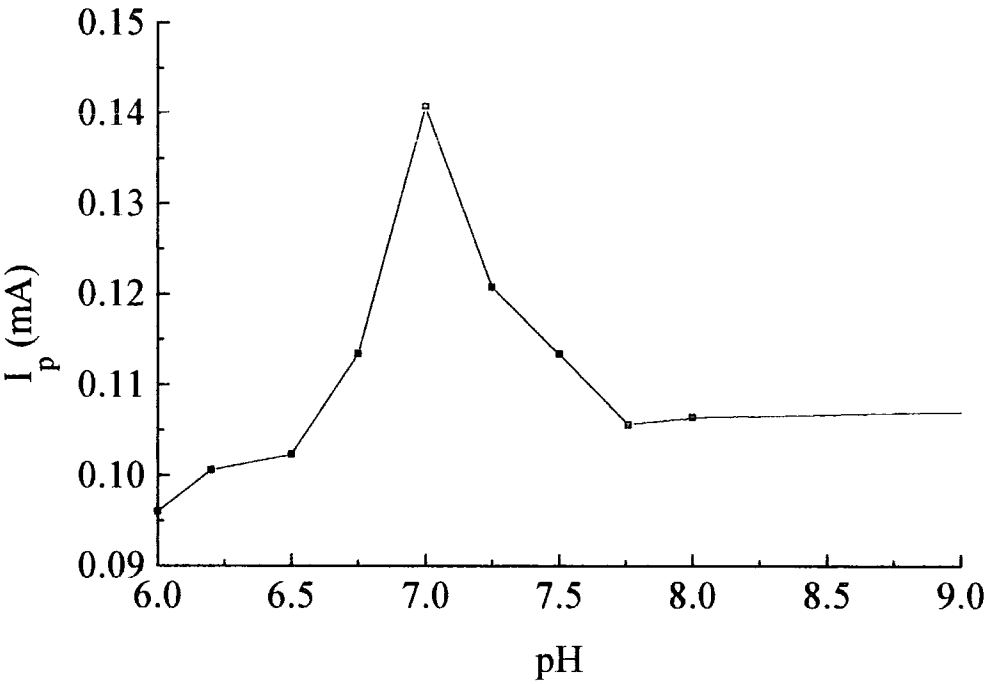

Figure 3.3.2.1.1. Peak Current Density dependence on pH for a 1 x 10^{-4} mol dm^{-3} trimipramine hydrochloride solution.

3.3.2.2 Variation of the Conditioning Potential

The optimum conditions for accumulation of the tricyclic antidepressants were initially determined using a desipramine hydrochloride solution (1 x 10^{-4} mol dm^{-3}) in a phosphate buffer (0.05 mol dm^{-3}, pH 7).

Using a bare screen-printed electrode (SPE), the square wave voltammogram (SQW) gave an initial oxidation peak at +0.57 V (vs. Ag/AgCl). This peak tended to decrease in intensity as successive runs were performed while the intensity of a second peak at +0.18 V grew (figure 3.3.2.2.1.).

When an SPE that was coated with the membrane material was used, the second peak at +0.18 V was more significant. On successive runs the height of the peak at +0.18 V increased. This suggested that as the first species was oxidised more of the second species was produced with a lower redox potential.

The signal at +0.18 V was further enhanced by applying a negative potential of –0.2 V to the electrode, after the +0.57 V (generating the monomer cation radical). This means that the optimum experimental conditions used for accumulation were 20s at +0.57 V followed by 30 s at –0.2V. The applied negative potential probably preconcentrates the cation radical, thereby reducing the decrease in peak current due to diffusion of this intermediate species.

Figure 3.3.2.2.2 shows the effect of repeated experiments using a 1 x 10^{-5} mol dm^{-3} trimipramine hydrochloride solution in phosphate buffer. As can clearly be seen the peak current density (from peak at +0.18 V) rapidly increases over the first hour of accumulation time. After this, the current density begins to decline. Such a decrease in current density was also noted by Wang *et al.* who believed that it was due to the formation of an inhibiting film. This hypothesis may be correct, since the ECE process could potentially form oligomers of greater size than a dimer. This could be facilitated by the monomer cation radical reacting with a cation monomer rather than another radical unit, leading to a radical dimer unit which could then continue reacting. These larger oligomers could potentially be a source of this inhibiting film, which reduces the current density, by physically blocking the cyclodextrin binding sites.

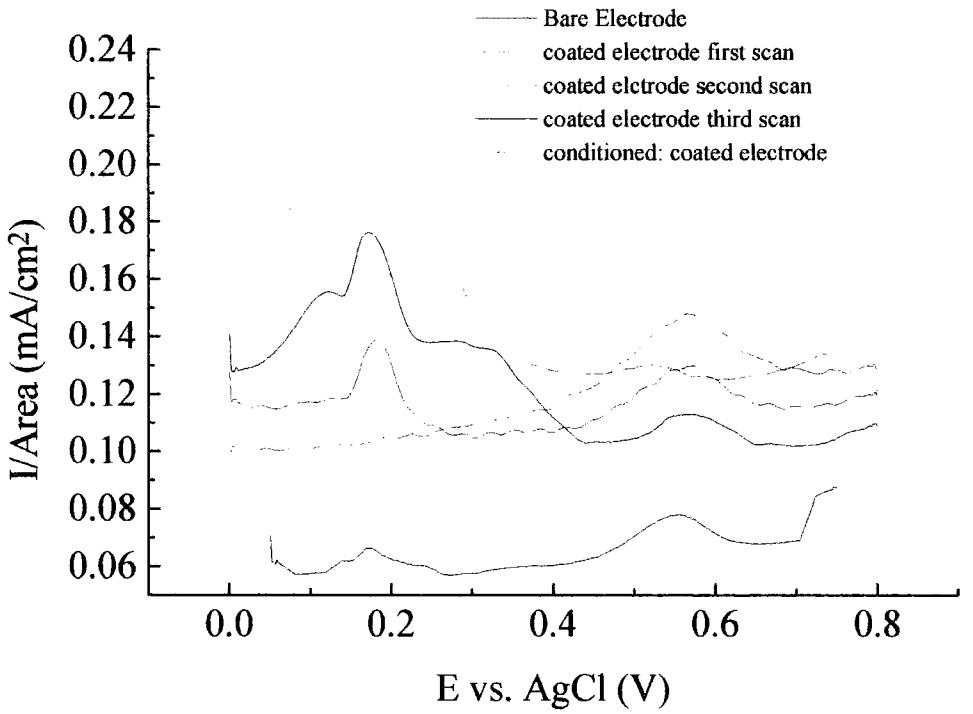

Figure 3.3.2.2.1. Effect of applying a conditioning potential to a 1 x 10^{-4} mol dm^{-3} desipramine hydrochloride solution.

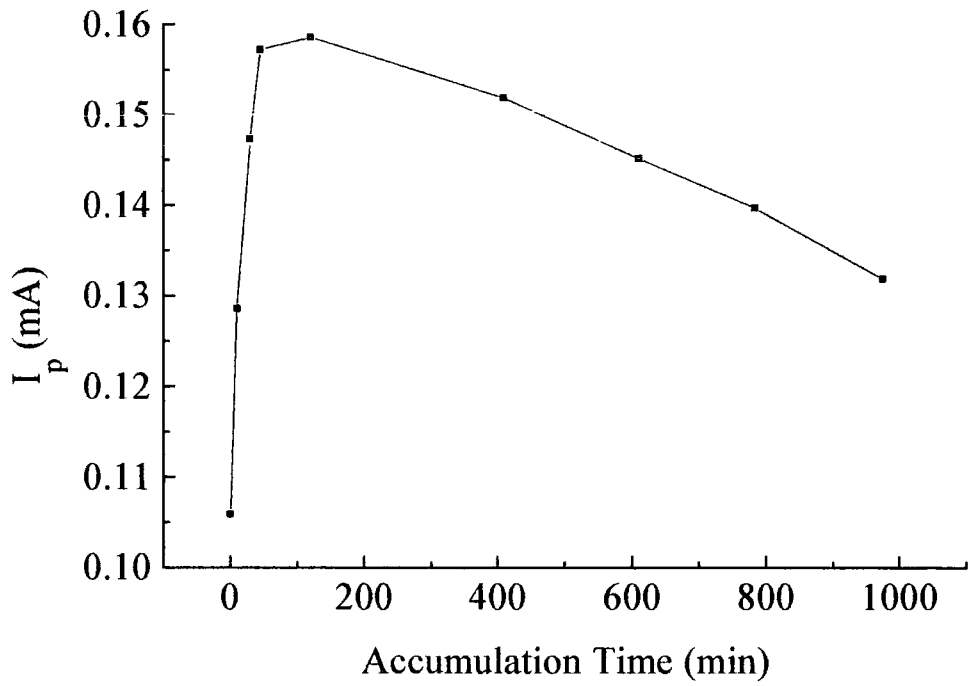

Figure 3.3.2.2.2. Variation of peak current at +0.18 V (vs. AgCl) with Conditioning Potential.

3.3.2.3 Concentration Dependence

Using the optimum conditions described in the previous section the peak current density at +0.18 V (after conditioning) was recorded for desipramine, imipramine and trimipramine hydrochlorides over the concentration range between 1 x 10^{-9} and 1 x 10^{-4} mol dm^{-3} (figure 3.3.2.3a). Shown in figure 3.3.2.3b is the electrode response from a solution containing1 x 10^{-9} to 1 x 10^{-4} mol dm^{-3} of imipramine hydrochloride.

With solutions more concentrated than 1 x 10^{-4} mol dm^{-3}, the peak at +0.18 V decreased whilst the peak at +0.57 V increased (figure 3.3.2.3c). The decrease in the +0.18 V peak is probably due to the greater production of higher molecular weight oligomers at this higher concentration; the observed shoulder may be tentatively ascribed to the production of a trimer. The position of this oxidative wave is the same as that observed in the exhaustive electrolysis of a solution containing 1 x 10^{-4} mol dm^{-3} imipramine (section 3.3.2.4).

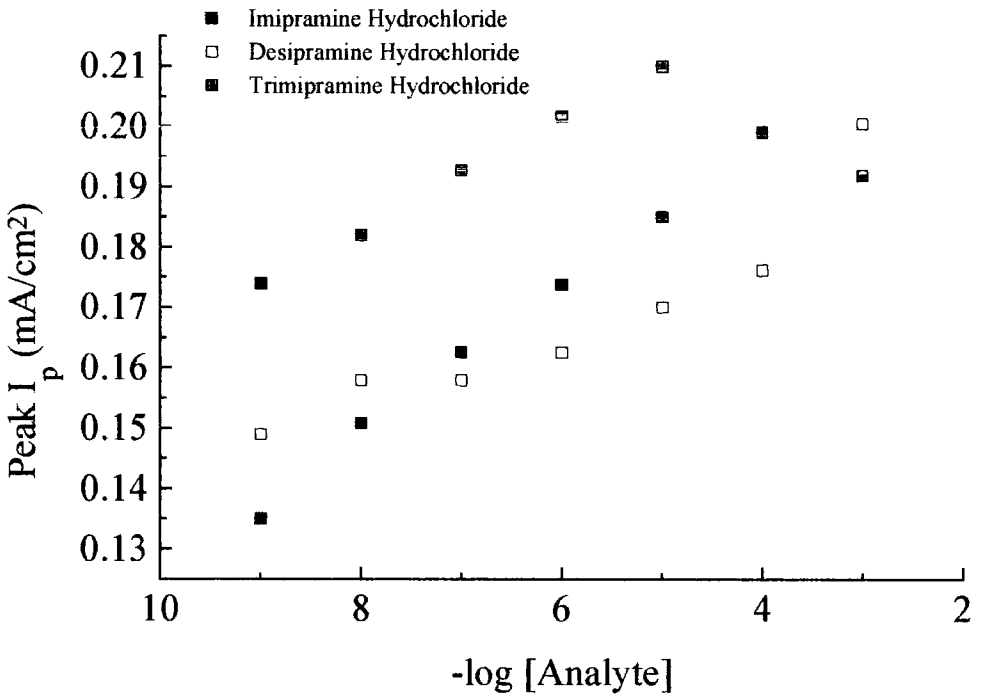

Figure 3.3.2.3a. Concentration dependence versus peak height for imipramine, desipramine and trimipramine hydrochloride in phosphate buffer.

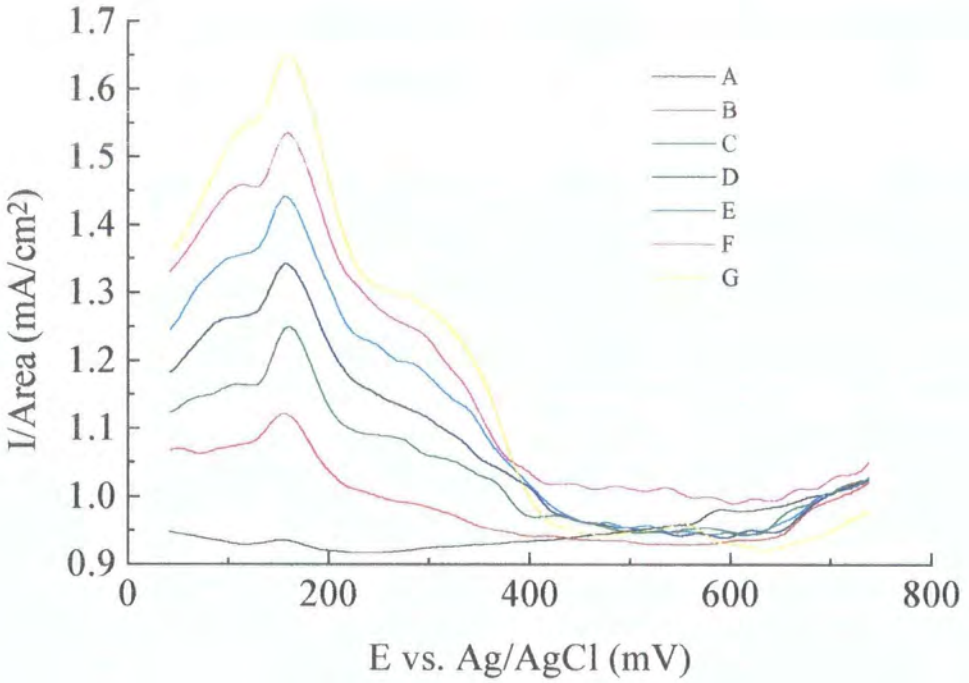

Figure 3.3.2.3b. Electrode response to varying concentration of imipramine hydrochloride in phosphate buffer (0.05 mol dm^{-3}, pH 7). A: background, B: 1 x 10^{-9} mol dm^{-3}, C: 1 x 10^{-8} mol dm^{-3}, D: 1 x 10^{-7} mol dm^{-3}, E: 1 x 10^{-6} mol dm^{-3}, F: 1 x 10^{-5} mol dm^{-3}, G: 1 x 10^{-4} mol dm^{-3}.

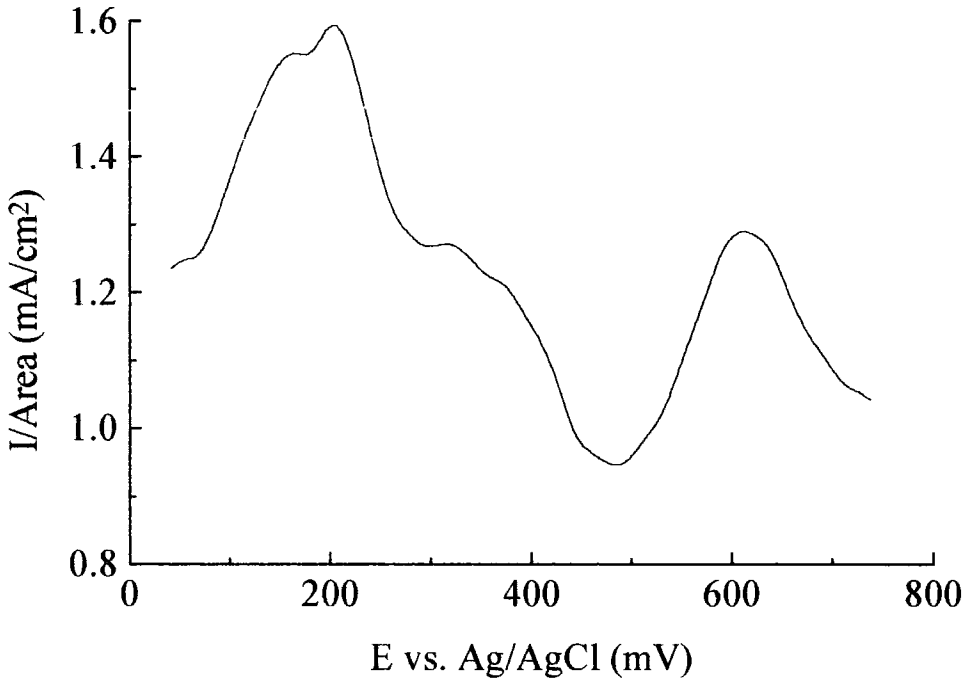

Figure 3.3.2.3c. Response trace for 1 x 10^{-3} mol dm^{-3} imipramine in phosphate buffer.

3.3.2.4 Mechanism of Detection

3.3.2.4.1 Mechanistic Analysis using Glassy Carbon Electrodes

A square wave voltammogram of a solution containing 1 x 10^{-4} mol dm^{-3} imipramine hydrochloride in phosphate buffer (0.05 mol dm^{-3}, pH 7) was run using a glass carbon electrode. Data were analysed using Model 271 Cool Kinetic Analysis Software. This data analysis showed the oxidation to be consistent with a two step ECE mechanism (scheme 3.3.2.4). The mechanistic scheme is initiated by a one electron oxidation at nitrogen with formation of a radical cation (rate limiting step). This radical ion can exist in several resonance forms. The radical cation then dimerises, and the dimerisation is accompanied by the loss of two protons per dimer (hence the pH dependence). The dimer, being more easily oxidised than the monomer, is oxidised at a lower potential (72 mV vs. Ag/AgCl) to produce the dication, with the loss of two electrons per dimer.

Figure 3.3.2.4.1.1 shows the current response obtained when performing square wave voltammetry experiments on both a fresh 1 x 10^{-4} mol dm^{-3} imipramine solution and one which had been exhaustively electrolysed at +0.57 V (vs. Ag/AgCl). The peak at 809 mV is associated with the formation of the radical cation, which then undergoes a coupling reaction to form the dimer. The dimer is then oxidised at the lower potential of 72 mV to form the stable cation. Present in the voltammogram of the electrolysed solution was another peak at 315 mV. This may be due to the oxidation of trimer molecules, formed from the dimer via a coupling reaction with another radical cation.

The results obtained using the alkylated cyclodextrin modified electrodes were also analysed. The results from three voltammograms obtained using (shown in figure 3.3.2.4.1.2);

1. A bare screen-printed electrode,
2. A modified electrode without conditioning at +0.57 V (vs. Ag/AgCl),
3. A modified electrode with conditioning at +0.57 V (vs. Ag/AgCl).

The greatly increased peak current density and enhanced sensitivity upon modification of the electrode was evident. The voltammogram without conditioning exhibited only a single peak at 550 mV (vs. Ag/AgCl). Again, this peak is consistent with a one-electron oxidation process involving the formation of a radical cation species by removal of an electron from the ring nitrogen.

However, upon applying the conditioning potential, a second peak at 178 mV (vs. Ag/AgCl) appears. The analysis of this peak shows it to be due to a two-electron oxidation, the dimer species formed after the coupling reaction is being oxidised to a cationic species. In contrast to the exhaustively electrolysed solution, there appears to be no separate third peak at 316 mV. However, the shoulder of the dimer oxidation peak is at the correct potential and does consistently increase in height, until at the highest concentration studied it does appear as an indication of a peak. As there will always be some trimer formed, the shoulder is always present in the voltammograms, although it appears only at the highest concentration.

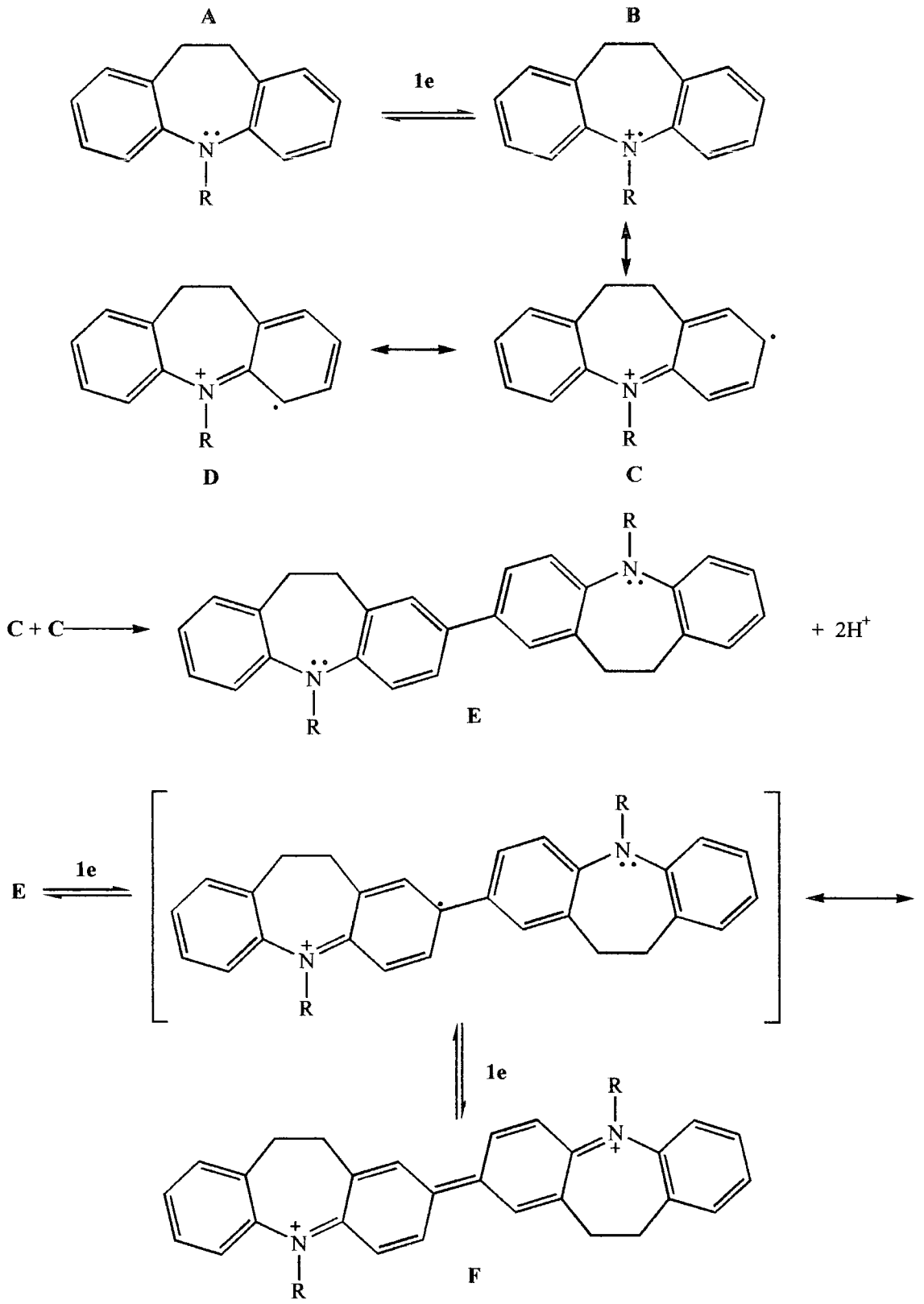

Scheme 3.3.2.4 Mechanism of imipramine oxidation.

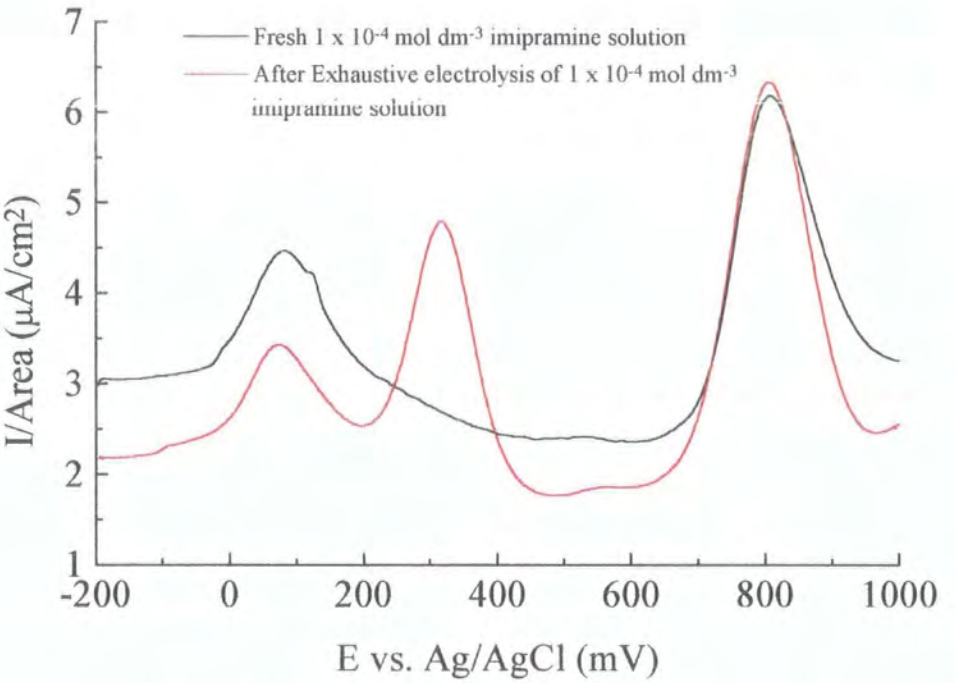

Figure 3.3.2.4.1.1. Square wave voltammogram of a 1 x 10^{-4} mol dm^{-3} imipramine solution in phosphate buffer, before and after exhaustive electrolysis.

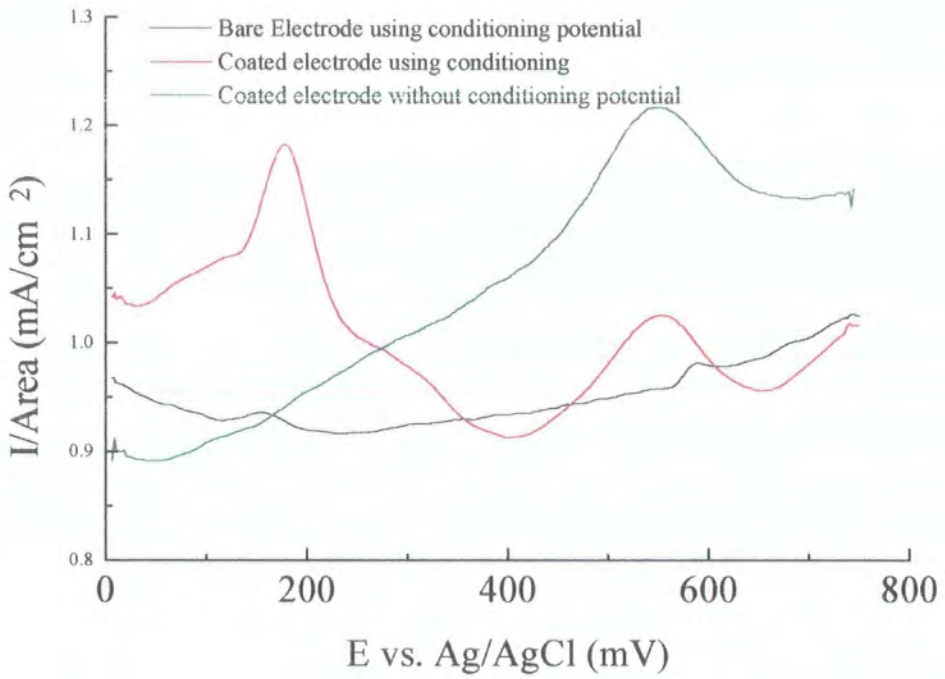

Figure 3.3.2.4.1.2. Comparison of voltammograms for a 1 x 10^{-4} mol dm^{-3} imipramine hydrochloride solution in pH 7 phosphate buffer.

3.3.2.5 Effect of the Background Electrolyte

The effect of varying the background electrolyte was studied in order to gain further insight into the mechanism. Square wave voltammograms of 1 x 10^{-4} mol dm^{-3} imipramine hydrochloride were recorded in 0.1 mol dm^{-3} NaCl (pH 6.5), 0.1 mol dm^{-3} $NaClO_4$ (pH 7.15), acetate buffer (pH 4.5), cacodylate buffer (pH 7.2) and phosphate buffer (pH 7.0) using the optimum conditions described earlier (section 3.2.1.2.1). Oxidation peaks were not observed in the presence of acetate, perchlorate or cacodylate. In a background of 0.1 mol dm^{-3} NaCl, two peaks were observed at 747 mV and 1107 mV (vs. Ag/AgCl), whose intensity varied with concentration down to 1 x 10^{-5} mol dm^{-3} imipramine hydrochloride. When a background of 1 x 10^{-3} mol dm^{-3} NaCl with increasing levels of KH_2PO_4 was used, a peak was observed at 100 mV (figure 3.3.2.5.1). The response in the presence of phosphate showed the peaks discussed earlier (section 3.3.2.3).

These results may be correlated with the variation in the lipophilicities of the anions used. Lipophilic anions are known to form relatively strong inclusion complexes with cyclodextrins via hydrophobic and/or hydrogen bonding, with larger binding constants than non-lipophilic anions (e.g. 33 dm^3 mol^{-1} for ClO_4^-[22] and 1.6 dm^3 mol^{-1} for Cl^-[23]). This relatively strong binding may block the cyclodextrin cavity and consequently prevent substrate inclusion thereby prohibiting the transport of the substrate to the electrode surface. As a consequence no redox peaks are observed. The less lipophilic anions chloride and phosphate have been shown by NMR studies to be included, only to a very small extent into α-cyclodextrin cavities[23]. Since these anions are associated with the periphery of the cyclodextrin, it is plausible that they may stabilise the radical cation once it has been formed by ion-pairing interactions. The phosphate ions are the only anions capable of facilitating the detection of very low levels of analyte. The phosphate anions, $H_2PO_4^-$ and HPO_4^{2-} can act as both hydrogen bond donors and acceptors. It seems likely that the alkylated cyclodextrin on the membrane surface has associated with it a phosphate anion that can form an ion pair with the imipramine through electrostatic and direct hydrogen bonding. The phosphate anion may then also stabilise the intermediate radical cation once it is formed.

Though the use of a chloride background also led to the detection of imipramine, the response was severely reduced (a detection limit of 1 x 10^{-5} compared to 1 x 10^{-9} mol dm^{-3} with HPO_4^{2-}).

The signal amplification observed with the modified electrodes may be due to a co-operative response. The encapsulating membrane can be considered to act as a lipophilic matrix within which large lipophilic anions (i.e. the tetraphenyl borate salt) and alkylated cyclodextrin ionophore are embedded. The cyclodextrin ionophore may form inclusion complexes with the anions (of the electrolyte solution) either strongly, hence blocking the cavity (lipophilic anions), or may be weakly associated with them, facilitating ion exchange. The cationic analyte is then attracted to the membrane surface where a small change in the electrolytic environment triggers the co-operative response. Such interactions have been widely studied in phospholipids and other biological membranes[24], and it is possible that polymer membranes with embedded anionic sites may be involved in similar interactions.

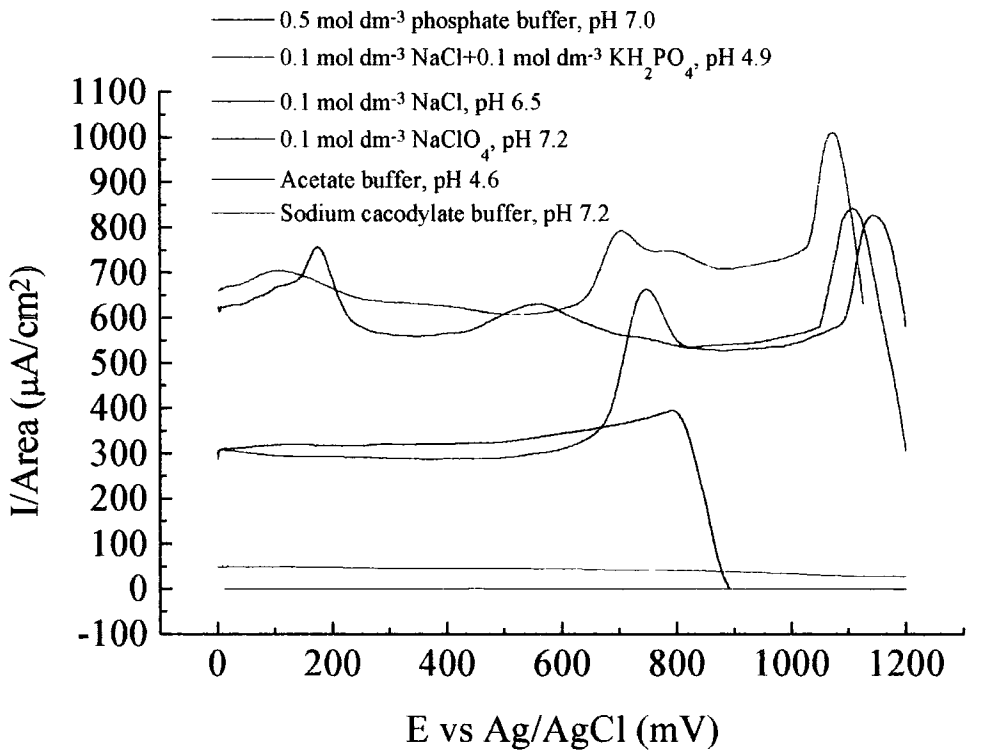

Figure 3.3.2.5.1. Effect of anions on square wave voltammograms of 1 x 10^{-4} mol dm^{-3} solutions of imipramine hydrochloride using coated screen-printed electrodes.

3.3.2.6 Summary

The interactions between cyclodextrins and tricyclic antidepressants have been studied previously[25]. However this was the first instance where modified cyclodextrins had been used to aid preconcentration of these analytes. The amperometric sensors reported showed subnanomolar levels of detection could be achieved by depositing alkylated cyclodextrins in a plasticised polymer matrix on to a screen printed carbon electrode. The resulting sensor possessed the detection limit required to facilitate detection of the analytes in clinical media.

3.4 References

1. ed. Dollery C., Therapeutic Drugs. Churchill Livingstone, London, 1991
2. Rang H. P., Dale M. M., Ritter J. M., Pharmacology. 3rd ed., Churchill Livingstone, London, 1995
3. ed. Klaus F., Analytical Profiles of Drug Substances. Academic Press, vol. 14. 1985
4. Scoggins B. A., Maguire K. P., Norman T. R., Burrows G. D., *Clin. Chem.*, 1980, **26**(1), 5-17
5. Paz L., Townshead A., *Anal. Commun.*, 1996, **33**, 31-33
6. Jourdil N., Pinteur B., Vincent F., Marka C., Bessard G., *J. Chromatogr., B.*, 1993, **613**, 59-65
7. Eap C. B., Koeb L., Baumann P., *J. Chromatogr. B.*, 1994, **652**, 97-103
8. Suckow R. F., Cooper T. B., *J. Pharm. Assoc.*, 1981, **70**(3), 257-261
9. Chen A. G., Wing Y. K., Chiu H., Lee S., Chen C. N., Chan K., *J. Chromatogr. B.*, 1997, **693**, 153-158
10. Spector S., Spector N. L., Almeida M. P., *Psychopharmacol. Commun.*, 1975, **1**, 421-429
11. Stefan R. I., Baiuescu G. E., Ionescu M. I., Enachescu I., Bunaciu A. A., Cosofret V. V., *Revista de Chimie*, 1994, **45**(10), 903-907
12. Hopkala H., Misztal G., *Pharmazie*, 1996, **51**(2), 96-99
13. Bersier P. M., Bersier J., *Electroanalysis*, 1994, **6**, 171-191
14. Frank S. N., Bard A. J., Ledwith A., *Electrochem. Soc.*, 1975, **122**, 898-904
15. Wang J., Bonakdar M., Morgan C., *Anal. Chem.*, 1986, **58**, 1024-1028
16. Biryol I., Uslu B., Kucukyavuz Z., *J. Pharm. Biomed. Anal.*, 1996, **15**, 371-381
17. Khidaru M., *Electroanalysis*, 1993, **5**, 521-523
18. Kataky R., Kelly P. M., Parker D., Patti A. F., *J. Chem. Soc., Perkin Trans.* 2, 1994, 2381-2382
19. Kataky R., Palmer S., *Electroanalysis*, 1996, **8**(6), 585-590
20. Kereichuk A. S., Pantsurkin V. I., Ptukha E. V., Potemkin K. D., Chekryshkina L. A., *Zhurnal Analiticheskoi Khimii*, 1989, **45**(3), 569-574
21. Ambrose J. F., Nelson R. F., *J. Electrochem. Soc.*, 1986, 1159-1164
22. Matsui Y., Ono M., Tokunaga S., *Bull. Chem. Soc. Jpn.*, 1997, **70**, 535-541

23. Yamashoji Y., Fujiwara M., Matsushita T., Tanaka M., *Chem. Lett.*, 1993, 1029-1032

24. Bond J. D., Huth G. C., Modern Biochemistry. Plenum Press, NY, 1986, ch. 10

25. Takisawa N., Hall D. G., Wyn-Jones E., Brown P., *J. Chem. Soc., Faraday Trans. 1*, 1988, **84**(9), 3059-3070

Chapter Four

A Study of Cyclodextrin Enantioselectivity

4.1 Introduction

The work in this chapter reports the studies performed relating to enantioselectivity in complexation with cyclodextrins. The primary analyte of interest was the β-blocker propranolol. This analyte was chosen because clinically the racemate is administered, but only the S(-) enantiomer is therapeutically active as a β-blocker[1,2]. *Therefore a means of determining the concentration of the therapeutically active enantiomer is of significant interest. Various other clinical analytes of a similar structure have also been studied, with the aim of gaining a better understanding of the nature of the enantioselectivity shown by cyclodextrins. The chiral centre of the clinical analytes was in a position β to the aromatic ring system. Another group of compounds has also been studied for purposes of comparison, including a series of benzylamine derivatives with the chiral centre α to the aromatic ring. The aim was to assess the effect of shifting the position of the chiral centre on the enantioselectivity.*

4.1.1 How to distinguish enantiomers?

It has been well known for many years that it is desirable to separate enantiomers of drug compounds because, at best, one enantiomer would be inactive and at worst, it would be toxic. A prime example of this is penicillamine where the (S)-enantiomer is an antiarthritic drug whereas the (R)-enantiomer is extremely toxic.

During the last decade, rapid progress has been achieved in the use of chiral stationary phases for both GLC and HPLC. This has been due largely to the synthesis of new chiral stationary phases which have incorporated modified cyclodextrins. Peralkylated cyclodextrins have proved to be among the most successful of the chiral stationary phases developed recently, and they have been successfully used in the separation of ephedrine enantiomers[3]. Indeed, many molecular modelling studies have been performed on such systems in an attempt to understand the mechanism of enantioselectivity[4,5].

NMR has also been used to distinguish between enantiomers. Although this technique cannot distinguish between enantiomers directly because the resonance of the enantiomeric nuclei are isochronous, diastereoisomers may be distinguished because certain resonances will be anisochronous[6]. This approach requires the use of a chiral auxiliary that will convert the mixture of enantiomers into a diastereoisomeric mixture. As long as there is a sufficiently large chemical shift non-equivalence to give a baseline resolution of the appropriate signals, then integration gives a direct measure of diastereoisomeric composition. This can then be directly related to the enantiomeric composition of the original mixture. There are three types of chiral auxiliary available (figure 4.1.1.1). Lanthanide shift reagents (LSR) and chiral solvating agents (CSA) form diastereoisomeric complexes with substrate enantiomers and may be used directly; chiral derivatising agents (CDA) require the separate formation of discrete diastereoisomers prior to NMR analysis. Care has to be taken to prevent kinetic resolution or racemisation of the derivatizing agent during derivatization[7]. Cyclodextrins have been used as chiral complexing agents to help resolve enantiomers; for example Greatbanks[8] has used β-cyclodextrin to distinguish the enantiomers of propranolol with moderate success.

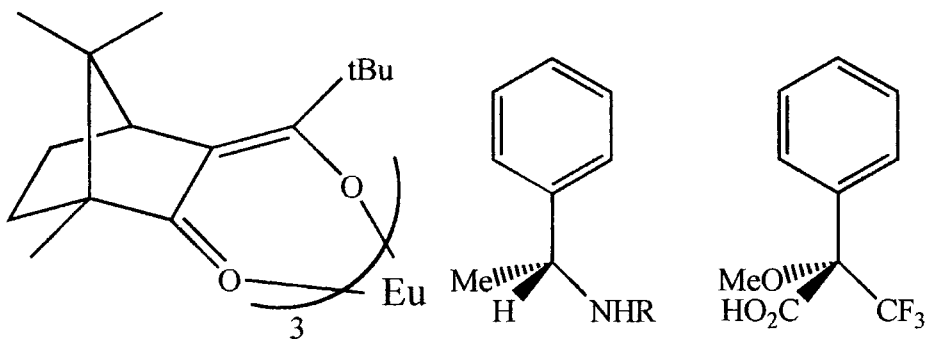

Tris(pivaloyl-d-camphorato) -Europium (Eu[pvc]$_3$) LSR

(R)-1-phenyl ethylamine CSA

(S)-MTPA CDA

Figure 4.1.1.1. Examples of Chiral Auxiliaries used in chiral NMR analysis.

Potentiometric methods of analysis have also been used for chiral discrimination. Initially these studies were focused on the discrimination of primary α-aryl ammonium ions, such as the α-phenylethyl ammonium ion. The ionophore used for such work needs to be both enantiomerically pure and sufficiently lipophilic to facilitate

incorporation in a solvent polymeric membrane. Initial research used derivatized crown ether compounds[9,10,11], which showed quite good enantiomer selectivity and some structural selectivity over competing primary ammonium ions. However, the chiral ionophores such as the crown-ether derivatives synthesised by Lehn, showed poor selectivity against alkali and alkaline earth metal ions, and were only suitable for chiral primary ammonium ions.

Another technique that has been used to differentiate between enantiomers is electrospray mass spectrometry (ESMS). Since ESMS is a 'soft' ionisation technique these weakly bound complexes are not broken up in the ionisation process. However, this technique does require either that the two enantiomers be run separately and the intensities of the signals produced compared[12], or that one of the enantiomers be deuterium labelled. This isotopic substitution allows both enantiomers to be injected simultaneously and owing to the slight mass difference, the intensities can easily be measured[13].

4.1.2 Longitudinal Relaxation and its application to the study of host-guest complexes

Longitudinal magnetisation exists due to the difference between the population of the nuclear spin states, α and β. At thermal equilibrium N_α and N_β obey the Boltzmann distribution law. After this equilibrium is disturbed by the introduction of a radio-frequency (RF) pulse, the new distributions N_α' and N_β' return to their original distributions, as a result of longitudinal relaxation which is a first order process. It follows that this relaxation involves population changes, so the processes involved are those which induce transitions between spin states. The relaxation process may be characterised by either a rate constant R_1, or its reciprocal, a relaxation time, T_1.

Longitudinal relaxation occurs through five main mechanisms (table 4.1.2.1) and the extent to which each of these mechanisms contributes to the relaxation process depends upon the species under investigation[14]. For the species used as a probe in this work, the proton, the dominant sources of relaxation are probably the dipole-dipole and spin-

rotation relaxation, though no attempt was made to investigate the relative contribution of these mechanisms.

Mechanism	Interaction	Maximum R (s^{-1})	Correlation time (s)
Quadrupolar	Electric	10^{6}	τ_θ typically 10^{-12} - 10^{-10}
Spin-Rotation	Magnetic	10^{2}	τ_θ typically 10^{-13} - 10^{-11}
Dipole-dipole	Magnetic	1	τ_θ typically 10^{-12} - 10^{-10}
Shielding anisotropy	Magnetic	10^{-1}	τ_θ typically 10^{-12} - 10^{-10}
Scalar coupling	Magnetic	10^{-1}	τ_θ typically $>10^{-6}$

Table 4.1.2.1. Summary of relaxation mechanisms.

The formation of host guest complexes has a profound effect upon the longitudinal relaxation rates of both the host and guest. The association of the molecules leads to changes to the reorientation mobility of both the host and guest, resulting in changes to τ_c (rotational correlation time) and hence R_1. The resulting changes in the relaxation rate of associated molecules have been used to help gain a clearer picture into their complexes.

Lehn and coworkers[15] used relaxation rate measurements at various temperatures and in various solvents to investigate 'bouquet-shaped' molecules based around a β-cyclodextrin core. The interest in these highly modified cyclodextrins was as bilayer ion channels. The relaxation rate measurements gave information concerning the orientation of the functionalised side chains relative to the axis of the cavity. Lipkowitz[16] used T_1 measurements in conjunction with molecular modelling to investigate the binding of tryptophan by α-cyclodextrin. The work showed some modest selectivities, related to the preferential inclusion of the (R)-enantiomer in the cyclodextrin cavity. Better enantioselectivity results were shown by this technique

when Bates[17] studied the interactions of ephedrine with 'poly'octyl-α-cyclodextrin. Significant changes in the relaxation rates of protons associated with the cyclodextrin complex of the (+)-enantiomer ($R_{1(Free)} = 5.8\ s^{-1}$, $R_{1(Bound)} = 1.2\ s^{-1}$ for ephedrine NH (8.2 ppm) proton). Taken together with other data, this implied that the (+)-ephedrine was preferentially included into this modified cyclodextrin.

4.1.3 Pulsed Gradient Spin-Echo (PGSE)

Measurement of diffusion coefficients using the PGSE technique[18] has been shown to be very useful in gaining information on the degree of association of complexing organic host guest systems. Molecular diffusion coefficients are quite sensitive to structural changes, binding and association phenomena. This method is particularly useful when the host macrocycle has a much larger molecular volume than the guest. This situation leads to a large difference in their diffusion coefficients. Upon complexation two distinct situations can occur,

a) slow-exchange between the free and bound component on the NMR timescale, which leads to the bound guest possessing a diffusion coefficient that matches that of the host.

b) fast-exchange, wherein the observed diffusion coefficient (D_{obs}) of the guest will be the weighted average of the diffusion coefficients of the free guest (D_{free}) and that of the bound guest (D_{com}) (equation 1). This allows the calculation of the association constant of the complex.

$$D_{obs} = n_1 D_{free} + n_2 D_{com};\ n_1 + n_2 = 1 \qquad (1)$$

In the experiments three distinct diffusion coefficients are measured. The diffusion coefficient for both components and for a 1:1 mixed solution. These D values are determined by measuring the intensity of a spin-echo in the presence and absence of pulsed gradients. The spin-echo is produced by the incomplete refocusing of the signal when the molecules diffuse in the presence of an applied field gradient. From the data obtained, the diffusion coefficients may be calculated using equation 2;

$$\ln\left(\frac{A_g}{A_o}\right) = -(\gamma g \delta^2)^2(\Delta - \delta/3)D \qquad (2)$$

where A_g and A_o are the echo intensities in the presence and in the absence of the pulsed gradients respectively, g is the gradient strength (Gcm^{-1}), D is the self diffusion coefficient of the observed spins (cm^2s^{-1}), δ is the length of the diffusion gradient, Δ is the time separation between the edges of the diffusion gradients and γ is the gyromagnetic ratio.

The technique has been applied widely to the investigation of host-guest association complexes[19,20]. Cohen[21] applied the technique to the study of cyclodextrin association complexes and the association constants for γ-cyclodextrin (host) with various 12-crown-4 compounds (guests) were obtained.

4.1.4 Propranolol Hydrochloride

Propranolol was the first β-blocker drug to achieve widespread therapeutic use for angina and hypertension. The therapeutic activity of the compound resides solely in the S(-) enantiomer, although the R(+) isomer has been shown to have membrane stabilising effects. The drug acts as a competitive antagonist at both the β_1 and β_2 adrenoceptors (against isoprenaline and adrenaline). In practice it reduces the effect of exercise or excitement on heart rate, cardiac output and arterial pressure. Propranolol is effective at levels of up to 300 μgl^{-1} (1 x 10^{-6} mol dm^{-3}) in plasma; levels above this lead to total β blockage and hence cardiac failure.

The preferred analytical method for determining propranolol involves the use of HPLC with a sensitivity of 2 μgl^{-1} (7 x 10^{-9} mol dm^{-3}). A variety of stationary phases have been used, only some of which have been able to resolve the enantiomers[1]. Other methods used to monitor drug levels are more indirect as they rely on measuring the heart rate and blood pressure[22].

The need to resolve, and assess the relative properties of, the enantiomers of this drug is acute. At present the racemate is used clinically. The detection method therefore requires enantiomer separation to monitor the concentration of the therapeutic enantiomer.

4.2 Experimental

The structures of the chiral analytes studies;

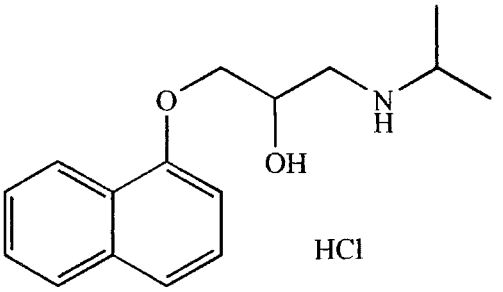

Propranolol Hydrochloride

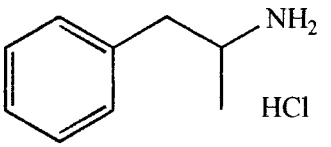

Amphetamine Hydrochloride

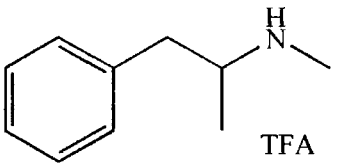

Methamphetamine Trifluoroacetate

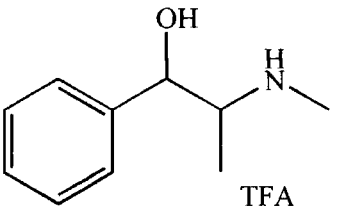

Ephedrine Trifluoroacetate

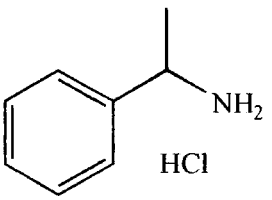

Methyl Benzylamine Hydrochloride

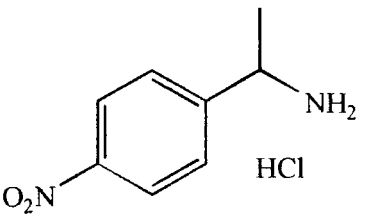

Methyl-4-nitrobenzylamine Hydrochloride

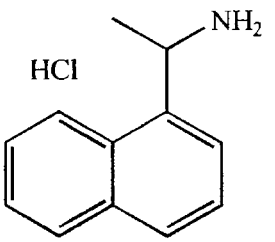

1-(1-Naphthyl)ethylamine Hydrochloride

4.2.1 Potentiometric Experimental

4.2.1.1 Potentiometric Calibration

All measurements were performed using constant volume dilution (section 5.1.2). Calibration experiments were performed with the enantiomers of propranolol, methyl benzylamine, 1-(1-naphthyl)ethylamine hydrochlorides and methyl-4-nitrobenzylamine. The membranes used were;

Propranolol:2,6 didodecyl-β-cyclodextrin (1.2 %), PVC (32.8 %), *o*NPOE (65.6 %) and TKB (0.4 %)

Amphetamine: 2,6 didodecyl-β-cyclodextrin (1.2 %), PVC (32.8 %), *o*NPOE (65.6 %) and TKB (0.4 %)

Methyl benzylamine: 2,6 didodecyl-α-cyclodextrin (1.2 %), PVC (32.8 %), *o*NPOE (65.6 %) and TKB (0.4 %)

1-(1-Naphthyl)ethylamine: 2,6 didodecyl-β-cyclodextrin (1.2 %), PVC (32.8 %), *o*NPOE (65.6 %) and TKB (0.4 %)

Methy-4-nitrobenzylamine: 2,6 didodecyl-α-cyclodextrin (1.2 %), PVC (32.8 %), BBPA (65.6 %) and TKB (0.4 %)

For each enantiomer the electroactive membranes were conditioned in 1 x 10^{-3} mol dm^{-3} analyte for 12 h prior to use.

The initial solution was 1 x 10^{-2} mol dm^{-3} analyte, and the diluent solution was de-ionized water.

R(+) and S(-) propranolol hydrochloride, S(+) and R(-) amphetamine hydrochloride, R(+) and S(-) methyl benzylamine hydrochloride, R(+) and S(-) 1-(1-naphthyl)ethylamine hydrochloride and R(+) and S(-) methyl-4-nitrobenzylamine hydrochloride were supplied by Sigma (Poole, Dorset, UK).

4.2.1.2 Interference Experiments

Interference studies were performed on the enantiomers of propranolol hydrochloride and methyl-4-nitrobenzylamine hydrochloride.

All measurements were made using the continuous volume dilution (section 5.1.2), the selectivity coefficients were determined using the mixed solution method (section 5.1.3). The membranes used were;

Propranolol: 2,6 didodecyl-β-cyclodextrin (1.2 %), PVC (32.8 %), *o*NPOE (65.6 %) and TKB (0.4 %)

Methyl-4-nitrobenzylamine: 2,6 didodecyl-α-cyclodextrin (1.2 %), PVC (32.8 %), BBPA (65.6 %) and TKB (0.4 %)

The interferents used in this work were 'clinical background' cations (1.45×10^{-1} mol dm^{-3} NaCl, 4.3×10^{-3} mol dm^{-3} KCl and 1.26×10^{-3} mol dm^{-3} $CaCl_2$) for both enantiomeric analytes. Sodium chloride, potassium chloride and calcium chloride present at a concentration of 1×10^{-2} mol dm^{-3} were also used as interferents in experiments with propranolol. The initial solutions consisted of 1×10^{-2} mol dm^{-3} analyte with the required interferent.

All the solutions were prepared using de-ionized water.

4.2.1.3 Longitudinal Relaxation Rate Measurements

Longitudinal relaxation rate measurements were performed on the following combinations of enantiomeric analytes and cyclodextrin host molecules;

1. R(+) and S(-) Propranolol with 2,6 didodecyl-β-cyclodextrin
2. S(+) and R(-) Amphetamine with 2,6 didodecyl-α-cyclodextrin
3. S(+) and R(-) Amphetamine with 2,6 didodecyl-β-cyclodextrin
4. (1S, 2R)-(+) and (1R, 2S)-(-) Ephedrine with 2,6 didodecyl-α-cyclodextrin
5. S(+) and R(-) Methamphetamine with 2,6 didodecyl-α-cyclodextrin

The solutions were prepared as described previously in section 5.3.1.

4.2.1.4 Pulse Gradient Spin Echo

The NMR diffusion experiments were performed as described earlier section 4.1.4. The host-guest complexes investigated were;

1. R(+) and S(-) Propranolol with 2,6 didodecyl-β-cyclodextrin
2. S(+) and R(-) Amphetamine with 2,6 didodecyl-β-cyclodextrin
3. (1S, 2R)-(+) and (1R, 2S)-(-) Ephedrine with 2,6 didodecyl-α-cyclodextrin
4. (1S, 2R)-(+) and (1R, 2S)-(-) Ephedrine with 2,6 didodecyl-3-methyl-α-cyclodextrin

The solutions were prepared and experiments were performed as described in section 5.3.3.

4.3 Electrochemical Response Studies

4.3.1 Propranolol, Ephedrine and Amphetamine.

The behaviour of various lipophilic cyclodextrin derivatives as ionophores for the enantiomers of these clinically relevant compounds was studied using ion-selective electrodes (figure 4.3.1.1.).

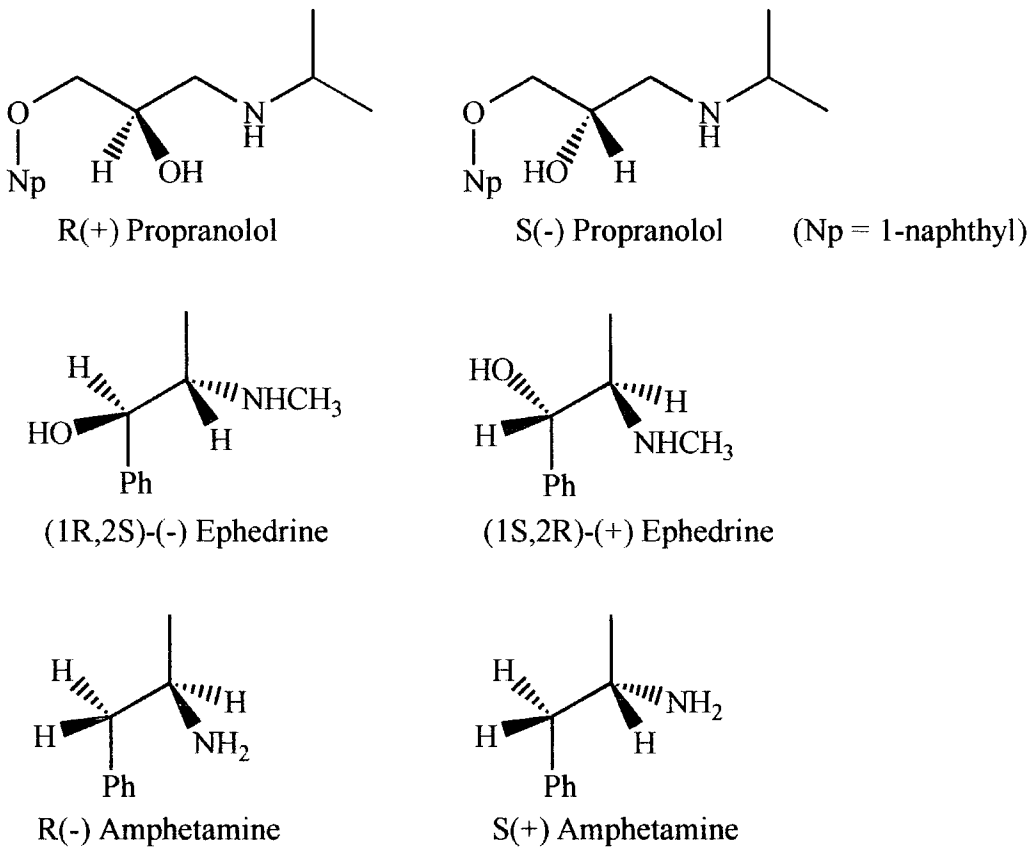

Figure 4.3.1.1. Clinically relevant chiral analytes studied.

The electrode responses to both R(+) and S(-) propranolol hydrochloride with 2,6 didodecyl-β-cyclodextrin as the ionophore were very good. The calibration experiments showed a near Nernstian response (57.0 mV/decade) and good limits of detection (~10^{-5} mol dm^{-3}) for both enantiomers. The response was also present in the presence of interfering cations. The interferents used were a simulated 'clinical background' of sodium (1.45 x 10^{-1} mol dm^{-3}), potassium (4.3 x 10^{-3} mol dm^{-3}) and

calcium (1.26 x 10^{-3} mol dm^{-3}) chlorides. Also used were the individual constituents of the clinical background at a concentration of 1 x 10^{-2} mol dm^{-3}. These interferents caused no effect on the electrode response: in all cases studied Nernstian responses and excellent limits of detection were observed (table 4.3.1.1.). This behaviour was characterised by the excellent selectivity coefficients that were achieved, $-\log K_{ij}^{pot}$, overall ≥ 4.0 against clinical background and $-\log K_{ij}^{pot} \geq 3.5$ for the individual interferents. In each case the initial potential was recorded, and the reading was significantly higher for the R(+) enantiomer with respect to the S(-). This showed that the ionophore was more sensitive towards the (+) than the (-) enantiomer. For propranolol this difference in the measured electrode potential (ca. 30 mV) corresponded to a free energy difference of 2.9 kJ mol^{-1}

$$\Delta E_{+/-} = E_{Initial_+} - E_{Initial_-} \qquad (1)$$

$$\Delta G_{+/-} = -nF\Delta E_{+/-} \qquad (2)$$

In addition, a good enantioselectivity $K_{+/-}$=3.2 was found ($K_{+/-} = E_{R+} - E_{S-}/S$), where $E_{R+} - E_{S-}$ is the difference in initial potentials for the R(+) and S(-) sensitive electrodes, and S is the gradient[9].

It is likely that the (+)-propranolol interacts more favourably with the cyclodextrin than the (-) diastereoisomeric complex. The small free energy difference of 2.9 kJ mol^{-1} is consistent with the energies associated with a single hydrogen-bonding interaction. This stabilising interaction could conceivably be present in the (+)-propranolol cyclodextrin complex and absent in the diastereoisomeric complex.

R(+) Propranolol Hydrochloride				
	Initial E (mV)	**Gradient (mV/decade)**	**Limit of Detection (mol dm^{-3})**	**-log K_{ij}**
Calibration	251	57.5	2.9×10^{-5}	
'Clinical'	301	56.1	1.4×10^{-5}	4.0
Na^+	258	55.6	9.1×10^{-6}	4.0
K^+	293	60.9	1.7×10^{-5}	3.8
Ca^{2+}	327	33.1	3.3×10^{-5}	3.5

S(-) Propranolol Hydrochloride				
	Initial E (mV)	**Gradient (mV/decade)**	**Limit of Detection (mol dm^{-3})**	**-log K_{ij}**
Calibration	239	57.0	1.1×10^{-5}	
'Clinical'	270	61.9	7.9×10^{-6}	4.3
Na^+	239	57.3	6.9×10^{-6}	4.2
K^+	261	62.7	1.6×10^{-5}	3.8
Ca^{2+}	264	30.6	2.3×10^{-5}	3.6

Table 4.3.1.1. Response of ISEs incorporating 2,6 didodecyl-β-cyclodextrin to R(+) and S(-) propranolol hydrochloride. 'Clinical' is a simulated background of clinical ions as chloride salts (1.45×10^{-1} mol dm^{-3} Na^+, 4.3×10^{-3} mol dm^{-3} K^+, 1.26×10^{-3} mol dm^{-3} Ca^{2+}). The initial potentials were recorded at 298 K relative to an external calomel reference electrode connected by a saturated KCl salt bridge.

The electrochemical results for S(+) and R(-) amphetamine hydrochloride also showed excellent response characteristics with 2,6 didodecyl-β-cyclodextrin as the ionophore. The electrodes showed a Nernstian response (~ 61 mV/decade) and reasonable limits of detection (LD $\geq 2.4 \times 10^{-4}$ mol dm^{-3}). The results with the ionophore were significantly better than those previously reported[17] when 'poly'octyl-α-cyclodextrin (contains 15.4 octyl groups and 2.6 OH groups on average[23]) was used as the ionophore. This may be due to several factors. One such factor is that is that it may be preferable for amphetamine to be included in the more rigidly defined dialkylated cyclodextrin (due to the complete retention of the 3[OH]—[O]2 intramolecular hydrogen bonding) rather

than the more conformationally mobile 'poly'alkalyted host (table 4.3.1.2). Analysis of the results for both ionophores showed better results for the (+) enantiomer, inferring the existence of some additional interaction between the (+) enantiomer and cyclodextrin that was not present in the diastereoisomeric complex.

Ionophore: 2,6 Didodecyl-β-cyclodextrin				
	Initial E (mV)	**Gradient (mV/decade)**	**limit of detection (mol dm^{-3})**	$\Delta E_{E_+ - E_-}$ **(mV)**
S(+) amphetamine	322	61.3	2.4×10^{-4}	35
R(-) amphetamine	283	62.4	3.5×10^{-5}	
Ionophore: 'poly'octyl-β-cyclodextrin[17]				
	Initial E (mV)	**Gradient (mV/decade)**	**limit of detection (mol dm^{-3})**	$\Delta E_{E_+ - E_-}$ **(mV)**
S(+) amphetamine	215.5	50.0	2.5×10^{-4}	88.5
R(-) amphetamine	127.0	37.0	unstable	

Table 4.3.1.2 Calibration results for S(+) and R(-) amphetamine hydrochloride at 298 K.

Further experiments were carried out on (+) and (-) ephedrine hydrochloride using the dialkylated cyclodextrin 2,6 didodecyl-α-cyclodextrin, allowing comparison with the results using 'poly'octyl-α-cyclodextrin obtained previously[17]. The results with the new ionophore showed the same trend as noted previously for this analyte and with the other analytes studied in this section. A slightly sub-Nernstian response was obtained (55.0 and 54.0 mV/decade respectively for (+) and (-) enantiomers). The limits of detection were unstable with respect to time (table 4.3.1.3). From the initial potentials recorded (E^o_{init}), the (+) ephedrine appears to be the preferred guest, with a difference in the initial potentials of 9mV. Whilst this result was in the same sense as observed using the 'poly'octyl cyclodextrin, the ΔE value has been reduced. In addition, the difference in free energies calculated from the electrochemical and PGSE data (see section 4.3.3) are not consistent (though both data sets show the (+) enantiomer to be the more stable).

This could be related to the instability of the electrochemical response obtained for both enantiomers, leading to a ΔE value that was smaller than expected.

Ionophore: 2,6 Didodecyl-α-cyclodextrin[a]				
	Initial E (mV)	**Gradient (mV/decade)**	**Limit of detection (mol dm^{-3})**	$\Delta E_{E_+ - E_-}$ **(mV)**
(1S,2R)-(+) Ephedrine	343.0	55.0	Unstable	9
(1R,2S)-(-) ephedrine	335.0	54.0	Unstable	
Ionophore: 'poly'octyl-α-cyclodextrin[b]				
	Initial E (mV)	**Gradient (mV/decade)**	**Limit of detection (mol dm^{-3})**	$\Delta E_{E_+ - E_-}$ **(mV)**
(1S,2R)-(+) Ephedrine	233	60.0	2.5×10^{-7}	26
(1R,2S)-(-) ephedrine	207	50.0	5.0×10^{-7}	

Table 4.3.1.3. Calibration results and enantioselectivity values for (+) and (-) ephedrine hydrochloride at 298 K. [a] membrane composition, ionophore, PVC, *o*NPOE, TKB. [b] membrane composition, ionophore, PVC, BBPA, TKB.

4.3.2 Benzylamine Derivatives

A series of chiral α-methyl-benzylamine derivatives was studied (figure 4.3.2.1) in an attempt to gain some insight into the nature of their binding interaction with lipophilic cyclodextrins.

The response to R(+) and S(-) methyl benzylamine was studied using 2,6 didodecyl-α-cyclodextrin. As can be seen from the results shown (table 4.3.2.1.) the (+) enantiomer showed a Nernstian response (60.9 mV/decade), with a good limit of detection (8.9×10^{-5} mol dm^{-3}). The S(-) enantiomer showed a super-Nernstian response (64.6 mV/decade) and a comparable limit of detection to that of the (+) enantiomer (8.9×10^{-5} mol dm^{-3}). However, the difference in initial potentials apparently favours the (-) enantiomer. The response to these analytes was poorer than that observed for the clinical analytes discussed above (section 4.3.1). Also, the sensitivity of the cyclodextrins appears to favour inclusion of the (-) enantiomers, as opposed to the (+)

ones noted in the clinical analytes. It must be remembered that in these compounds the chiral centre is α to the aromatic group, in contrast to the amphetamine series of molecules, where it was β.

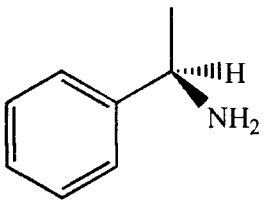

R(+)-α-Methyl benzylamine

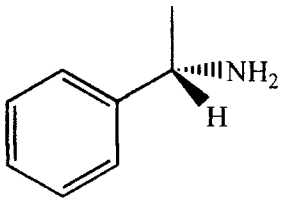

S(-)-α-Methyl benzylamine

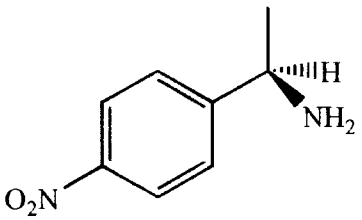

R(+)-α-Methyl-4-nitrobenzylamine

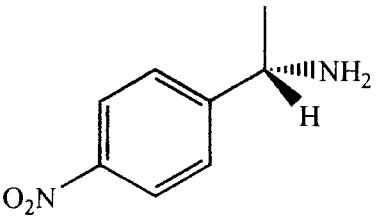

S(-)-α-Methyl-4-nitrobenzylamine

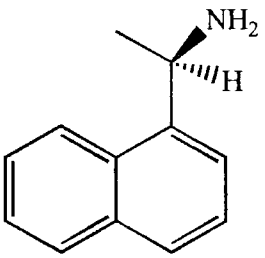

R(+)-1-(1-Naphthyl)ethylamine

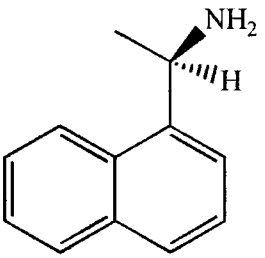

S(-)-1-(1-Naphthyl)ethylamine

Figure 4.3.2.1. Chiral α-methyl-benzylamine and naphthylethylamine derivatives studied.

	Initial E (mV)	Gradient (mV/decade)	Limit of Detection (mol dm^{-3})	$\Delta E_{E_+ - E_-}$ (mV)
R(+) Methyl benzylamine	213	60.9	8.9×10^{-5}	13
S(-) Methyl Benzylamine	231	64.6	8.9×10^{-5}	

Table 4.3.2.1 Calibration and enantioselectivity results for R(+) and S(-)-α-methyl benzylamine at 298 K. Membrane composition, 2,6 didodecyl-α-cyclodextrin, PVC, *o*NPOE, TKB.

Calibration and a limited set of selectivity measurements were performed with R(+) and S(-) methyl-4-nitrobenzylamine (table 4.3.2.2). It was also decided to observe the effect of changing the plasticizer from the phenolic *o*NPOE to the non-aromatic BBPA, since it is not unreasonable to hypothesise that the cyclodextrin cavity may include the *o*NPOE and hence affect the electrodes response characteristics. Indeed α-cyclodextrins have been by shown Inoue[24] to include *o*-nitrophenol. The results (table 4.3.2.2) revealed that changing the plasticizer from *o*NPOE to BBPA had only a minor effect upon the electrode response. A slight increase in the limit of detection for both analytes was found. One notable effect of changing the plasticizer was to increase the $\Delta E_{-/+}$ value from 6mV to approximately 30 mV. This change may be related to the removal of the competing inclusion of the plasticizer. The selectivity coefficients recorded for both enantiomers were good in a simulated clinical background ($-\log K_{ij}^{pot}$, overall ≥ 2.6).

The R(+) and S(-) enantiomers of the 1-(1-naphthyl)ethylamine (NEA) molecule were also examined. The calibrations were performed using 2,6 didodecyl-β-cyclodextrin as the ionophore. Results for both enantiomers (table 4.3.2.3) showed a super-Nernstian gradient (68 mV/decade and 66.3 mV/decade for R(+) and S(-) respectively) with moderate limits of detection. Again, comparison of the initial electrode potentials (E_{init}^{o}) for both enantiomers showed that the (-) diastereoisomeric pair was bound more strongly (higher E_{init}^{o} value).

S(-) Methyl-4-nitrobenzylamine					
Plasticizer		**Initial E (mV)**	**Gradient (mV/decade)**	**LD (mol dm^{-3})**	**-log K_{ij}^{pot}**
BBPA	**Calibration**	252	61.8	1.5×10^{-6}	
	Clinical	241	59.9	3.8×10^{-4}	2.6
***o*NPOE**	**Calibration**	240	60.3	1.2×10^{-5}	
R(+) Methyl-4-nitrobenzylamine					
Plasticizer		**Initial E (mV)**	**Gradient (mV/decade)**	**LD (mol dm^{-3})**	**-log K_{ij}^{pot}**
BBPA	**Calibration**	220	61.3	6.7×10^{-6}	
	Clinical	214	55.6	2.8×10^{-4}	2.7
***o*NPOE**	**Calibration**	234	60.7	1.4×10^{-5}	

Table 4.32.2 Calibration and selectivity data for R(+) and S(-) methyl-4-nitrobenzylamine hydrochloride at 298 K. LD = Limit of Detection.

	Initial E (mV)	**Gradient (mV/decade)**	**Limit of detection (mol dm^{-3})**	$\Delta E_{E_- - E_+}$ **(mV)**
R(+) NEA	219	67.7	1.2×10^{-4}	33
S(-) NEA	252	66.3	1.1×10^{-5}	

Table 4.3.2.3. Calibration and enantioselectivity results for R(+) and S(-) 1-(1-naphthyl)ethylamine at 298 K. Membrane composition, 2,6 didodecyl-β-cyclodextrin, PVC, *o*NPOE, TKB.

It may be that the pendant arm of the S(-) enantiomer is able to rotate into such an orientation, that the interactions between it and the cavity rim are less unfavourable than for the R(+). When the chiral centre is further away from the aromatic group, as in the clinical analytes, the additional rotational freedom may allow the (+) enantiomers to gain a more compatible orientation with respect to the cyclodextrin.

4.3.3 Summary

These electrode response studies serve to highlight the level of enantiodifferentiation in working potentiometric electrodes. When the chiral centre is α to the aryl group, the S(-) enantiomer was bound more strongly, whereas with a chiral centre β to the aryl group, the (+) enantiomer is always the more strongly bound. To determine why this should be the case requires the use of methods of analysis that probe solution structure directly, such as NMR.

4.4 Solution NMR Studies of Host Guest Complexes

NMR may be applied as a powerful tool in the study of the inter- and intra- molecular interactions often present in cyclodextrin inclusion complexes. Various NMR techniques have been used to study the interactions between 2,6 didodecyl-α- and 2,6 didodecyl-β-cyclodextrins with different arylammonium ions. All of the NMR spectra were obtained in $CDCl_3$ solutions, using the trifluoroacetate salts of the chiral arylammonium ions.

4.4.1 Chemical Shift Effects

Monitoring the effects of complexation by observing changes in the chemical shift of selected resonances in host guest complexes is a widely used technique[25,26,27]. The inclusion of a guest into the cavity of cyclodextrin will affect the local magnetic environment of protons H_3 and H_5 on the inside of the cavity, as well as those of the guest molecule. This alteration in the proton environment leads to a change in the chemical shift of the relevant signals. Such changes can provide information on the relative orientations and interactions between the host and guest molecules.

Earlier studies[17] using FTIR and NMR reported the behaviour of complexes of ephedrine with 'poly'octyl-α-cyclodextrin. These studies identified the existence of a strong intramolecular NH---OH interaction in both the free and bound states. The diastereotopic NH_2 hydrogens in the ephedrine trifluoroacetate were highly anisochronous in $CDCl_3$ ($\Delta\delta$ = 1.03 ppm), which is consistent with the preferential

population of a single conformation where the two hydrogens are in inequivalent magnetic environments. When the cyclodextrin was added, the (+) ephedrine (molar ratio 1:2.5 host:guest at 298 K) showed an increase in the shift non-equivalence to 1.17 ppm, with the higher frequency NH proton (9.42 ppm) shifted to higher frequency when bound (9.53 ppm), whereas the (-) ephedrine showed no change. This suggested that N-H interactions were important in determining the relative structures of the two diastereoisomeric complexes, possibly involving intermolecular hydrogen-bonding of one of the NHs to the cyclodextrin host. This interpretation agrees with the results of NMR titration experiments performed by Petersheim[28] which provided evidence showing that the ammonium group of ephedrine (and pseudoephedrine) underwent hydrogen-bonding interactions with the secondary oxygens of β-cyclodextrin. The studies showed the 2' and 3' hydroxyl resonances of the β-cyclodextrin undergo exchange broadening with increasing concentration of drug, the degree of exchange broadening was dependent upon the drug enantiomer present.

In this work, the study has been extended to include several other β-arylammonium cations. In addition, a further study of ephedrine, using 2,6 didodecyl-α-cyclodextrin as host has been undertaken in order to gain further understanding of the inclusion process.

The ^{1}H NMR spectra of propranolol (298 K, $CDCl_3$) clearly shows the diastereotopic ammonium protons are anisochronous ($\Delta\delta$ = 1.07 ppm) in the free state (figure 4.4.1.1). This could be due to the presence of intramolecular hydrogen bonding, which was supported by the observation of a weak IR band at 3590 cm^{-1} in solution, whose position was independent of concentration (figure 4.4.1.2). Upon complexation with 2,6 didodecyl-β-cyclodextrin, the shift non-equivalence was 1.04 ppm for both enantiomers. However, for the complex with the R(+) enantiomer the shifts were 0.08 and 0.09 ppm to higher frequency, whilst in the complex with S(-) propranolol, shifts of 0.01 and 0.05 to lower frequency were observed for NH_a and NH_b (NH_a denotes the proton resonating at higher frequency than NH_b). This behaviour can be seen in figure 4.4.1.3.

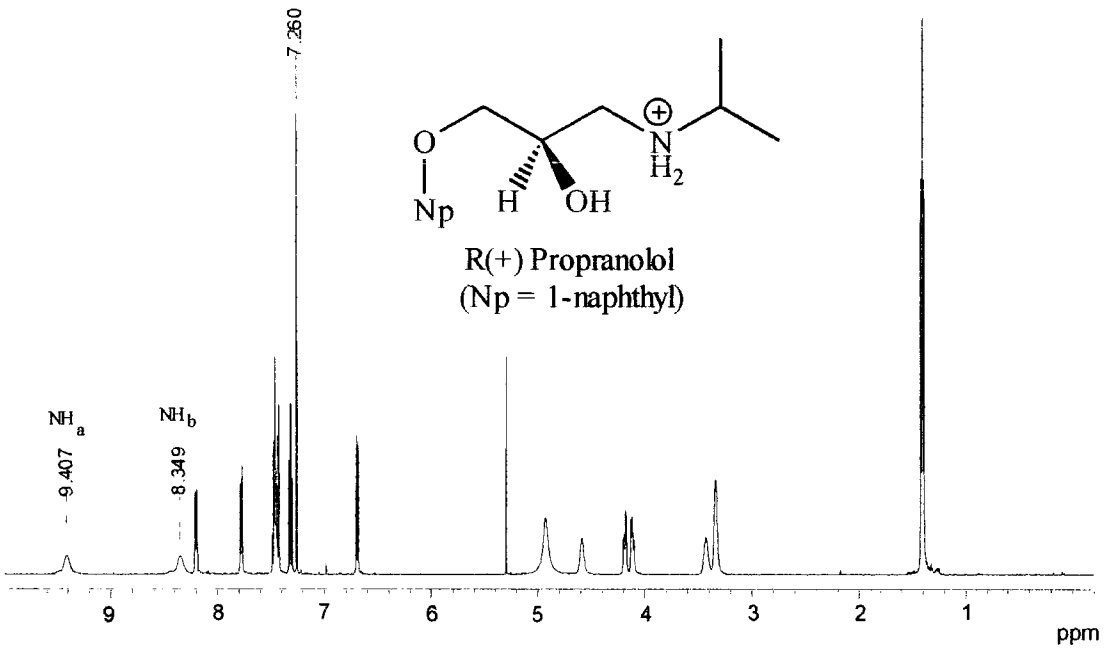

Figure 4.4.1.1. ^{1}H NMR of R(+) Propranolol, showing the anisochronous NH_2 protons.

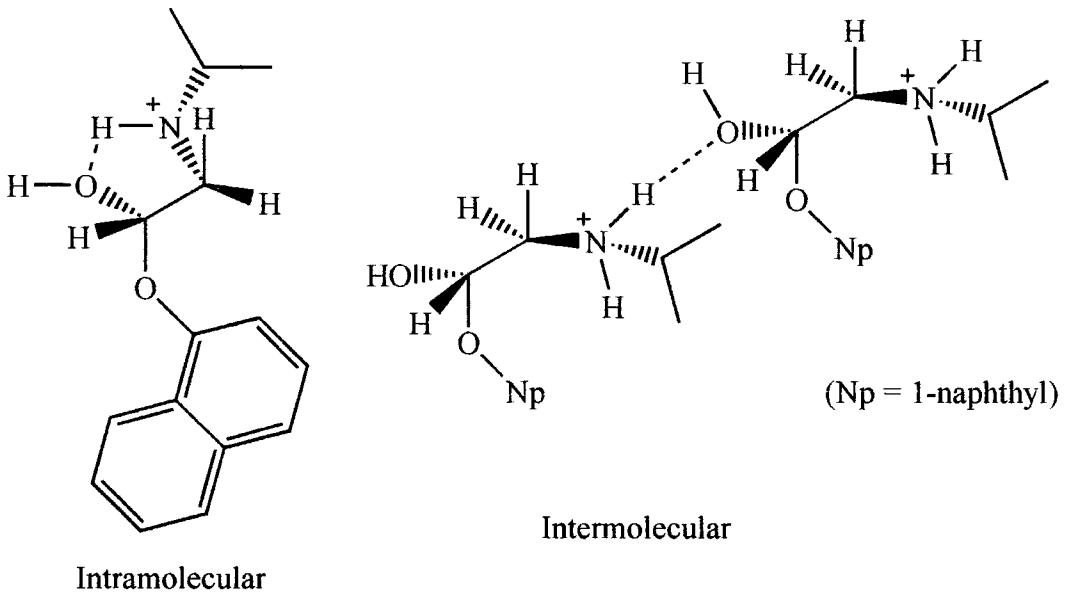

Figure 4.4.1.2. Intra- and Inter- molecular +N-H—O hydrogen bonding in Propranolol.

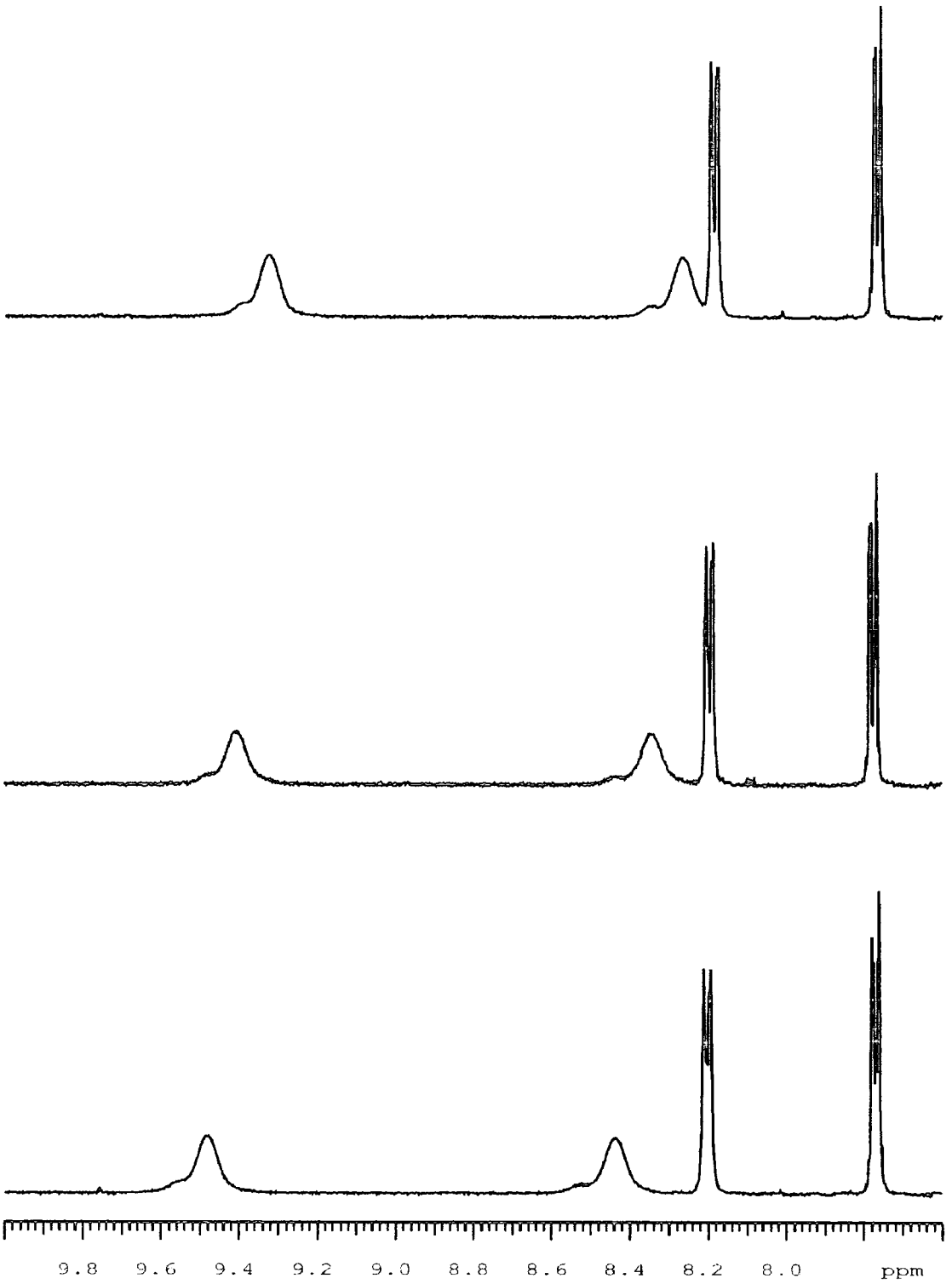

Figure 4.4.1.3. Changes in the ^{1}H NMR spectra of protonated propranolol in the presence of 2,6 didodecyl-β-cyclodextrin. R(+) propranolol, lower; S(-) propranolol, upper; no cyclodextrin, centre.

This behaviour is consistent with the formation of a slightly more well defined hydrogen bonded structure in the complex of (+) with respect to that formed between (-) propranolol and the cyclodextrin.

Unfortunately, due to the complexity of the spectra, and the overlap of certain signals, changes in coupling constants could not be measured with any confidence, to allow information to be acquired on any rotational changes in the pendent arm upon complexation. Also, observation of the chemical shifts of the aryl region proved inconclusive (indeed as it would for this entire series of compounds) since any shift changes that occurred were very small. For all these complexes changes in the chemical shifts of H_3 and H_5 of the cyclodextrin could be envisaged since they are situated on the interia of the cyclodextrin cavity. Indeed, a study of these protons has led to hypotheses about the direction and depth of guest inclusion into the cavity[25,27]. Unfortunately in the case of the complexes of propranolol with 2,6 didodecyl-β-cyclodextrin (due to peak overlap), it was impossible even at 500 MHz to discern which protons were due to H_3 or H_5.

In the case of amphetamine it was found (table 4.4.1.1) that the ammonium proton signal shifted to higher frequency for both enantiomers in the presence of both 2,6 didodecyl-α- and β-cyclodextrin. The change was greater for the complexes with the alkylated β-cyclodextrin. The shift was probably due to formation of hydrogen bonds between the ammonium group and the oxygens of the secondary hydroxyls in the cyclodextrin. The changes were greater for the complex with β-cyclodextrin, showing that the environment of those protons was being affected to a greater extent, probably due to a better size fit between the analyte and host. The changes in the position of the H_3 signal (4.01 ppm) could this time be measured (though H_5 (3.8 ppm) was still unavailable due to peak overlap). Although both the alkylated α- and β-cyclodextrin hosts induced a change in the chemical shifts of the ammonium protons of amphetamine (table 4.4.1.1), only the complex with 2,6 didodecyl-α-cyclodextrin showed any enantioselectivity. The slight difference may be due to different orientations of the guest aromatic within the cavity. This variation in guest orientation may still be present in the β-cyclodextrin complex but the poorer host-guest fit probably means it does not affect the signals to such an extent.

Guest	Host	$\Delta\delta_{NH(Free)}$	$\Delta\delta_{NH(Bound)}$	ΔNH_a	ΔNH_b
R(+) Propranolol	2,6 didodecyl-	1.07	1.04	+0.08	+0.09
S(-) Propranolol	β-cyclodextrin	1.07	1.04	-0.01	-0.05
(+) Methamphetamine	2,6 didodecyl-	0.16	0.15	+0.32	+0.38
(-) Methamphetamine	α-cyclodextrin	0.16	0.19	+0.28	+0.33
(+) Ephedrine	'poly'octyl-α-	1.03	1.17	+0.11	-0.1
(-) Ephedrine	cyclodextrin	1.03	1.03	0	0
(+) Ephedrine	2,6 didodecyl-	1.05	1.05	+0.42	+0.4
(-) Ephedrine	α-cyclodextrin	1.05	0.97	+0.3	+0.4
R(+) Amphetamine	2,6 didodecyl-	-	-	+0.25	-
S(-) Amphetamine	β-cyclodextrin	-	-	+0.25	-
R(+) Amphetamine	2,6 didodecyl-	-	-	+0.15	-
S(-) Amphetamine	α-cyclodextrin	-	-	+0.19	-

Table 4.4.1.1. Effect of complexation upon the NMR shifts for ammonium protons of the guests (Ephedrine with 'poly'octyl-α-cyclodextrin data from ref.17).

Methamphetamine trifluoroacetate was also studied, and the diastereotopic ammonium protons were found to be anisochronous ($\Delta\delta$ = 0.16), though not to the same extent as for propranolol and ephedrine, due to the lack of internal hydrogen bonding (figure 4.4.1.4). Upon complexation, the NH proton signals for both enantiomers were shifted to higher frequency (table 4.4.1.1) with the (+) enantiomer being affected marginally more. Again, it seems that both enantiomers are hydrogen bonding to the host cyclodextrin and the (+) enantiomer appears to shift the most.

The work previously reported[17] on the complexation of ephedrine was continued by observing the effects of complexation with 2,6 didodecyl-α-cyclodextrin. As discussed previously in this section, the two diastereotopic ammonium protons of ephedrine are anisochronous ($\Delta\delta$ = 1.05 ppm) due to the intramolecular hydrogen bonding between one of the ammonium protons and the hydroxyl group. Upon complexation with the cyclodextrin host, a shift to higher frequency for the ammonium signals of both enantiomers was observed (table 4.4.1.1), showing that the environment around these

protons has been altered. In contrast to the results for the complexation with 'poly'octyl-α-cyclodextrin, no noticeable increase in the anisochronaity of the two protons in the (+) enantiomer was noted. However, there is a decrease for the (-) enantiomer. The complexation of the ephedrine enantiomers caused a shift in the signals due to the H_3 proton of the cyclodextrin host ($\Delta\delta_{H3(+)} = 0.02$, $\Delta\delta_{H3(-)} = 0.03$) which may be related to the inclusion of the aromatic ring into the cyclodextrin cavity. These results are not the same as those observed for the 'poly'octyl system. This is not surprising as the didodecyl-α-cyclodextrin cyclodextrin probably has a more rigidly defined cavity geometry, because of the greater degree of 3(OH)—(O)2, hydrogen-bonding.

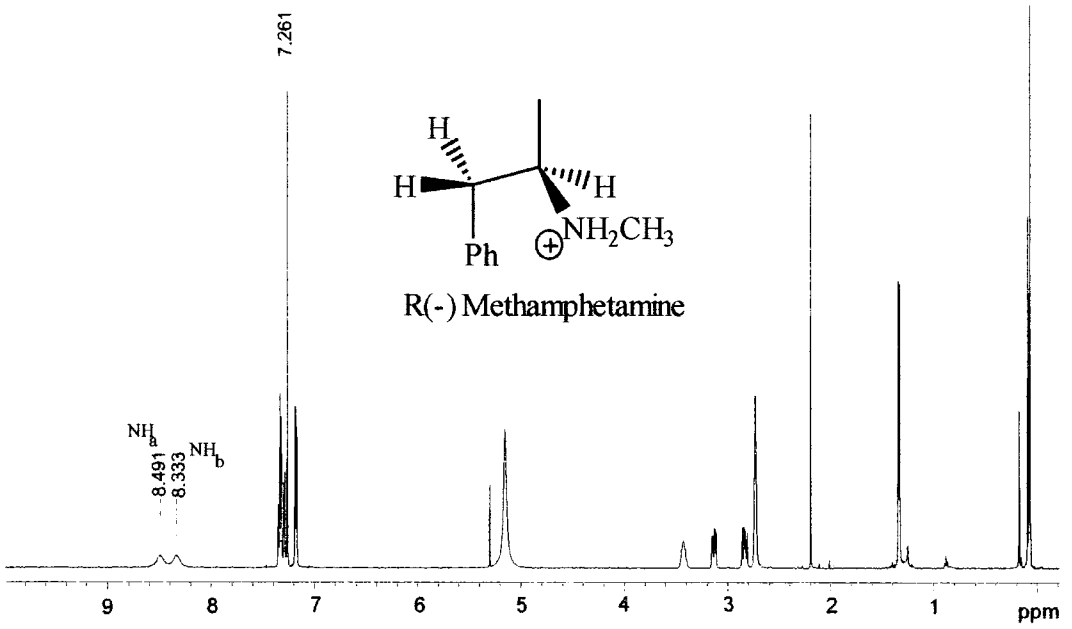

Figure 4.4.1.4. ^{1}H NMR spectra of Methamphetamine trifluoroacetate (3.3×10^{-2} mol dm^{-3}, 298 K, $CDCl_3$). Highlighted are the NH_a and NH_b ammonium protons.

For amphetamine and methamphetamine it is not surprising that the differences in chemical shift changes between enantiomers are similar. Both analytes have mobile side chains, because there is no intramolecular hydrogen bonding. In both ephedrine and propranolol this free rotation is restricted, making it harder for the pendant chain to orientate itself into a suitable conformation to allow maximum stabilising interactions between the guest and host.

4.4.2 Relaxation Rate measurements

Measurements following the changes in proton relaxation rates ($R_1 = 1/T_1$) for the host and guest molecules were used in an effort to define further the structural differences in the diastereoisomeric complexes. This method is useful because it is known that the measured relaxation rates are sensitive to a wide variety of factors including solvent, temperature, relative conformational population, exchange dynamics and intermolecular distances. This study was performed to compare R_1 data obtained for the diastereoisomeric complexes under controlled conditions, and to elucidate reasons for any differences, paying particular attention to the behaviour of the NH protons.

Guest	Host	Observed Proton	Relaxation Rate						
			free (+)	Bound (+)	ΔR_1	free (-)	Bound (-)	ΔR_1	$\Delta\Delta R_1$
amphetamine	2,6 $C_{12}\beta$CD	NH_3	12.7	3.4	-9.3	12.7	4.7	-8.0	1.3
		H_3	0.64	0.78	+0.14	0.64	0.84	+0.2	0.06
Propranolol	2,6 $C_{12}\beta$CD	NH_a	8.6	9.6	+1.0	8.6	5.5	-3.1	4.1
		NH_b	8.8	8.6	-0.2	8.8	5.4	-3.4	3.2
Ephedrine	'Poly'$C_8\alpha$CD	NH_a	4.3	6.5	+2.2	4.3	6.5	+2.2	0.0
		NH_b	5.8	1.15	-4.65	5.8	6.9	+1.1	5.75
		H_3	2.0	3.5	+1.5	2.0	2.1	+0.1	1.4
Ephedrine	2,6$C_{12}\alpha$CD	NH_a	7.9	3.5	-4.4	7.9	4.6	-3.3	1.1
		NH_b	7.4	4.5	-2.9	7.4	5.3	-2.1	0.8
		H_3	0.60	0.75	+0.15	0.60	0.80	+0.2	0.05
Methamphetamine	2,6$C_{12}\alpha$CD	NH_a	11.9	6.6	-5.3	11.9	5.3	-6.6	1.3
		NH_b	11.6	6.6	-5.0	11.6	5.4	-6.2	1.2
		H_3	0.61	0.78	+0.17	0.61	0.76	+0.15	0.02
Amphetamine	2,6$C_{12}\alpha$CD	NH_3	11.2	1.9	-9.3	11.2	3.5	-7.7	1.6

Table 4.4.2.1. Comparative relaxation rates (s^{-1}) for chiral arylammonium ions in the presence of alkylated cyclodextrins.

As can be seen from table 4.4.2.1 the relaxation rates for the NH_2^+ protons of propranolol are enantiomer dependent. The rates for both NH protons in the more weakly bound complex with S(-) propranolol showed a marked decrease upon complexation. With the R(+) enantiomer an increase by 1.0 s^{-1} for NH_a was found while NH_b remained unchanged.

Generally, R_1 values decrease through inhibition of relaxation mechanisms that decrease the local reorientation correlation time through increased molecular motion. Relaxation rates may be increased following complexation with a large host molecule, due to a decrease in molecular motion, ω, as a result of the association with the large molecule. The establishment of a new relaxation pathway such as that provided by hydrogen bonding between a guest and host also needs to be taken into account. Molecular modelling studies have been performed between propranolol and native β-cyclodextrin by Armstrong[29]. It was suggested that the inclusion complex was formed by the inclusion of the naphthalene ring into the cyclodextrin cavity with the pendant arm available for hydrogen bonding to the secondary hydroxyls of the host. The distances calculated between the NH_2^+ group of both enantiomers and cyclodextrin hydroxyls are shown in table 4.4.2.2. The shortest distances are between NH_2^+ -- 3[OH], for the R(+) enantiomer, and NH_2^+ – 2[OH] for the S(-) enantiomer.

	NH_2^+ – 2[OH] / Å	NH_2^+ – 3[OH] / Å
R(+) Propranolol	3.3	2.8
S(-) Propranolol	3.8	4.5

Table 4.4.2.2. Calculated distances from the NH_2 group of protonated propranolol to the secondary hydroxyl groups of the β-cyclodextrin[29].

This pattern is consistent with the data obtained from the R_1 measurements. An increase in relaxation rate for NH_a was found. This proton (NH_a) of the R(+) enantiomer is probably hydrogen bonding to the host 2,6 didodecyl-β-cyclodextrin (3[OH] of the cyclodextrin), NH_b meanwhile may now be hydrogen bonding (as the proton donor) to 2[O]. This possible hydrogen bonding coupled, with the expected increase in relaxation rate due to inclusion, may be enough to compensate for the

decrease in relaxation rate due to inhibition of relaxation caused by hydrogen-bonding to water dissolved in the solvent. The S(-) enantiomer shows a decrease in rate for both NH_2^+ protons, although the decrease is less for NH_b. This is consistent with neither of the NH_2^+ protons being able to hydrogen bond to the host (distances are too great) and their inability to relax via water in the solvent. The absence of these relaxation mechanisms leads to a decrease in the relaxation rate of the NH_2^+ protons.

For all the other analyte-cyclodextrin complexes studied (table 4.4.2.1) it was found that the relaxation rate was decreased upon complexation. This is indicative of the suppression of at least one dipolar relaxation pathway that effectively increases the local motional mobility, hence decreasing the local reorientation correlation time. This process may be related to changes in the hydrogen-bonding state of the NH_3^+ and NH_2^+ protons, which in the free state are probably hydrogen-bonded to residual water (from the salt or solvent). Complex formation will cause a decrease in the extent of this relaxation mechanism, as hydrogen bonding to the host cyclodextrin becomes competitive. Counteracting this tendency is the increase in R_1 values expected when a small guest associates with a large molecule. Given the opposing nature of these mechanisms on R_1, the overall observed effect will be a function of the difference in equilibrium constants for formation of the diastereoisomeric complexes and the change in the degree of NH—O hydrogen bonding. In these analyte-cyclodextrin complexes the evident decrease in relaxation rates could well be due to a decrease in hydrogen bonding.

4.4.3 Pulsed-Gradient Spin-Echo Measurements of Complex Stabilities

Pulsed-gradient spin echo NMR measurements of diffusion coefficients (section 4.2.1.4) were kindly performed by Professor Yoram Cohen. The association constants for 1:1 complex formation between the trifluoroacetate salts of the enantiomers of propranolol, ephedrine and amphetamine with 2,6 didodecyl-α- and β-cyclodextrin were calculated.

Table 4.4.3.1 shows the results obtained for all the systems studied. The complex between R(+) propranolol and 2,6 didodecyl-β-cyclodextrin is the most strongly bound. The association constant ($K_a = 222 \pm 58$ dm^3 mol^{-1}) is consistent with reported affinities of β-cyclodextrin for 1-substituted naphthyl derivatives[30]. The S(-) enantiomer was more weakly bound ($K_a = 66 \pm 17$ dm^3 mol^{-1}), corresponding to a free energy difference of 2.8 kJ mol^{-1}. Both the sense and the magnitude of this enantioselectivity are consistent with the electrochemical studies and values estimated from chiral HPLC methods[23].

In the two other cases studied, a more modest selectivity was observed, but the (+) enantiomer was always the more strongly bound. As a control, a cyclodextrin host with the 3[OH] alkylated was used in conjunction with ephedrine: no enantioselectivity was observed ($K_a = 113$ dm^3 mol^{-1} for (-) ephedrine, $K_a = 113$ dm^3 mol^{-1} for (+) ephedrine). Alkylation of the 3[OH] position removes the intramolecular hydrogen bonding network from the cyclodextrin. The interaction between 3[OH]—[O]2 provides conformational rigidity to the host molecule. Prior electrochemical response studies had also showed that complete alkylation of these lipophilic cyclodextrins removes the enantiodiscrimination for ephedrine and its stereoisomers[17].

System	CD ($x10^{-5}$ cm^2s^{-1})	Analyte ($x10^{-5}$ cm^2s^{-1})	K_a (dm^3mol^{-1})	$K_{(+)}/K_{(-)}$
2,6 $C_{12}\alpha CD$	0.32±0.01	-	-	-
S(-) Ephedrine	-	0.66±0.02	-	-
R(+) Ephedrine	-	0.66±0.02	-	-
2,6 $C_{12}\alpha CD$+ R(+) Ephedrine	0.28±0.01	0.51±0.01	142±21	1.25±0.25
2,6 $C_{12}\alpha CD$+ S(-) Ephedrine	0.28±0.01	0.54±0.01	114±15	-
2,6C_{12}3$C_1\alpha CD$	0.39±0.01	-	-	-
2,6C_{12}3$C_1\alpha CD$+S(-) Ephedrine	0.31±0.01	0.52±0.01	113±19	1.00±0.24
2,6C_{12}3$C_1\alpha CD$+R(+) Ephedrine	0.31±0.01	0.52±0.01	113±19	-
2,6$C_{12}\beta CD$	0.33±0.01	-	-	-
S(+) Amphetamine	-	0.69±0.01	-	-
R(-) Amphetamine	-	0.69±0.02	-	-
2,6$C_{12}\beta CD$+S(+) Amphetamine	0.31±0.01	0.48±0.01	163±28	1.60±0.37
2,6$C_{12}\beta CD$+R(-) Amphetamine	0.31±0.01	0.51±0.01	102±16	-
S(-) Propranolol	-	0.59±0.02	-	-
R(+) Propranolol	-	0.59±0.02	-	-
2,6$C_{12}\beta CD$+S(-) Propranolol	0.30±0.01	0.53±0.02	67±17	3.31±1.2
2,6$C_{12}\beta CD$+R(+) Propranolol	0.24±0.01	0.45±0.02	222±58	-

Table 4.4.3.1 Diffusion coefficients (D in cm^2s^{-1}) of the chiral ammonium salts and of the cyclodextrins studied in the free and in 1:1 solutions along with association constants (K_a in dm^3mol^{-1}) derived from the data. Measurements were made at 283 K.

4.5 Conclusions

The data from both the NMR and electrochemical response studies show, for this range of analytes, that the (+) enantiomer is more strongly bound. The variation in the strength of complexation between enantiomers is probably due to an increase in the degree of hydrogen bonding observed upon complexation of the (+) enantiomer (involving NH_a). The complexation of propranolol shows this best, and the R(+) enantiomer is more strongly bound by 2.6 – 2.9 kJ mol^{-1} (evidence from PGSE and electrochemistry). There is evidence that stabilising NH – O interactions are present between propranolol and 2,6 didodecyl-β-cyclodextrin that are absent in the weaker isomeric complex. Earlier molecular modelling calculations are consistent with this result, showing that NH_2^+ – OH distances in the complex with (+) propranolol are short enough to allow hydrogen bonding, while the corresponding distances in (-) propranolol are longer.

The case of the benzylamine derivatives is different. Although too much emphasis should not be placed on the electrochemical data without corroborating evidence, it can be deduced that in all the cases studied, the (-) was more the strongly bound. This change in preference may be due to a number of reasons, not least of which would be the different position of the chiral centre: here being α to the aromatic ring rather than further along a pendent chain. However, more experiments need to be done relate this change to the precise solution structure of the complex.

It must also be noted here that enantioselectivity is only a small part of the overall association constants for pairs of diastereoisomers. The forces involved are typically 1-2 orders of magnitude weaker than those responsible for general complexation, the main energy gain coming from the substitution of the energetically unfavourable polar-apolar interactions between the included water and the cyclodextrin cavity with the more favourable apolar-apolar interactions between the guest and cavity. This can be seen by referring back to table 4.4.3.1. In all of the cases studied the enantiodiscrimination free energy difference is consistently an order of magnitude smaller than that required to form the complexes. Even so, the relatively small amount of energy involved is enough to dictate the selectivity of the host cyclodextrin for the

potential chiral guest molecule. The enantiodiscrimination observed here is clearly the result of the overall effect of some nonbonding interactions, and in particular is due to the difference in hydrogen-bonding between the guest molecules and the host.

4.6 References

1. ed. Dollery C., Therapeutic Drugs. Churchill Livingstone, London. 1991
2. Barett A. M., Cullum V. A., *Br. J. Pharmac.*, 1968, **34**, 43-55
3. Lipkowitz K. B., Pearl G., Coner B., Peterson M. A., *J. Am. Chem. Soc.*, 1997, **119**, 600-610
4. Kohler J. E. H., Hohla M., Richters M., Konig W. A., *Chem. Ber.*, 1994, **127**, 119-126
5. Black R., Parker C. G., Zimmerman S. S., Lee M. L., *J. Comput. Chem.*, 1996, **17**, 931-939
6. Cram D. J., Mateos J. L., *J. Am. Chem. Soc.*, 1959, **81**, 2756-2762
7. Parker D., *Chem. Rev.*, 1991, **91**, 1441-1457
8. Greatbanks D., Pickford R., *Magn. Reson. Chem.*, 1987, **25**, 208-215
9. Bussmann W., Lehn J-M., Oesch U., Plumere P., Simon W., *Helv. Chim. Acta.*, 1981, **64**(3),657-661
10. Peacock S. C., Cram D. J., *J. Chem. Soc., Chem. Commun.*, 1976, 282-284
11. Behr J-P., Lehn J-M., Vierling P., *Helv. Chim. Acta.*, 1982, **65**(6), 1853-1867
12. Haskins N. J., Saunders M. R., Camilleri P., *Rapid Commun. Mass Spectrom.*, 1994, **8**, 423-426
13. Sawada M., Taki Y., Yamada H., Hirayama S., Kaneda T., Tanaka T., Kamada K., Mizooku T., Takeuchi S., Ueno K., Hirose K., Tobe Y., Naemura K., J. *Am.Chem. Soc.*, 1995, **117**, 7726-7736
14. Kidd G. R., NMR of newly assessable nuclei, 1983, vol. 1
15. Canceill J., Julien L., Lacombe L., Lehn J-M., *Helv. Chim. Acta*, 1992, **75**, 791-812
16. Lipkowitz K. B., Raghothama S., Yang J-A., *J. Am. Chem. Soc.*, 1992, **114**, 1554-1562
17. Bates P. S., Kataky R., Parker D., *J. Chem. Soc., Perkin Trans. 2*, 1994, 669-675
18. Stejskal E. O., Tanner J. E., *J. Chem. Physics*, 1965, **42**(1), 288-292
19. Cohen Y., Mayzel O., *J. Chem. Soc., Chem. Commun.*, 1994, 1901-1902
20. Mayzel O., Aleksiuk O., Grynszpan F., Baili S. E., Cohen Y., *J. Chem. Soc., Chem. Commun.*, 1995, 1183-1184
21. Gafni A., Cohen Y., *J. Org. Chem.*, 1997, **62**, 120-125

22. ed. Bishop M. L., Duben-Engelkirk J. L., Fody E. P., Clinical Chemistry: Principles, Procedures, Correlations. 2nd ed. J. B. Lipponcott. Philadelphia. 1985. Ch. 25
23. Bates P. S., Patti A. F., Parker D., *J. Chem. Soc., Perkin Tras. 2*, 1994, 657-668
24. Inoue Y., Takashi Y., Chujo R., *Carbohydr. Res.*, 1985, **144**, C4-C11
25. Li S., Purdy W. C., *Anal. Chem.*, 1992, **64**, 1405-1412
26. Ndou T. T., Mukundan S., Warner I H., *J. Incl. Phenom. Molec. Recog. Chem.*, 1993, **15**, 9-25
27. Sakurai T., Saitou E., Hayashi N., Hirasawa Y., Inoue H., *J. Chem. Soc., Perkin Trans. 2*, 1994, 1929-1935
28. Mularz E. A., Cline-Love L. J., Petersheim M., *Anal. Chem.*, 1988, **60**, 2751-2755
29. Armstrong D. W., Ward T. J., Armstrong R. D., Beesley T. E., *Science*, 1986, **232**, 1132-1135
30. ed. Szeitli J., Osa T., Cyclodextrins in 'Comprehensive Supramolecular Chemistry' ed. Atwood J. L., MacNicol J. E. D., Voglt F., vol.3, Pergamon, Oxford, 1996

Chapter Five

General Experimental Procedures

5.1 Potentiometric Methods

5.1.1 Ion-selective Membrane Composition

The electroactive membranes were prepared containing the appropriate ionophore (1.2 %), o-nitrophenyloctyl ether (*o*NPOE), bis(butylpentyl)adipate (BBPA) or bis(2-ethylhexyl)sebacate (DOS) (65.6 %), PVC or Tecoflex SG80 (32.8 %) and Sodium tetrakis[3,5-bis(trifluoromethyl)phenyl]borate (TKB) or potassium tetrakis(4-chlorophenyl)borate (KTClPB) (0.4 %) in 6 cm^3 THF (see figure 5.1.1.1 for structures).

The membranes were cast according to the procedure described by Moody[1].
The PVC, *o*NPOE, DOS and KTClPB were obtained from Fluka. Tecoflex SG80 was obtained from Thermedics Inc. (USA), TKB was synthesised in this laboratory.

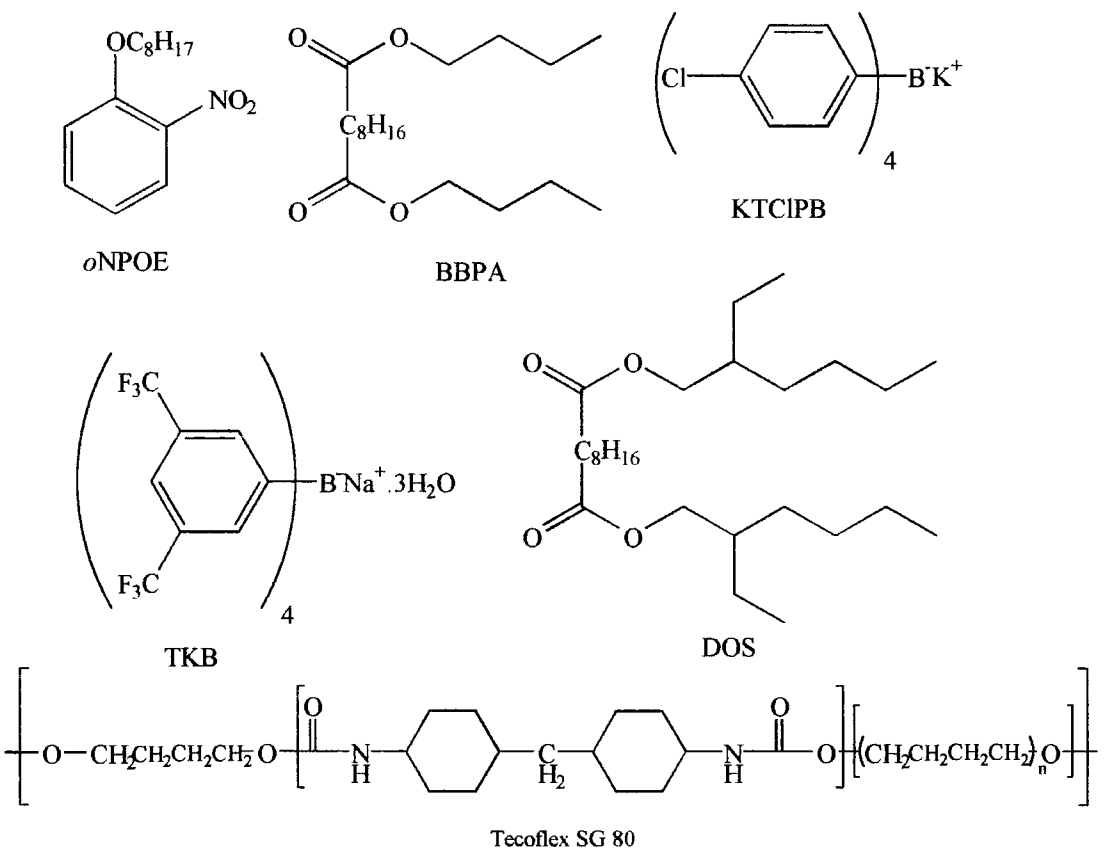

Figure 5.1.1.1. Membrane Constituents.

5.1.2 Constant Volume Dilution Method.

This method was first introduced by Horvai *et al.*[2] in 1976 and has since been widely used as a calibration method and also in the determination of electrode parameters. With this method the concentration of an analyte ion can be varied with time or diluent volume. If the electrode response follows the Nernst equation then the measured potential difference E, is proportional to log c as long as the activity coefficient remains constant. The electrode will then produce a linear response of E versus t.

The method requires the continuous dilution of a fixed volume of solution containing the primary ion, either by water, for a calibration graph or by a background electrolyte, for selectivity measurements. The system must also have efficient stirring to maintain a homogenous solution during the experiment[3].

Derivation of the log c $\leftrightarrow$ t relationship;

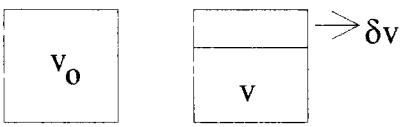

After a given time interval a small volume of solution δv is removed from the cell and replaced with diluent which does not contain the primary ion,

$$v_0 - v_D = \delta v \qquad (1)$$

This gives the new lower concentration (c') of the primary ion in the cell by the equation,

$$c' = \frac{cv}{v_0} = \frac{c(v_0 - \delta v)}{v_0} \qquad (2)$$

Re-arranging and substituting $\delta c = c' - c$

$$\frac{\delta c}{c} = -\frac{\delta v}{v_o} \qquad (3)$$

If the dilution is continuous $\delta v \rightarrow dv$,

$$\frac{dc}{c} = \frac{dv}{v_o} \qquad (4)$$

If the flow rate is w (m^3s^{-1}), then dv = wdt,
substituting for dv and integrating,

$$\int_{c_0}^{c} \frac{dc}{c} = -\int_{0}^{t} \frac{wdt}{v_0} \qquad (5)$$

$$\text{then } \ln c = \ln c_0 - \frac{wt}{v_0} \qquad (6)$$

where c_0 : initial concentration of primary ion

c : concentration of primary ion at time t

As the results are initially in the form of potential difference vs. time and the graphs presented are in the form potential difference vs. -log c, the following conversion is used for time into -log c,

$$-\log c = -\log c_0 + \log\left(e^{-wt/v_0}\right) \qquad (7)$$

This technique was used as the standard method for obtaining calibration and selectivity measurements. The constant volume dilution system was set-up as shown in figure 5.1.2.1. The solution was drawn through the constant volume cell and past the frit of the T-junction reference electrode (figure. 5.1.2.2) vessel to waste and the electrode response was monitored with respect to time.

The flow rate was measured by timing the filling of a 10 ml volumetric flask by the waste solution. The volume of the constant volume cell was calculated by measuring the time taken to fill the cell from the input to the output. This time was then converted to a volume using the flow rate calculated earlier. The system was thermostatted at 298 K.

The constant volume cell and T-junction reference cell were both made in-house. A 7mm disc of the electroactive membrane was cut and mounted in a Philips IS(561) electrode body (Philips Analytical, Eindhoven, Netherlands). The inner filling solution was 1 x 10^{-3} mol dm^{-3} ammonium chloride (Merck, UK), and the reference electrode was a single junction calomel electrode (ATI Russell, Fife, Scotland) with saturated potassium chloride as the bridging solution. The peristaltic pump was a Minipuls 3 (Gilson).
The Philips body electrode and reference electrode were connected to a high impedance buffer amplifier, which was attached to a digital multimeter (Keithley) and a chart recorder.

The parameters required for equation 7 were calculated to be;
Flow rate (w) = 0.8 ml min^{-1}
Cell volume (v_o) = 2.34 ml

A stable reading was obtained with the initial solution flowing before the dilution was initiated.

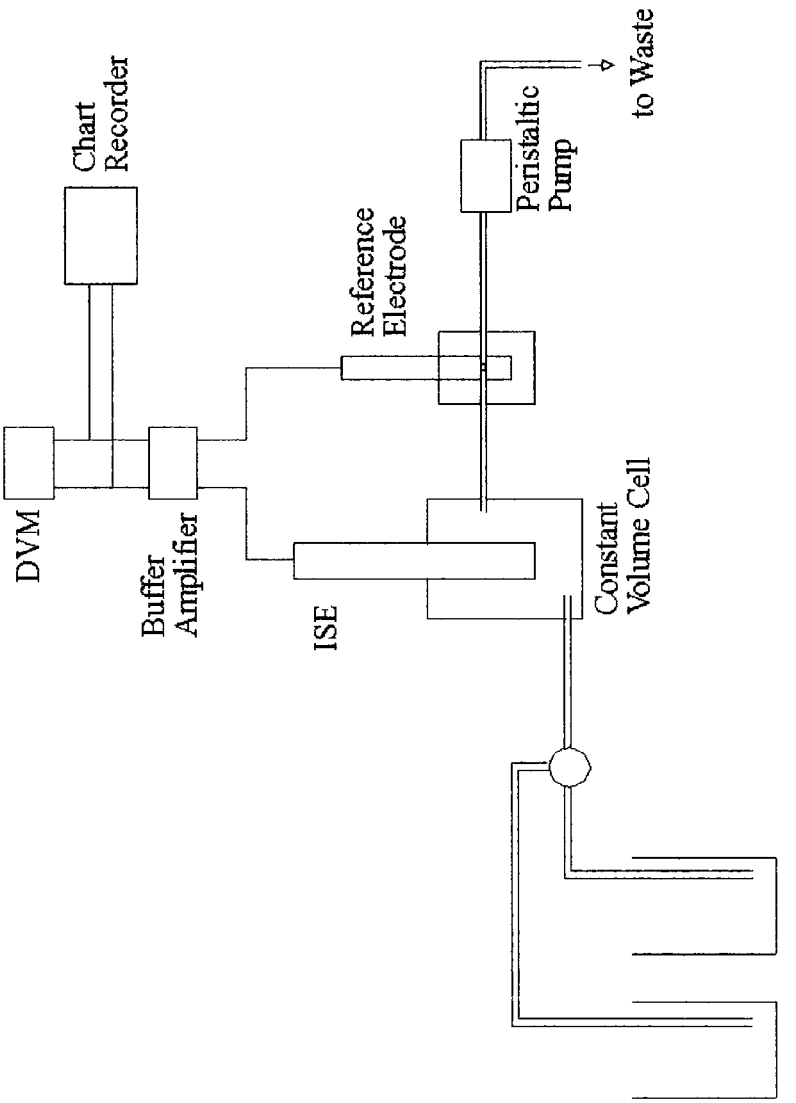

Figure 5.1.2.1. Constant volume dilution schematic.

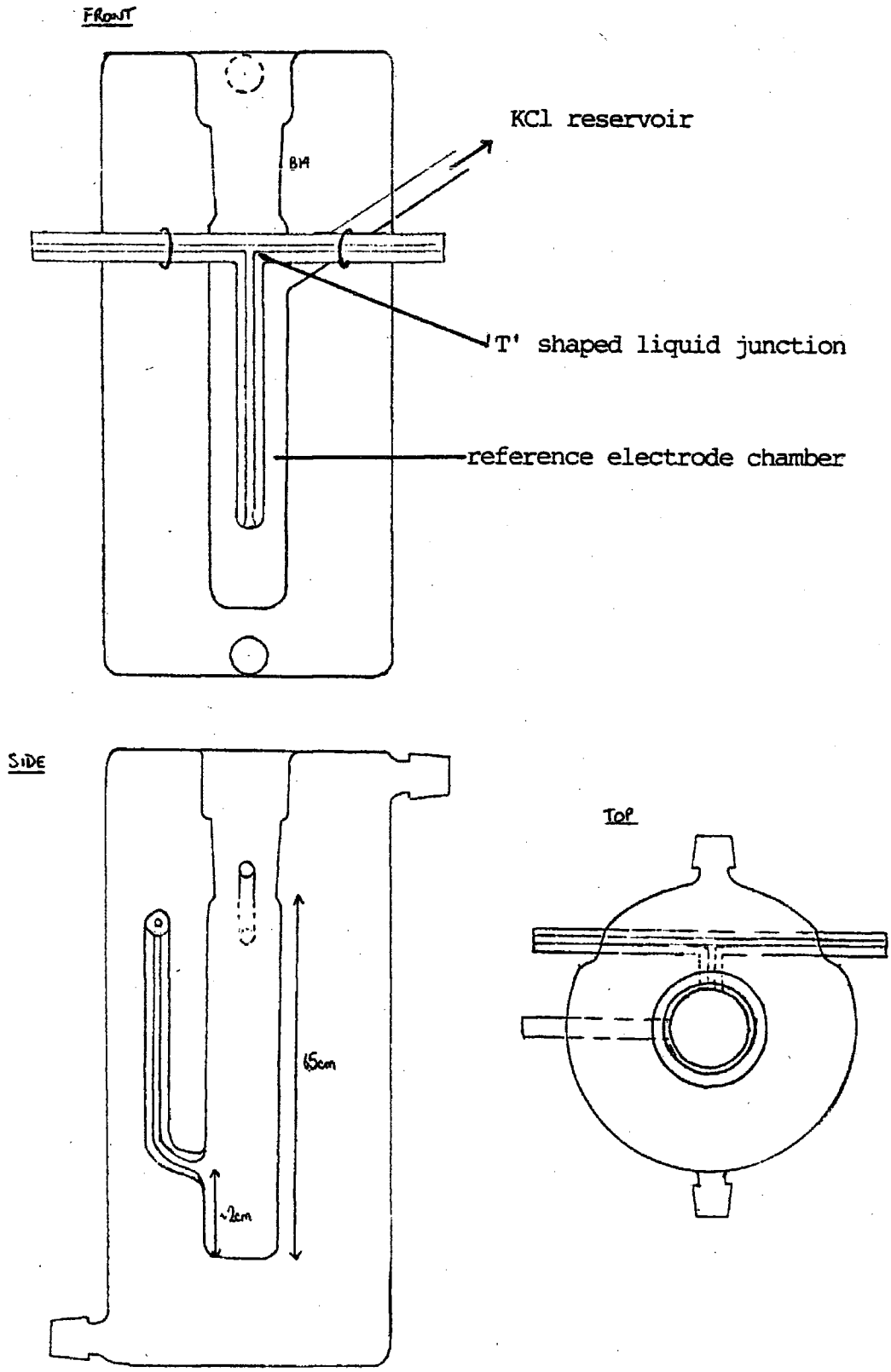

Figure 5.1.2.2. Schematic of Reference Cell.

5.1.3 Fixed Interferent Method

To calculate the selectivity coefficient the fixed interferent method (FIM) was used[4]. The method involves the variation of either the interferent or the primary ion concentration while the other is kept constant.

a) Fixed primary ion concentration.
The concentration of the primary ion is kept constant and the interferent ion concentration is varied.

b) Fixed interferent ion concentration.

The concentration of the interferent ion is kept constant while the concentration of the primary ion is varied. This method is preferred as it usually provides a more realistic simulation of the situation in samples. Indeed, this was the method used in the interference studies. The selectivity coefficient for the concentration of interferent can be obtained from a plot of E vs. -log c.

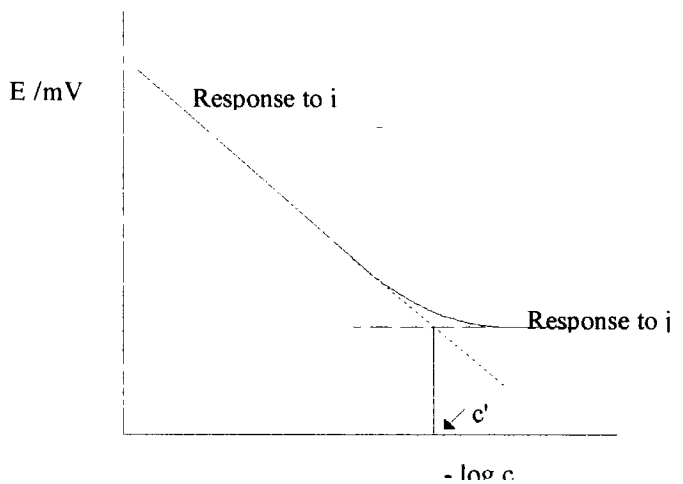

Figure 5.1.3.1. Mixed Solution Plot.

If the plot of E vs. -log c levels out at low concentrations, the point where the two extrapolated linear regions intersect is the point c', where the electrode is responding equally to both the primary and interferent ions, see figure 5.1.3.1.
At high concentrations the potential difference only depends on the primary ion,

$$E_i = E_0 + k \log c_i \qquad (1)$$

At low concentrations the potential will depend only on the interferent ion,

$$E_j = E_0 + k \log\left(k_{ij} c_j^{z_i/z_j} \right) \qquad (2)$$

At the point c' the electrode is responding equally to both ions i.e. this concentration of primary ion as the interferent ion, therefore,

$$c' = k_{ij} a_j^{z_i/z_j} \qquad (3)$$

therefore giving,

$$k_{ij} = \frac{c'}{c_j^{z_i/z_j}} \qquad (4)$$

If however the plot of E vs. -log c does not level out at lower concentrations of the primary ion then the following can method can be used, as in figure 5.1.3.2,

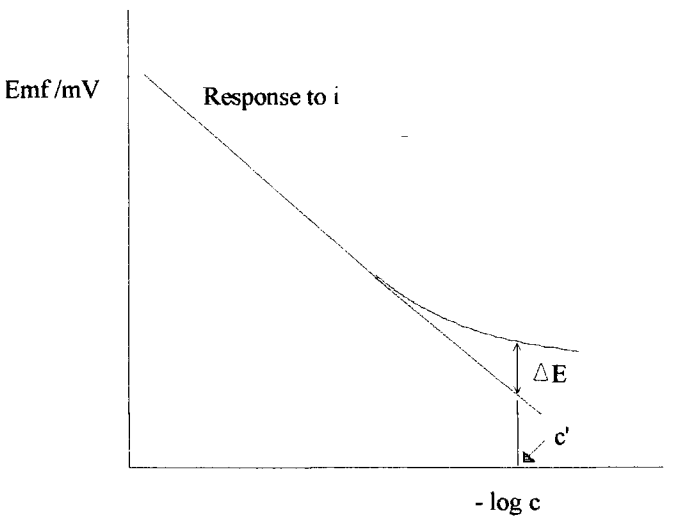

Figure 5.1.3.2.

For pure ion i calibration,

$$E_i = E_0 + k \log c_i \qquad (5)$$

For the mixed solution,

$$E' = E_0 + k \log\left(c_i + k_{ij} c_j^{z_i/z_j} \right) \qquad (6)$$

When $c_i = c' = k_{ij}c_j$ the difference in potential, ΔE, between the pure primary ion solution and the mixed ion solution, each with primary ion concentration c' is,

$$\Delta E = E' - E_i = k \log 2 \qquad (7)$$

$$\Delta E = \frac{2.303RT}{z_i F} \log 2 \qquad (8)$$

$$\Delta E \cong \frac{18}{z_i} \text{mV} \qquad (9)$$

Therefore c' can be found by extrapolating the linear section of the plot from high concentration to the point at which the deviation between the two lines is $18/z_i$ mV.

5.1.4 Flow Injection Analysis

The Flow Injection Analyser was configured as shown in figure 5.1.4.1. The carrier was drawn through the injector, dispersion coil and detector, to waste, by the peristaltic pump (Ismatec SA, Switzerland). Samples were introduced into the flow system by means of a six-port manual injector with a sample loop volume of 250 µl.

The dispersion coil consisted of 1 m Teflon tubing (1m, i.d. 0.5 mm, o.d. 1 mm). The detector cell configuration was a macro wall-jet system (figure 5.1.4.2). This consisted of a potentiometric wall-jet cell arrangement with small effective volume with a macro ion-selective electrode as the detector. A Philips IS-560 electrode body (Philips Analytical, Eindhoven, Netherlands) and a single junction calomel electrode (ATI

Russell, Fife, Scotland) with bottom ceramic-frit were fitted into the detector cell body. The reference electrolyte (1 x 10^{-1} mol dm^{-3} KCl) flowed continuously around the reference electrode frit, forming a thin film of flowing solution around the ion-selective electrode as it entered the reservoir. The carrier stream impinged directly onto the ion-selective membrane surface through a capillary. The capillary to electrode membrane distance was approximately 2 mm.

The ion-selective electrode and reference electrode were connected to an amplifier unit (Molspin Ltd, Newcastle, UK) which supplied a voltage gain of three. The amplifier was then connected to a digital multimeter (Metex M4650CR), and the EMF response was displayed on a PC.

All measurements were performed at room temperature. For each analyte sample, multiple injections of that sample were made to check the reproducibility of the potential difference measured. The flow rate of the system was measured by timing the filling of a 10 ml volumetric flask, flow rate 4 ml min^{-1}. In all the measurements, a steady potential for the carrier solution was obtained before injecting the first sample.

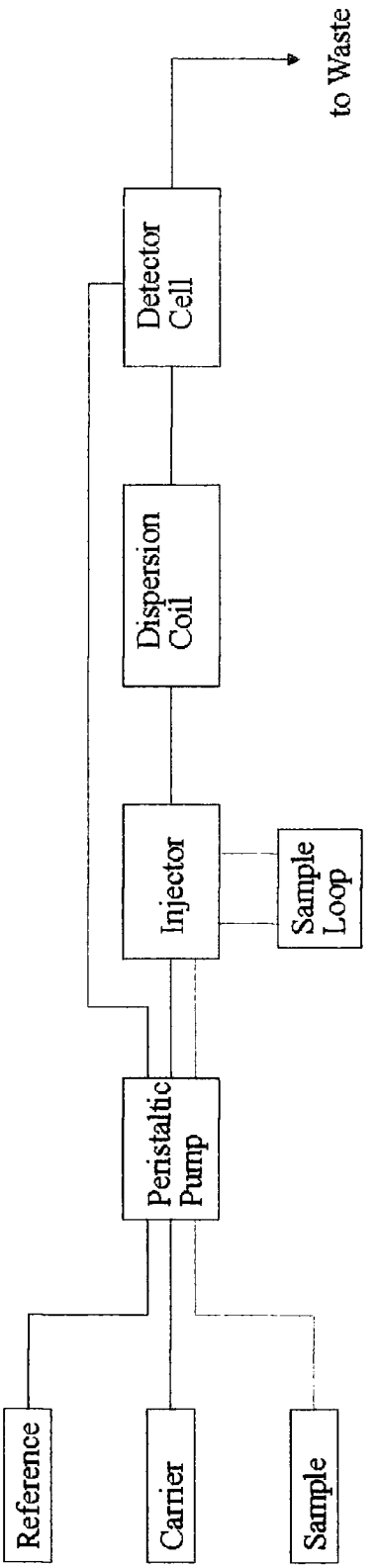

Figure 5.1.4.1. Schematic of Flow Injection Analyser.

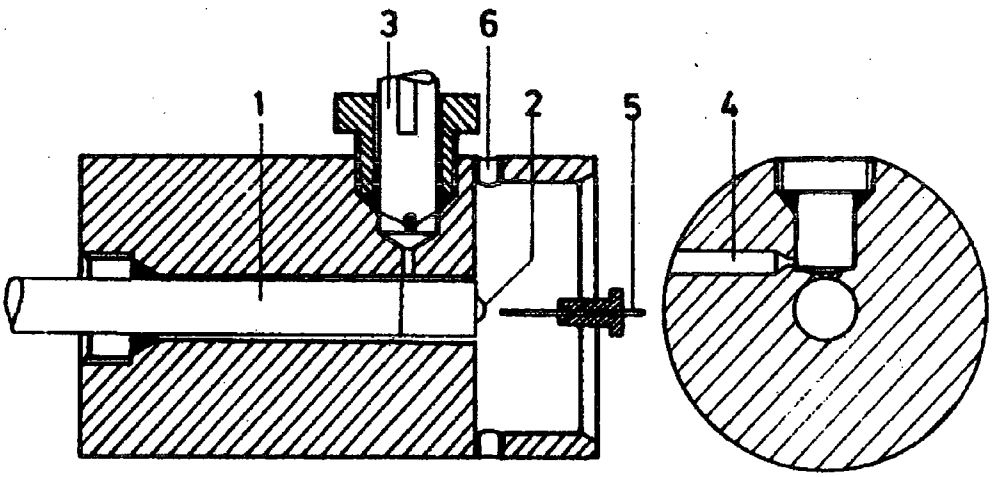

Figure. 5.1.4.2. Flow Injection Analyser Detector Cell[5]. 1, ISE; 2, ion-selective membrane; 3, reference electrode; 4, bore for continuously streaming reference electrolyte; 5, jet; 6, outlet.

5.1.5 Protein Interference Dip Tests

The electroactive membranes were mounted in Philips IS-560 electrode bodies and the reference electrode was a double junction silver-silver chloride (RE15, Unicam) with 10% Potassium nitrate as bridge solution.
The protein solutions studied were,

1) 40 g/l Bovine Serum Albumin
2) 0.55 g/l α_1-acid glycoprotein
3) Pooled Human Serum

For each of the protein interferents studied two solutions were prepared,

1. containing 1 x 10^{-3} mol dm^{-3} analyte in 'clinical background' cations,
2. 1 x 10^{-3} mol dm^{-3} analyte with the protein and 'clinical background' cations.

The ISE and reference electrode were placed in the stirrer protein-free solution and the potential difference recorded after 20 min. The electrodes were then washed before being placed in the protein containing solution, the potential difference was again

recorded after 20 min. After re-washing the electrodes in de-ionised water, they were returned to the aqueous solution. This process was repeated 10 times for each pair of solutions.

All solutions were prepared using de-ionised water.
All measurements were made at 298 K.
Both the electrodes were connected to a buffer amplifier and the EMF response was recorded on a digital multimeter (Keithley).

5.2 Amperometric Experimental

5.2.1 Square Wave Voltammetry

This technique was used for all the amperometric experiments performed due to its quantitative nature. The equipment was set-up in three configurations;

1) A glassy carbon working electrode (BAS Technical, Stockport, UK) with a silver-silver chloride reference electrode and a platinum wire counter. The working electrodes were polished with 0.05 μm alumina slurry (Buchler, Lake Buff, USA), washed thoroughly and dried before use. The glassy carbon electrode was used either uncoated or coated with an alkylated cyclodextrin solution depending on the actual experiment.
2) A screen printed PVC substrate which consisted of a carbon working electrode (surface area, 0.12 cm^2) and a silver-silver chloride reference electrode (Cambridge Life Sciences, Ely, UK) with a separate platinum wire counter electrode.

   The surface of the working electrode could be modified as required by depositing 1μl aliquots of membrane material onto its surface. The modification used depended upon the analyte of interest.

5.2.2 Controlled Potential Coulometry

A MF-1056 electrolysis cell (BAS Technical, Stockport, UK) was used for the controlled potential coulometry. This consisted of a porous carbon working electrode, a silver chloride reference and a platinum wire counter electrode.

In these experimental set-ups the voltammograms were recorded using an EG & G PARC (Princeton, NJ, USA) Model 263 or M273 with model M270/250 software. Data analysis was performed using EG & G Model 271 Cool Kinetic Analysis Software.

5.3 NMR Experimental

5.3.1 Longitudinal Relaxation (R_1) Experimental

The experiments were performed on a Bruker AMX 500 spectrometer using the standard inversion recovery technique[6].

Paramagnetic oxygen was excluded from the samples by a repetitive 'freeze-pump-thaw' process carried out under an argon atmosphere. For each complex investigated, four solutions were prepared with the guest being present as the trifluoroacetate salt;

1) Free guest, 3.3×10^{-2} mol dm^{-3}
2) Free host cyclodextrin, 1.32×10^{-2} mol dm^{-3}
3) R enantiomer guest (3.3×10^{-2} mol dm^{-3}) +
   host cyclodextrin (1.32×10^{-3} mol dm^{-3})
4) S enantiomer guest (3.3×10^{-2} mol dm^{-3}) +
   host cyclodextrin (1.32×10^{-3} mol dm^{-3})

Each solution was prepared in 0.7 ml d-chloroform. All the solutions were deoxygenated by a repetitive 'freeze-evacuate-thaw' process carried out under an argon atmosphere. The guest analyte was in the form of a trifluoroacetate salt, the preparation of which is described in section 5.3.2.

5.3.2 Preparing the trifluoroacetate salt

A solution of the required analyte hydrochloride in de-ionized water was basified to pH 9/10 with 4 mol dm^{-3} sodium hydroxide. The resulting solution was extracted into dichloromethane. The combined organic residues were dried over anhydrous potassium carbonate and filtered. An excess of trifluoroacetic acid was added and the resulting solution was dried under reduced pressure to give a viscous oil.

5.3.3 Pulse Gradient Spin Echo (PGSE)

The PGSE diffusion experiments were performed at 283 K on a Bruker ARX500 spectrometer equipped with a BGU pulsed gradient unit on a B-VT-2000 temperature control unit. Data was collected using a commercial 5 mm inverse probe equipped with shelf-shielded g-gradients on 5 x 10^{-3} mol dm^{-3} samples in d-chloroform. The guest molecule was in the form of a trifluoroacetate salt, the preparation of which is described in section 5.3.2.

5.4 References

1. Craggs A., Moody G. J., Thomas J. D. R., *J. Chem. Educ.*, 1974, **51**(8), 541-544
2. Horvai G., Toth K., Pungor E., *Anal. Chim. Acta*, 1976, **82**, 45-54
3. Kelly P. M., Proposed Reference Method for the measurement of ionised calcium in blood, PhD thesis, Newcastle, 1993
4. Umezawa Y., Umezawa K., Sato H., *Pure & Appl. Chem.*, 1995, **67**(3), 507-518
5. Jeney J., Toth K., Lindner E., Pungor E., *Microchem. J.*, 1992, **45**, 232-247
6. Behr J. P., Lehn J-M., *J. Am. Chem. Soc.*, 1976, 98, 1743-1747

Appendix

Research Colloquia, Conferences and Publications

The author attended the following lecture courses:

NMR Spectroscopy, by Dr. A. M. Kenwright, Dr. P. G. Steel and Prof. D. Parker

Diffraction Techniques, by Prof. J. A. K. Howard

Physical Chemistry of Polymers, by Prof. R. W. Richards

The author attended the following colloquia between October 1994 and September 1997.

1994

October 4 Prof. N.L. Owen, Brighton Young University, Utah, USA
Determining Molecular Structure – the INADEQUATE NMR way

November 2 Dr. P. G. Edwards, University of Wales, Cardiff
The Manipulation of Electronic and Structural Diversity in Metal Complexes – New Ligands

December 7 Prof. D. Briggs, ICI and University of Durham
Surface Mass Spectrometry

December 13 Prof. H. A. O. Hill
Making use of one electron after another

1995

January 18 Dr. G. Rumbles, Imperial College, London
Real and Imaginary Third Order Non-linear Optical Materials

February 1 Dr. T. Cosgrove, Bristol University
Polymers do it at Interfaces

February 17 Prof. B. Birch, Luton University
Disposable Sensors

May 4 Prof. A. J. Kresge, University of Toronto
The Ingold Lecture Reactive Intermediates: Carboxylic-acid Enols and Other Unstable Species

November 9 Prof. R. J. P. Williams
Metals in Health and Disease

November 17 Prof. D. Bergbreiter, Texas A&M, USA
Design of Smart Catalysts, Substrates and Surfaces from Simple Polymers

November 23 Dr. P. Levy
Drug Abuse in Sports

1996

January 10 Dr. B. Henderson, Waikato University, NZ
Electrospray Mass Spectrometry – a new sporting technique

January 17 Prof. J. W. Emsley, Southampton University
Liquid Crystal: More than Meets the Eye

February 28 Prof. E. W. Randall, Queen Mary & Westerfield College
New Perspective in NMR Imaging

March 13 Prof. D. Graner, Manchester University
Mushrooming in Chemistry

April 30 Dr. L. D. Pettit, Chairman, IUPAC Commision of Equilibrium Data
PH-metric studies using very small quantities of uncertain purity

May 1 Prof. M. J. Pilling
Chemistry in the Atmosphere

October 4 Dr. P. D. Woods
Triplet State Interactions in DNA model Systems

October 22 Prof. B. J. Tighe, Department of Molecular Sciences and Chemistry, University of Aston
Making Polymers for Biomedical Application – can we meet Nature's Challenges?

October 29 Prof. D. M. Knight, Department of Philosophy, University of Durham
The purpose of Experiment – A look at Davy and Faraday

November 6 Dr. M. Duer, Chemistry Department, Cambridge
Solid-state NMR Studies of Organic Solid to Liquid-crystalline Phase Transitions

November 12 Prof. R. J. Young, Manchester Materials Centre, UMIST
New Materials – Fact or Fantasy?

November 18 Prof. G. A. Olah, University of Southern California, USA
Crossing Conventional Lines in my Chemistry of the Elements

November 27 Dr. R. Templer, Imperial College, London
Molecular Tubes and Sponges

December 3 Prof. D. Phillips, Imperial College, London
A Little Light Relief

1997

February 6 Prof. P. Bartlett, University of Southampton
Integrated Chemical Systems

February 18 Prof. Sir James Black, The James Black Foundation/King's College London
My Dialogues with Medicinal Chemists

February 25 Prof. A. G. Sykes, University of Newcastle
The Synthesis, Structure and Properties of Blue Copper Proteins

March 6 Prof. Klara Toth, Technical University of Budapest, Budapest
Scanning Electrochemical Microscopy

May 7 Prof. Harrington
Molecular Pathology Studies of Nerve Systems

Conferences

The author attended the following meetings:

1. Short Papers in Pharmaceutical Analysis, Royal School of Pharmacy, London, 24th October 1995
2. Advances and Applications in Capilliary Electrophoresis and Related Technology, Sunderland, 24th January, 1996
3. ESEAC '96, Durham, 25-29th March, 1996
4. Electrochem '96, Bath, 16–19th September, 1996
5. Scottish Dalton Meeting, Edinburgh, 6th February, 1997

Publications

1. Local anaesthetics measured by lipophilic β-cyclodextrin-based ion-selective electrodes
   Ritu Kataky and Simon Palmer
   Electroanalysis, 1996, **8**(6), 585-590

2. Selectivity in the binding and detection of charge diffuse ions
   David Parker, Ritu Kataky, Patricia M. Kelly and Simon Palmer
   Pure & Appl. Chem, 1996, **68**(6), 1219-1223

3. Alkylated cyclodextrin based potentiometric and amperometric electrodes applied to the measurement of tricyclic antidepressants
   Ritu Kataky, Simon Palmer, David Parker and Dominic Spurling
   Electroanalysis. Accepted for Publication

4. Enantiomer discrimination using lipophilic cyclodextrins studied by electrode response, pulsed-gradient spin-echo (PGSE) NMR and relaxation rate measurements
   Ayelet Gafni, Yoram Cohen, Ritu Kataky, Simon Palmer and David Parker
   J. Chem. Soc., Perkin Trans. 2. Accepted for Publication

5. Cyclodextrin-modified potentiometric and amperometric electrodes in flow injection analysis
   Ritu Kataky, Klara Toth, Zsofia Feher and Simon Palmer
   Analyst, In Preparation